

The Influence of s - d Exchange Interaction on the Gap Anisotropy and Anisotropy of the Lifetime of Normal State Charge Carriers of Layered Cuprates

Todor M. Mishonov*, Nedeltcho I. Zahariev[†], Albert M. Varonov[‡]

*Georgi Nadjakov Institute of Solid State Physics, Bulgarian Academy of Sciences
72 Tzarigradsko Chaussee Blvd., BG-1784 Sofia, Bulgaria*

2 December 2022

Abstract

The anisotropy of the electron scattering rate and lifetime $\Gamma_{\mathbf{p}} = 1/\tau_{\mathbf{p}}$ observed by Angle Resolved Photoemission Spectroscopy (ARPES) is evaluated using s - d Kondo-Zener exchange Hamiltonian used previously to describe superconducting properties of high- T_c cuprates; for correlation between critical temperature T_c and BCS coupling constant, for example. The performed qualitative analysis reveals that “cold spots” correspond to nodal regions of the superconducting phase where the superconducting gap is zero, because the exchange interaction is annulled. Vice versa, “hot spots” and intensive scattering in the normal state correspond to the regions with maximal gap in the superconducting phase. We have obtained that separable kernel postulated in the Fermi liquid approach to the normal phase is the same kernel which is exactly calculated in the framework of the s - d approach in the Linear Combination of Atomic Orbital (LCAO) approximation for CuO_2 plane. In this sense, at least on the qualitative level, the superconducting cuprates are described by one and the same Hamiltonian applied to their superconducting and normal properties. For the overdoped cuprates having conventional Fermi liquid behavior we derived the corresponding Stoss-integral for the s - d interaction in the framework of LCAO approximation which is the central result of the present study. Repeating the thermodynamics we observed that for optimally doped cuprates $2\Delta_{\text{max}}/T_c$ is in good agreement with Pokrovsky theory for anisotropic gap superconductors.

*mishonov@gmail.com

[†]zahariev@issp.bas.bg

[‡]varonov@issp.bas.bg

CONTENTS

Contents	ii
1 Introduction	1
1.1 Basic notions of the elementary kinetics	3
1.1.1 Transport cross-section of two dimensional coulomb scattering	3
1.1.2 Linear temperature dependence of the in-plane resistivity	4
2 Basic electronic properties of CuO₂ plane	7
2.1 Band structure in LCAO approximation	8
2.2 Influence of strong s - d correlation on Cu site	18
2.3 BCS reduction	18
2.4 Pokrovsky theory of anisotropic gap superconductors	20
2.5 Calculation of T_c of CuO ₂ plane	22
2.6 Why the exchange amplitude J_{sd} can have antiferromagnetic sign	24
2.7 Short consideration of the unique properties CuO ₂ plane	27
3 Fermi liquids	30
3.1 Fermi liquid reduction and inter-layers electric field fluctuations	30
3.2 Zero sound for ferromagnetic sign of s - d exchange interaction	34
3.3 Fermi liquid behavior of overdoped cuprates	38
4 Solution of the kinetic equation and derivation of the conductivity	42
4.1 Re-scaling of energy	47
5 Discussion and conclusions	53
5.1 Psychoanalysis of the phenomenology	53
5.2 “In the beginning was the Hamiltonian, and the \hat{H} was by the God, and \hat{H} was the God.” Saint John (citation by memory)	53
5.3 Small quantum of history	54
5.4 Results	55
Bibliography	58

INTRODUCTION

It took almost 50 years between the experimental discovery of superconductivity to its theoretical explanation. Nowadays history repeats itself with high-temperature superconductivity; it's been more than 35 years since its discovery with no convincing theoretical candidate in sight despite that qualitative understanding has been already achieved [1]. One of the first proposed mechanism for cuprates was the extended Hubbard model between $\text{Cu}3d$ and $\text{O}2p$ states in the CuO_2 plane [2, 3], but it is still an open question whether the Hubbard model can quantitatively describe high temperature superconductivity [4]. Currently the t - J [5] and t - J - U [6] models are on the agenda of the theoretical studies [7] both of them descendants of the Hubbard model.

In this work the Shubin-Kondo-Zener s - d exchange interaction [8, 9, 10] with the Linear Combination of Atomic Orbitals (LCAO) Hamiltonian in the CuO_2 plane of optimally and overdoped cuprates is studied. Röhler for the first time noted that the $\text{Cu}4s$ - $3d_{x^2-y^2}$ hybridization seems to be the crucial quantum chemical parameter controlling related electronic degrees of freedom [11, 12]. The obtained results with s - d exchange interaction described here convincingly support this observation as they qualitatively agree with contemporary calculations and experiments.

For optimally doped and overdoped cuprates LCAO approximation for the electron bands [13] agrees with Local Density Approximation (LDA) band calculations [14, 15]. A remarkable property of the high-temperature superconducting hole doped cuprates is the correlation between the critical temperature T_c and the $\text{Cu}4s$ energy level discovered with LDA band calculations [16]. One of the results from this study qualitatively agrees with this correlation using one and the same calculated s - d exchange interaction.

This interaction is also used to calculate the anisotropy of the electron scattering rate and lifetime which again qualitatively agrees with the one observed by Angle Resolved Photoemission Spectroscopy (ARPES) experiments. This experimental technique has been widely used to study cuprates [17, 18, 19, 20, 21, 22, 23, 24, 25, 26, 27, 28, 29, 30, 31, 32] and for the observed scatter-

ing rate anisotropy the phenomenology of “hot spots” by Hlubina and Rice [33] and “cold spots” by Ioffe and Millis [34] on the Fermi surface was introduced. The regions with strong scattering and short lifetime are coined hot spots and the cold spots are the regions with the longest lifetime or the weakest scattering. This hot/cold spot phenomenology is applicable roughly speaking when cuprates demonstrate Fermi liquid behavior for optimally and overdoped regime.

Last but not least, for a ferromagnetic sign of the s - d exchange interaction a propagation of zero sound is predicted. Already for half a century different kinds of zero sound have been theoretically studied extensively and this topic continues to attract a great deal of interest within the scientific community. For instance, recent studies include two-dimensional zero-sound [35, 36] and shear [37] zero sound for p -type interaction [38]. We can finally conclude that except for ^3He thin films, two dimensional structures with large exchange interaction with ferromagnetic sign will soon become an interesting object for the realization of the old idea of Landau [39, 40].

As it is well known the basic superconducting state for overdoped cuprates is well described by a simple mean-field theory with a d -wave superconducting gap [41, 42]. The purpose of the present study is to describe the anisotropy of the lifetime of the normal charge carriers using the s - d exchange interaction which naturally explains gap anisotropy of the superconducting phase. The use of one and the same Hamiltonian, for both the normal and superconducting phase, is only the first step on the right track.

To summarize, using the LCAO method with the s - d exchange interaction two properties of the high- T_c cuprates are described: 1) the correlation of the $\text{Cu}4s$ energy level and T_c for the superconducting regime and 2) the anisotropy of the lifetime of charge carriers on the Fermi surface in the normal phase measured by ARPES experiments. In addition, the microscopic Hamiltonian leads to the prediction of zero sound propagation along the diagonals (“through the cold spots”), but only for ferromagnetic sign of the s - d exchange interaction, i.e. for non-superconducting cuprates.

After this extended review of the Hamiltonian used to explain the superconducting properties, in Sec. 3.1 we perform Fermi liquid reduction of the exchange s - d Hamiltonian and suggest a possible explanation of the phenomenology of “hot” and “cold” spots used to describe the normal properties of high- T_c cuprates. A short version of this study is given in Ref. [43] For a lateral illustration of the Fermi liquid theory we analyze in Sec. 3.2 the imaginary case of a layered perovskite which is not superconducting, but has ferromagnetic sign of the exchange amplitude J_{sd} . For such perovskites we predict propagation of zero sound; a short version of this study can be found in Ref. [44]. In Sec. 3.3 using the same Hamiltonian and notions we analyze Fermi liquid behavior of overdoped cuprates where Ohmic resistance is quadratic with temperature $\varrho_\Omega = A_\Omega T^2$. We calculate the coefficient A_Ω which is determined by s - d exchange interaction. The explicit formula for the scattering rate Eq. (123) in the Landau Fermi liquid theory for the Stoss-integral is the central result of the present study. We reproduced here the results of our short communications [43] and [44] in order to represent a complete and coherent picture of the normal and superconducting properties of high- T_c cuprates and to introduce a common system of notions and notations.

The main qualitative conclusion of the work is that the phenomenology of the normal properties can be derived from the s - d Hamiltonian used to describe the superconducting properties.

In the discussion and conclusion Chap. 5 we analyze: A) the motivation of the phenomenology, B) what compromises are necessary to build a coherent picture and C) we try to mention some seminal papers which in our opinion are important to create a complete mosaic. For a general review of the physics of cuprates we recommend the monograph by Plakida [45]. For the physics of metal-insulator transitions in transitional-metal oxides see the classical monograph by Mott [46, Chap. 6]. However, we wish to emphasise that our attention is concentrated on the overdoped cuprates with doping level far from the Mott transition.

1.1 Basic notions of the elementary kinetics

1.1.1 Transport cross-section of two dimensional coulomb scattering

Let us consider scattering by two dimensional Coulomb potential in a text-book style

$$U(r) = \frac{Ze^2}{r}, \quad r = |\mathbf{r}| = \sqrt{x^2 + y^2}, \quad e^2 \equiv \frac{q_e^2}{4\pi\epsilon_0}. \quad (1)$$

Our first step is to calculate the matrix elements between normalized plane waves

$$\begin{aligned} \psi_i(\mathbf{r}) &= \frac{1}{\sqrt{S}} e^{i\mathbf{P}_i \cdot \mathbf{r}/\hbar}, & \psi_f(\mathbf{r}) &= \frac{1}{\sqrt{S}} e^{i\mathbf{P}_f \cdot \mathbf{r}/\hbar}, \\ P &= P_i = P_f, & \mathbf{P}_f &= \mathbf{P}_i + \hbar\mathbf{K}, & \hbar K &= 2P \sin(\theta/2), \end{aligned} \quad (2)$$

where θ is the angle between the initial p_i and final p_f momentum. For the distances L_x and L_y we suppose periodic boundary conditions and $S = L_x L_y$. Using the well-known integral

$$\int_0^{2\pi} \frac{d\varphi}{a + b \cos(\varphi)} = \frac{2\pi}{\sqrt{a^2 - b^2}}, \quad (3)$$

after some regularization and analytical continuation for the Fourier transform we obtain

$$\left(\frac{1}{r}\right)_{\mathbf{K}} = \int \frac{1}{r} e^{-i\mathbf{K} \cdot \mathbf{r}} dx dy = \frac{2\pi}{K}, \quad (4)$$

and for the matrix elements between the initial and final states we have

$$U_{f,i} = \int \psi_f^*(\mathbf{r}) U(r) \psi_i(\mathbf{r}) dx dy = \frac{2\pi Z e^2}{2(P/\hbar) \sin(\theta/2) S}. \quad (5)$$

Then for the density of final states per unit angle for free particles $P_E \equiv \sqrt{2mE}$ we have

$$\rho_f(E) = \frac{1}{2\pi} \sum_{\mathbf{P}} \delta(E - E_{\mathbf{P}}) = \frac{1}{2\pi} \frac{S}{(2\pi\hbar)^2} \int_0^\infty \delta\left(\frac{P^2}{2m} - \frac{P_E^2}{2m}\right) d(\pi P^2) = \frac{mS}{(2\pi\hbar)^2}. \quad (6)$$

And for the flux of the probability of incoming electron we have the product of the velocity v and the density of the probability $1/S$ of a plane wave

$$j_i = \frac{V_i}{S}, \quad V_i = \frac{P}{m}. \quad (7)$$

According to the second Fermi golden rule for the cross-section with dimension length in 2D we derive

$$\sigma(\theta) = \frac{2\pi}{\hbar} |U_{f,i}|^2 \frac{\rho_f}{j_i} = \frac{\pi}{4\hbar} \frac{(Ze^2)^2}{VE \sin^2(\theta/2)}, \quad E = \frac{P^2}{2m} \quad (8)$$

and using $\sin^2(\theta/2) = \frac{1}{2} (1 - \cos(\theta))$ one can easily calculate the transport section

$$\sigma_{tr} = \int_0^\pi \sigma(\theta) (1 - \cos \theta) d\theta = \frac{\pi^2}{2\hbar} \frac{(Ze^2)^2}{VE}. \quad (9)$$

For the applicability of the Born approximation the effective charge $|Z| \ll 1$. In the next subsection we incorporate this cross-section in the formula for the temperature dependence of the resistivity.

1.1.2 Linear temperature dependence of the in-plane resistivity

The mean free path l , impurity concentration n_{imp} and transport section σ_{tr} are involved in the well-known relation

$$ln_{imp}\sigma_{tr} = 1 \quad (10)$$

which determines the electrical conductivity in the Drude formula which we apply to the 2D case

$$\frac{1}{\varrho} = \sigma_{Drude} = \frac{n_e q_e^2 \tau}{m}, \quad \tau = \frac{l}{V}, \quad \Gamma_C \equiv \frac{1}{\tau} = n_{imp} \sigma_{tr} V = \frac{\pi^2 (Ze^2)^2 n_{imp}}{2\hbar E}, \quad (11)$$

where Γ_C is the Columb scattering rate, τ is the mean free time, and ϱ is the resistivity of the 2D conductor with dimension Ω in SI units. For a general introduction of kinetics of metals, see Refs. [47, 48, 49, 50].

High- T_c cuprates are layered materials, but in order to evaluate the contribution of the classical fluctuation of the electric field between conducting 2D layers in Ref. [51] was analyzed a plane capacitor model for a $(\text{CuO}_2)_2$ bi-layer. Imagine that a 2D plane is divided in small squares (plaquettes) with a side equal to the Cu-Cu distance, the in-plane lattice constant a_0 and the distance between the planes (double or single) is d_0 . The capacity of the considered small capacitor

$$C = \varepsilon_0 \frac{a_0^2}{d_0}. \quad (12)$$

For the square of the fluctuation charge $Q = Zq_e$ of this plaquette the equipartition theorem [52, 53, 54] with temperature in energy units

$$\frac{\langle Q^2 \rangle_T}{2C} = \frac{T}{2} \quad (13)$$

gives

$$(Zq_e)^2 = \langle Q^2 \rangle = CT = \varepsilon_0 \frac{a_0^2}{d_0} T, \quad (14)$$

where for brevity from now on we omit the brackets $\langle \rangle_T$ denoting thermal averaging. The used here and in Ref. [51] is actually the Nyquist theorem [55, Eq. (78.3)]

$$(\mathcal{E}^2)_\omega = 2\hbar\omega R(\omega) / \tanh(\hbar\omega/2T), \quad (15)$$

where $(\mathcal{E}^2)_\omega$ is the spectral density of the voltage $\mathcal{E} = E_z c_0$ between CuO_2 planes with distance c_0 , E_z is thermally fluctuating electric field between conducting layers, $R(\omega) = c_0/a_0^2 \sigma_z(\omega)$ is the resistance between two plaquettes with area a_0^2 , and $\sigma_z(\omega)$ is the conductivity of the layered cuprate in the dielectric direction. As it was recently proved, the general Callen-Welton fluctuation-dissipation theorem can be considered as a consequence of the Nyquist theorem [56, 57, 58].

The calculated in such a way averaged square of the fluctuating charge $Z^2 = Q^2/q_e^2$ has to be substituted in the differential Eq. (8) or transport Eq. (9) cross-section. Additionally, for the area density of the “impurities” we have to substitute in the mean free path the density of the plaquettes $n_{\text{imp}} = 1/a_0^2$. At these conditions the Drude formula Eq. (98) gives for 2D resistivity per square of CuO_2 plane

$$4\pi\epsilon_0 \varrho = \frac{m^2 T}{8\hbar^3 n_e^2 d_0} \quad (16)$$

and the 2D dimensional conductivity $\sigma_{\text{Drude}}/4\pi\epsilon_0$ has dimension velocity. In Gaussian system $4\pi\epsilon_0 = 1$, but all equations in the present paper are system invariant. For a bulk material where separate bi-layers are at distance c_0 , the 3D resistivity parallel to the conducting planes ρ_{ab} can be evaluated as

$$4\pi\epsilon_0 \rho_{ab} = \frac{m^2 c_0}{8\hbar^3 n_e^2 d_0} T. \quad (17)$$

In short, the linear behavior of the resistivity reveals that in layered materials thermal fluctuations of electric field determine the density fluctuations. Electrons scatter on the fluctuation of their own density which in some sense is a self-consistent procedure. A slightly different realization of the same idea is described in Ref. [13, Chap. 8]. Analogously, the wave scattering of the sunlight by the density fluctuations of the atmosphere determines the color of the sky; who would be blind for the blue sky [51]? In a maximal traditional interpretation, resistivity of the layered high T_c cuprates is simply Rayleigh scattering of Fermi quasiparticles on the electron density fluctuations in a layered metal.

However, our formula for the scattering rate $\Gamma = 1/\tau$, Eq. (98) naturally explains an isotropic scattering which does not agree with the spectroscopic data. If we consider the energy in Eq. (98) to be equal to the Fermi one ϵ_F the formula for the cross-section Eq. (9) predicts negligible anisotropy if it is applied to the CuO_2 plane while ARPES (Angle Resolved Photo-Emission Spectroscopy) data [23, 59, 31] reveals remarkable anisotropy of $\Gamma(\varphi)$ when we rotate on angle φ around (π, π) -point i.e. the center of the hole pocket.

Analysis of the normal conductivity per square CuO_2 plane in some cuprates gives that $\sigma/4\pi\epsilon_0 \gg v_{\text{Bohr}} \equiv e^2/\hbar$. This leads that in CuO_2 plane we have well-defined quasiparticles

(in the sense of Landau) as it is confirmed by ARPES data in nodal direction. That not only Fermi liquid but even Fermi gas approach do not reveals an "enemy of working class" in sense of Kivelson and Fradkin [59, Chap. 15, page 583].

It is obvious that the Coulomb scattering is not the only mechanism for creation of the scattering rate Γ and Ohmic resistivity. The purpose of the present work is to take into account the s - d exchange interaction which creates the pairing in the superconducting phase.

In the next chapter we recall the generic 4-band model for the CuO_2 plane and Shubin-Kondo-Zener exchange interaction applied to this "standard model".

BASIC ELECTRONIC PROPERTIES OF CuO₂ PLANE

Ideas and notions of the Landau-Fermi liquid theory were widely used to analyze the properties of normal high- T_c cuprates [45]. See, for example, the early papers by Carrington et al. [60], Hlubina and Rice [33], Stojkovic and Pines [61], and Ioffe and Millis [34] and the recent review by Varma [62]. The large anisotropy in the scattering rate along the Fermi surface of these materials was reported for first time by Shen and Schrieffer [63] and later by Valla *et al.* [64]. The cornerstone of the Boltzmann equation analysis of carriers kinetics is the strong anisotropy of their charge lifetime τ_p along the Fermi contour. The central concepts here are the “hot spots” where close to $(\pi, 0)$ and $(0, \pi)$ regions of the Fermi contour the electron lifetime is unusually short and the angle Resolved Photoemission Spectroscopy (ARPES) spectral function is very broad [17, 18] suggesting strong scattering [34]. For contemporary ARPES studies see Ref. [31] and references therein. Ioffe and Millis [34] however emphasized that the concept of “cold spots” along the BZ where electron lifetime is significantly longer and ARPES data reveal well defined quasiparticle peak, suggesting relatively weak scattering, which increases rapidly along the Fermi contour moving away from “cold spots”. Recent research on the physics of hot and cold spots can be found in Refs. [27, 41, 65]. This hot/cold spot phenomenology is applicable roughly speaking when cuprates demonstrate Fermi liquid behavior for optimally and overdoped regime.

For optimally doped and overdoped cuprates the Linear Combination of Atomic Orbitals (LCAO) approach for the electron bands [13] agrees with Local Density Approximation (LDA) band calculations [14, 15]. A remarkable property of the high-temperature superconducting hole doped cuprates is the correlation between the critical temperature T_c and the Cu4s energy level obtained within LDA band calculations [16].

It took almost 50 years since the experimental discovery of superconductivity till its theoretical explanation. Nowadays history repeats itself with regard to high-temperature superconduc-

tivity; it's been more than 35 years since its experimental realization with no convincing theory in sight in spite the fact that qualitative understanding has been already achieved [1, 66]. One of the first proposed mechanisms for cuprates was based on the extended Hubbard model involving interaction between $\text{Cu}3d$ and $\text{O}2p$ states in the CuO_2 plane [2, 3], however, it is still an open question whether the Hubbard model can quantitatively describe high temperature superconductivity [4]. For the time being, the t - J [5] and t - J - U [6] models, both descendants of the Hubbard model, are on the agenda of theoretical studies [7].

In this work, we explore the properties of the Shubin-Kondo-Zener s - d exchange interaction [8, 9, 10] within LCAO Hamiltonian in the CuO_2 plane of optimally and overdoped cuprates. To this end, we take advantage of the observation that in $\text{Cu}4s$ - $3d_{x^2-y^2}$ hybridization seems to be the crucial quantum chemical parameter controlling related electronic degrees of freedom [11, 12]. Moreover, we describe the anisotropy of the lifetime of the normal charge carriers using the s - d exchange interaction, which naturally explains the gap anisotropy of the superconducting phase. The main advantage of this our approach is the use of one and the same Hamiltonian to describe both the normal and superconducting phase.

This work is organized as follows. We review briefly the basic electronic properties of the CuO_2 plane in Chap. 2 using (i) the band structure in LCAO approximation, (ii) the Shubin-Kondo-Zener s - d exchange interaction, (iii) BCS reduction of the exchange interaction and (iv) Pokrovsky theory of anisotropic gap superconductors to evaluate T_c of CuO_2 plane. in Sec. 3.1, we perform Fermi liquid reduction of the exchange s - d Hamiltonian and suggest a possible explanation of the phenomenology of “hot” and “cold” spots used to describe the normal properties of high- T_c cuprates. For an illustration of the Fermi liquid theory we analyze in Sec. 3.2 the case study of a nonsuperconducting layered perovskite involving a ferromagnetic J_{sd} . For these perovskites, we unveil the propagation of zero sound. In Sec. 3.3 using the same Hamiltonian and notions, we analyze Fermi liquid behavior of overdoped cuprates where the Ohmic resistance is quadratic in temperature $\varrho_\Omega = A_\Omega T^2$. We calculate the coefficient A_Ω which is determined by s - d exchange interaction. The explicit formula for the scattering rate in the Landau Fermi liquid theory for the Stoss-integral is the central result of the present study. The main qualitative conclusion of the present article is that the phenomenology of the normal properties can be derived from the s - d Hamiltonian, see Chap. 5.

2.1 Band structure in LCAO approximation

A general review of electron band calculations in cuprates is given by Pickett [67], here we use and interpolation scheme of the band structure convenient for theoretical treatment of the exchange interaction, see e.g. Ref. [13] for more details. LCAO method completely dominates in the intuitive picture in quantum chemistry and simple quantum calculations. In LCAO, we have a Hilbert space spanned by the valence orbitals. Here we wish to point out that LCAO was used by Abrikosov [68] in an attempt to explain the metal-insulator phase transition in CuO_2 . Applying

LCAO to a CuO_2 plane, we have

$$\begin{aligned}\hat{\psi}_{\text{LCAO},\alpha}(\mathbf{r}) = \sum_{\mathbf{n}} \bigg[& \hat{D}_{\mathbf{n},\alpha} \psi_{\text{Cu}3d_{x^2-y^2}}(\mathbf{r} - \mathbf{R}_{\text{Cu}} - a_0 \mathbf{n}) \\ & + \hat{S}_{\mathbf{n},\alpha} \psi_{\text{Cu}4s}(\mathbf{r} - \mathbf{R}_{\text{Cu}} - a_0 \mathbf{n}) \\ & + \hat{X}_{\mathbf{n},\alpha} \psi_{\text{O}2p_x}(\mathbf{r} - \mathbf{R}_{\text{O}_x} - a_0 \mathbf{n}) \\ & + \hat{Y}_{\mathbf{n},\alpha} \psi_{\text{O}2p_y}(\mathbf{r} - \mathbf{R}_{\text{O}_y} - a_0 \mathbf{n}) \bigg],\end{aligned}\quad (18)$$

where $\mathbf{n} = (\tilde{x}, \tilde{y})$ designates the elementary cell with integer 2D coordinates $\tilde{x}, \tilde{y} = 0, \pm 1, \pm 2, \pm 3, \dots$. In the elementary cell with constant a_0 we have for the coordinates of the Cu ion $\mathbf{R}_{\text{Cu}} = (0, 0)$, and for the oxygen ions in \tilde{x} - and \tilde{y} -direction we have $\mathbf{R}_{\text{O},x} = (\frac{1}{2}, 0) a_0$ and $\mathbf{R}_{\text{O},y} = (0, \frac{1}{2}) a_0$. We write the LCAO wave function in the second quantization assuming that the atomic amplitudes $\hat{D}_{\mathbf{n},\alpha}$, $\hat{S}_{\mathbf{n},\alpha}$, $\hat{X}_{\mathbf{n},\alpha}$, and $\hat{Y}_{\mathbf{n},\alpha}$ in front of the atomic wave functions identified by ψ are Fermi annihilation operators. For illustration, we consider atomic functions of neighboring atoms as orthogonal.

In the generic 4 orbitals and 4 band model we have to take single site energies ϵ_d , ϵ_s and ϵ_p and the transfer integrals between neighboring atoms t_{sp} , t_{pd} and t_{pp} . Starting from the coordinate space \mathbf{n} , we arrive at the momentum space symmetric Hamiltonian

$$H_{\text{LCAO}} = \begin{pmatrix} \epsilon_d & 0 & t_{pd}s_x & -t_{pd}s_y \\ 0 & \epsilon_s & t_{sp}s_x & t_{sp}s_y \\ t_{pd}s_x & t_{sp}s_x & \epsilon_p & -t_{pp}s_x s_y \\ -t_{pd}s_y & t_{sp}s_y & -t_{pp}s_x s_y & \epsilon_p \end{pmatrix}, \quad (19)$$

where

$$s_x = 2 \sin\left(\frac{1}{2}p_x\right), \quad s_y = 2 \sin\left(\frac{1}{2}p_y\right).$$

Here a remark is due: in electron band calculations the Coulomb repulsion is not neglected but only calculated in a self-consistent way. Roughly speaking, the Hubbard U is incorporated in the single-site energies and the experimental observation of the Fermi surface, by ARPES for example, is a small hint of the applicability of the self-consistent approach as initial approximation.

The dimensionless quasi-momenta or phases $0 \leq p_x, p_y \leq 2\pi$ belong to 2D Brillouin zone (BZ) and for the eigenfunctions we have

$$\Psi_{\mathbf{P}} = \begin{pmatrix} D_{\mathbf{P}} \\ S_{\mathbf{P}} \\ X_{\mathbf{P}} \\ Y_{\mathbf{P}} \end{pmatrix} = \begin{pmatrix} -\epsilon_s \epsilon_p^2 + 4\epsilon_p t_{sp}^2 (s_x + s_y) - 32t_{pp}\tau_{sp}^2 s_x s_y \\ -4\epsilon_p t_{sp} t_{pd} (s_x - s_y) \\ -(\epsilon_s \epsilon_p - 8\tau_{sp} s_y) t_{pd} s_x \\ (\epsilon_s \epsilon_p - 8\tau_{sp} s_x) t_{pd} s_y \end{pmatrix}, \quad (20)$$

where $\epsilon_s = \epsilon - \epsilon_s$, $\epsilon_d = \epsilon - \epsilon_d$, $\epsilon_p = \epsilon - \epsilon_p$, $\tau_{sp}^2 = t_{sp}^2 - \frac{1}{2}\epsilon_s t_{pp}$. The true quasi-momentum is given by $\mathbf{P} = \frac{\hbar}{a_0} \mathbf{p}$; the dimensionless variables simplify the complicated notations and provide

formulas convenient for numerical analysis. Moreover, the band wave functions Ψ_p have to be normalized. Let us mention also that we make use of the assumption that atomic wave functions of neighboring atoms as orthogonal thus neglecting atomic overlapping.

In terms of energy, the secular equation of the band Hamiltonian

$$\det(H_{\text{LCAO}} - \epsilon \mathbb{1}) = \mathcal{A}xy + \mathcal{B}(x + y) + \mathcal{C} = 0 \quad (21)$$

is a 4-degree polynomial having 4 zeros, say $\epsilon_{b,p}$, with band index $b = 1, 2, 3, 4$. For the coefficients in the secular equation (21), after some algebra, we obtain

$$\mathcal{A}(\epsilon) = 16(4t_{pd}^2 t_{sp}^2 + 2t_{sp}^2 t_{pp} \epsilon_d - 2t_{pd}^2 t_{pp} \epsilon_s - t_{pp}^2 \epsilon_d \epsilon_s), \quad (22a)$$

$$\mathcal{B}(\epsilon) = -4\epsilon_p(t_{sp}^2 \epsilon_d + t_{pd}^2 \epsilon_s), \quad (22b)$$

$$\mathcal{C}(\epsilon) = \epsilon_d \epsilon_s \epsilon_p^2. \quad (22c)$$

Introducing the auxiliary parameters

$$t = \frac{\mathcal{A}}{8} + \frac{\mathcal{B}}{4}, \quad t' = \frac{\mathcal{A}}{16}, \quad \eta = -\frac{\mathcal{A}}{4} - \mathcal{B} - \mathcal{C} \quad (23)$$

the secular equation (21) providing the profile of the Constant Energy Curve (CEC) that can be written in the convenient formula

$$\eta = -2t [\cos(p_x) + \cos(p_y)] + 4t' \cos(p_x) \cos(p_y). \quad (24)$$

This exact form with energy dependent coefficients inspired many theorists to approximate LCAO CEC for $\epsilon_p = \epsilon_F$ by expressions inherent to relatively simple tight binding models on a square lattice. However, this is related to the profile of CEC only at fixed energy and cannot be used to describe the whole energy dependence of the conduction band or calculation of the Fermi velocity. As a rough approximation for small transfer integrals, one uses the approximation

$$\mathcal{C} = \epsilon_d \epsilon_s \epsilon_p^2 \approx (\epsilon_p - \epsilon_d)(\epsilon_d - \epsilon_s)(\epsilon_d - \epsilon_p)^2 \quad (25)$$

and thus η can be considered as a linear function of the band energy ϵ_p .

On the other hand, the shape of the hole pocket can be experimentally observed by analysing ARPES data. Then, CEC curve passes through the points $\tilde{D} = (p_d, p_d)$ and $\tilde{C} = (\pi, p_c)$, where

$$x_d = \frac{-\mathcal{B} + \sqrt{\mathcal{B}^2 - \mathcal{A}\mathcal{C}}}{\mathcal{A}} = \sin^2\left(\frac{p_d}{2}\right), \quad x_c = -\frac{\mathcal{B} + \mathcal{C}}{\mathcal{A} + \mathcal{B}} = \sin^2\left(\frac{p_c}{2}\right).$$

The parameters x_c and x_d can be used to fit CEC to the experimental data introducing

$$\mathcal{A}_f = 2x_d - x_c - 1, \quad (27a)$$

$$\mathcal{B}_f = x_c - x_d^2, \quad (27b)$$

$$\mathcal{C}_f = x_d^2(x_c + 1) - 2x_c x_d, \quad (27c)$$

satisfying the equation

$$\mathcal{A}_f xy + \mathcal{B}_f (x + y) + \mathcal{C}_f = 0, \quad (27d)$$

with

$$\frac{\mathcal{A}_f}{\mathcal{B}_f} = \frac{\mathcal{A}}{\mathcal{B}} \Big|_{\varepsilon=\epsilon_F}.$$

The fitting parameters x_c and x_d can be used to compare the result of electron band calculations and photo-emission data [13]. For our further analysis, we introduce convenient formulae in different representations

$$\frac{t}{t'} = 2 + 4 \frac{\mathcal{B}_f}{\mathcal{A}_f}, \quad (28)$$

i.e. the ratio t'/t can be calculated from electron band structure obtained from ARPES data for the Fermi contour. For example, According to ARPES data for $\text{Bi}_2\text{Sr}_2\text{Cu}_1\text{O}_{6+\delta}$, Ref. [20] obtains $p_d = 0.82 \text{ rad}$ and $p_c = 0.129 \text{ rad}$, which gives for this cuprate $t'/t = 0.492$. Furthermore we refer also to the dimensionless parameters [16]

$$r \equiv \frac{1}{2(1+s)}, \quad s(\epsilon_F) \equiv \frac{(\epsilon_s - \epsilon_F)(\epsilon_F - \epsilon_p)}{(2t_{sp})^2}. \quad (29)$$

The secular LCAO equation (21) provides the opportunity to calculate CEC in the BZ analytically

$$p_y = \pm \arcsin \sqrt{y}, \quad 0 \leq y = -\frac{\mathcal{B}x + \mathcal{C}}{\mathcal{A}x + \mathcal{B}} \leq 1. \quad (30)$$

After performing diagonalization, the band Hamiltonian of the free charge carriers takes the standard form

$$\hat{H}'^{(0)} = \sum_{b,\mathbf{p},\alpha} (\varepsilon_{b,\mathbf{p}}, -\epsilon_F) \hat{c}_{b,\mathbf{p},\alpha}^\dagger \hat{c}_{b,\mathbf{p},\alpha} \quad (31)$$

where $\hat{c}_{b,\mathbf{p},\alpha}^\dagger$ are the Fermi creation operators for electron in band “b” with momentum \mathbf{p} and spin projection $\alpha = \pm \frac{1}{2}$. The change of the Fermi operators (32) is related to diagonalization of the single particle Hamiltonian $\hat{H}'^{(0)}$. After summation on the bands, momenta and spin projections, we can return from momentum representation to the real space lattice wave function

$$\hat{\Psi}_{\mathbf{n},\alpha} = \begin{pmatrix} \hat{D}_{\mathbf{n},\alpha} \\ \hat{S}_{\mathbf{n},\alpha} \\ \hat{X}_{\mathbf{n},\alpha} \\ \hat{Y}_{\mathbf{n},\alpha} \end{pmatrix} = \frac{1}{\sqrt{N}} \sum_{b,\mathbf{p}} e^{i\mathbf{p} \cdot \mathbf{n}} \begin{pmatrix} D_{b,\mathbf{p}} \\ S_{b,\mathbf{p}} \\ e^{i\varphi_x} X_{b,\mathbf{p}} \\ e^{i\varphi_y} Y_{b,\mathbf{p}} \end{pmatrix} \hat{c}_{b,\mathbf{p},\alpha}, \quad (32)$$

where the phases $\varphi_x = p_x/2$, $\varphi_y = p_y/2$ are chosen so that the band Hamiltonian (19) and its eigenfunctions (20) are real. Moreover, for the Fermi operators we have $\{\hat{c}_{b,\mathbf{p},\alpha}, \hat{c}_{b',\mathbf{p}',\alpha'}^\dagger\} = \delta_{bb'}$, $\delta_{\mathbf{p}\mathbf{p}'}\delta_{\alpha\alpha'}$, $\{\hat{D}_{\mathbf{n},\alpha}, \hat{D}_{\mathbf{n}',\alpha'}^\dagger\} = \{\hat{S}_{\mathbf{n},\alpha}, \hat{S}_{\mathbf{n}',\alpha'}^\dagger\} = \{\hat{X}_{\mathbf{n},\alpha}, \hat{X}_{\mathbf{n}',\alpha'}^\dagger\} = \{\hat{Y}_{\mathbf{n},\alpha}, \hat{Y}_{\mathbf{n}',\alpha'}^\dagger\} = \delta_{\mathbf{n}\mathbf{n}'}\delta_{\alpha,\alpha'}$, and

the other anti-commutators are identically zero. In (32) $N = N_x N_y$ designates the number of elementary cells subjected to periodic boundary conditions along x - and y -axes; we imagine that the CuO_2 plane lies over a torus with N_x and N_y plaquettes. The spectrum is calculated with the aid of the secular equation (21) and the eigenvalues ϵ_b , thus, we can calculate the corresponding band wave function $\Psi_{b,\mathbf{p}} = \Psi(\epsilon_{b,\mathbf{p}})$ given in Eq. (20) for every band and momentum.

Our first approximation in this problem of physics of metals is to take into account only the conduction d -band of the CuO_2 plane and to omit further in the summation the completely empty s -band or the completely filled oxygen $2p$ -bands. The band structure computed with the aid of the Newton method [13] is depicted in Fig. 1. The conduction d -band, shown in green, is the 3rd ($b = 3$) from the bottom and it is crossed by the dashed Fermi level. Hereafter, we will omit the band index in all expressions supposing that only the band $b = 3$ contributes the most.

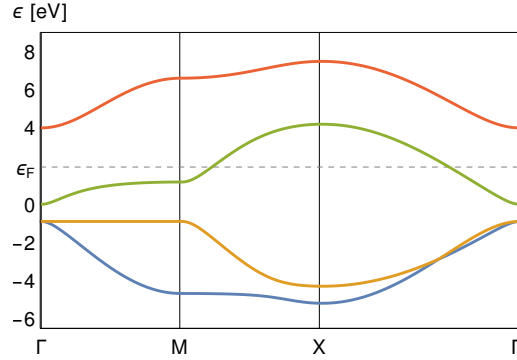


Figure 1: Energy bands $\epsilon_{\mathbf{p},b}$ of LCAO Hamiltonian (19) with input parameters $\epsilon_s = 4$ eV, $\epsilon_p = -0.9$ eV, $\epsilon_d = 0$ eV, $t_{sp} = 2$ eV, $t_{pp} = 0.2$ eV, $t_{pd} = 1.5$ eV, $f_h = 0.58$, $a_0 = 3.6$ Å and $T_c = 90$ K, chosen to be close to the values given in Refs. [14, 16]. The Fermi energy ϵ_F is given with dashed line. The labeled points in the quasi-momentum space are: $\Gamma = (0, 0)$, $M = (\pi, 0)$, $X = (\pi, \pi)$. The conduction $\text{Cu}3d_{x^2-y^2}$ band ($b = 3$) coincides in Γ point with the $\text{Cu}3d_{x^2-y^2}$ atomic level $\epsilon_d = 0$ which is chosen for the zero of the energy scale. We have two completely filled oxygen bands $b = 1, 2$ ($\epsilon_{\Gamma,1} = \epsilon_{\Gamma,2} = \epsilon_p$), and one completely empty $\text{Cu}4s$ band $b = 4$; $\epsilon_{\Gamma,4} = \epsilon_s$.

ϵ_s	ϵ_p	ϵ_d	t_{sp}	t_{pp} [69]	t_{pd}	f_h	a_0	T_c
4.0	-0.9	0.0	2.0	0.2	1.5	0.58	3.6 Å	90 K

Table 1: Single site energies ϵ and hopping amplitudes t and Fermi energy ϵ_F according to Eq. (38) of the LCAO Hamiltonian Eq. (19) in eV. The parameters values are chosen close to the ones given in Refs. [14, 16].

For the sake of simplicity, we can start with the $\text{Cu}3d_{x^2-y^2}$ level, $\epsilon_{\mathbf{p}}^{[0]} = \epsilon_d$, and apply several Newton iterations

$$\epsilon_{\mathbf{p}}^{[i+1]} = \epsilon_{\mathbf{p}}^{[i]} - \frac{\mathcal{A}xy + \mathcal{B}(x+y) + \mathcal{C}}{\mathcal{A}'xy + \mathcal{B}'(x+y) + \mathcal{C}'} \bigg|_{\epsilon=\epsilon_{\mathbf{p}}^{[i]}}. \quad (33)$$

Starting from the Γ point ($\epsilon(0, 0) = \epsilon_d$), we calculate the conduction band energy at some neighboring point in the momentum grid. The calculated in this way electron band structure is drawn in Fig. 1, cf. Ref. [13] where different parameters for the calculation were used. In such a way we can tabulate the energy $\epsilon_{\mathbf{p}}$ and further necessary $\chi_{\mathbf{p}} \equiv S_{\mathbf{p}} D_{\mathbf{p}}$ in a rectangular grid

$$\begin{aligned}
p_x &= \Delta p_x i_x, & i_x &= 0, \dots, N_x, & \Delta p_x &= \frac{2\pi}{N_x}, \\
p_y &= \Delta p_y i_y, & i_y &= 0, \dots, N_y, & \Delta p_y &= \frac{2\pi}{N_y}, \\
N_x &= 2K_x \gg 1, & N_y &= 2K_y \gg 1, \\
\epsilon_{\Gamma} &= \epsilon_{\text{bottom}} = \epsilon_{0,0} = \epsilon(0, 0) = \epsilon_d = 0, \\
\epsilon_{\text{M}} &= \epsilon_{\text{Van Hove}} = \epsilon_{0,\pi} = \epsilon_{\pi,0} = \epsilon(K_x, 0) = \epsilon(0, K_y), \\
\epsilon_{\text{X}} &= \epsilon_{\text{top}} = \epsilon_{\pi,\pi} = \epsilon(K_x, K_y).
\end{aligned} \tag{34}$$

Further we can use those tables for interpolation in arbitrary point of the momentum space \mathbf{q} in a rectangular grid, for example

$$\begin{aligned}
q_x &= \Delta p_x i, & i &= 0, \dots, M_x, & \Delta q_x &= \frac{2\pi}{M_x} \\
q_y &= \Delta p_y j, & j &= 0, \dots, M_y, & \Delta q_y &= \frac{2\pi}{M_y} \\
M_x &= 2L_x \gg N_x, & M_y &= 2L_y \gg N_y.
\end{aligned}$$

And further

$$\begin{aligned}
i_x &= \text{Int} \left(\frac{q_x}{\Delta p_x} \right), & c_x &= \frac{q_x}{\Delta p_x} - i_x \in (0, 1), \\
i_y &= \text{Int} \left(\frac{q_y}{\Delta p_y} \right), & c_y &= \frac{q_y}{\Delta p_y} - i_y \in (0, 1), \\
\epsilon_{\mathbf{q}} &\approx (1 - c_x)(1 - c_y) \epsilon(i_x, i_y) + c_x(1 - c_y) \epsilon(i_x + 1, i_y) \\
&\quad + (1 - c_x)c_y \epsilon(i_x, i_y + 1) + c_x c_y \epsilon(i_x + 1, i_y + 1),
\end{aligned} \tag{35}$$

and analogous bi-linear approximation for the hybridization function

The electron band velocity

$$v(\mathbf{p}) = \left| \frac{\partial \epsilon_{\mathbf{p}}}{\partial \mathbf{p}} \right|$$

of the conduction band is given in Fig. 2.

The behavior of the bilinear approximation for the hybridization function

$$\chi_{\mathbf{p}} \equiv S_{\mathbf{p}} D_{\mathbf{p}} \tag{36}$$

which is an important ingredient in our further consideration is shown in Fig. 3. Recall that the real dimensional quasimomentum is $\mathbf{P} = (\hbar/a_0) \mathbf{p}$. Moreover, we have to emphasize that the

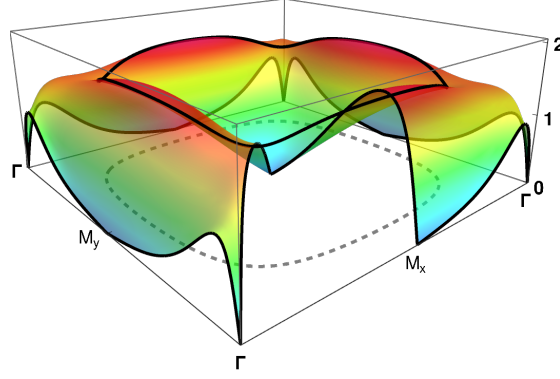


Figure 2: The velocity v_p of the conduction band as a function of quasi-momentum $p_x, p_y \in (0, 2\pi)$ with dimension energy and given in eV. The variable $V = (a_0/\hbar)v$ has dimension m/s. In the special points $\Gamma = (0, 0)$, $M = (\pi, 0)$, $X = (\pi, \pi)$ the band velocity is zero.

Coulomb interaction between the electrons is taken into account in a self-consistent way and we consider that the LCAO method is only an interpolation scheme of the local density band structure calculations. The inter-atomic transfer integrals and single site energies are the parameters of the named interpolation scheme.

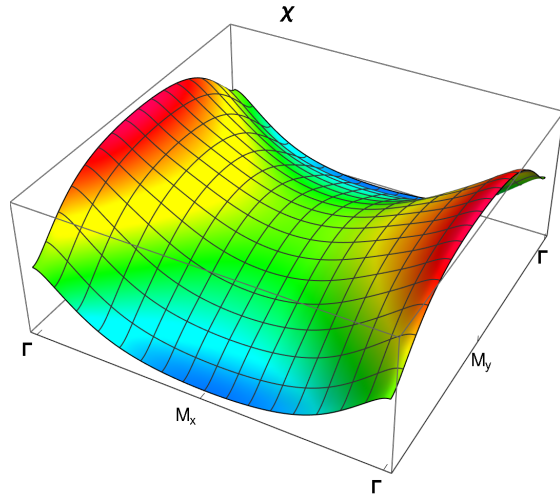


Figure 3: The hybridization function as function of quasi-momentum \mathbf{p} . This hybridization describes the amplitude electron from conduction $\text{Cu}3d_{x^2-y^2}$ band to be simultaneously $\text{Cu}4s$ electron.

From the canonical equation (21) for the spectrum, we easily derive the explicit equation for CEC

$$p_y(p_x; \epsilon) = \pm 2 \arcsin(\sqrt{y}). \quad (37)$$

The Fermi energy ϵ_F is determined by the hole filling factor, i.e. the relative area of the hole pocket S_p , and the area of the Brillouin zone $(2\pi)^2$, i.e.

$$f_h = \overline{\theta(\epsilon_{\mathbf{p}} - \epsilon_F)} = \frac{S_p}{(2\pi)^2}, \quad (38)$$

where the over-line stands for BZ averaging

$$\overline{F(\mathbf{p})} \equiv \int_0^{2\pi} \int_0^{2\pi} F(p_x, p_y) \frac{dp_x dp_y}{(2\pi)^2}. \quad (39)$$

In our brief review of the results of the electron properties of the CuO_2 plane it is also instructive to introduce the averaging on the Fermi surface $\epsilon_{\mathbf{p}} = \epsilon_F$; the Fermi contour in the 2D case

$$\langle f(\mathbf{p}) \rangle = \frac{\overline{f(\mathbf{p})\delta(\epsilon_{\mathbf{p}} - \epsilon_F)}}{\overline{\delta(\epsilon_{\mathbf{p}} - \epsilon_F)}}.$$

Averaging over the Fermi contour we introduce

$$\chi_{\text{av}} \equiv \exp \left\{ \frac{\langle \chi_{\mathbf{p}}^2 \ln |\chi_{\mathbf{p}}| \rangle}{\langle \chi_{\mathbf{p}}^2 \rangle} \right\} \quad (40)$$

and change of the normalization of the hybridization amplitude $\tilde{\chi} \equiv \chi/\chi_{\text{av}}$ whose averaging on the Fermi contour gives

$$\langle \tilde{\chi}_{\mathbf{p}}^2 \ln(\tilde{\chi}_{\mathbf{p}}^2) \rangle = 0. \quad (41)$$

The renormalized gap anisotropy is maximal in modulus amplitude in the pairing X-M direction

$$\tilde{\chi}_{\text{max}} = |\tilde{\chi}(p_x = p_c, p_y = \pi)|, \quad \epsilon = \epsilon_F. \quad (42)$$

Within these notations we introduce the effective mass of the charge carriers at the center of the hole pocket

$$\frac{1}{m_{\text{top}}} = -\frac{1}{E_0} \left. \frac{\partial^2 \epsilon_{\mathbf{p}}}{\partial p_x^2} \right|_{(\pi, \pi)}, \quad (43)$$

where

$$E_0 \equiv \frac{\hbar^2}{m_e a_0^2}.$$

Using the mass of the free electron, the introduced effective mass is dimensionless and E_0 is an energy parameter characterizing the CuO_2 plane.

Analogously we introduce the effective cyclotron mass m_c which for almost cylindrical in 3D Fermi surfaces is parameterized by the density of states per plaquette. According to the Shockley formula [55], we have

$$m_c = \frac{1}{2\pi m_e} \frac{d\mathcal{S}_P}{d\epsilon_F} = 2\pi E_0 \rho_F, \quad \mathcal{S}_P \equiv \frac{\hbar^2}{a_0^2} \frac{f_h}{(2\pi)^2}, \quad (44)$$

where m_e is the mass of the free electron, S_p is the area of the hole pocket in the quasi-momentum space \mathbf{P} , and m_c is again a dimensionless parameter.

Let's assume that in some space homogeneous high frequency vector-potential slightly changes all momenta of the electrons with an evanescent \mathbf{Q} . Therefore, we have $\mathbf{P} \rightarrow \mathbf{P} + \mathbf{Q}$ the total change of the electron energy ΔE (per plaquette) is parameterized by the reciprocal tensor of the effective optical mass, say m_{opt} ,

$$\begin{aligned}\Delta E &= 2 \sum_{\mathbf{p}} [\epsilon(\mathbf{p} + \mathbf{q}) - \epsilon(\mathbf{p})] \theta(\epsilon(\mathbf{p}) - \epsilon_F) \\ &= \mathbf{Q} \cdot \frac{N_e}{2m_e} \mathbf{m}_{\text{opt}}^{-1} \cdot \mathbf{Q}, \quad \mathbf{q} \equiv \frac{a_0}{\hbar} \mathbf{Q},\end{aligned}\quad (45)$$

where

$$N_e = 2 \sum_{\mathbf{p}} \theta[\epsilon(\mathbf{p}) - \epsilon_F]$$

is the total number of holes per plaquette and the factor 2 in front of momentum summation takes into account spin summation. In the brackets in Eq. (45) we recognize the second derivative, which in 2D space using the Gauss theorem for quadratic symmetry gives for the dimensionless optical mass

$$\frac{1}{m_{\text{opt}}} = \frac{\rho_F}{2E_0 f_h} \langle v^2 \rangle. \quad (46)$$

As a numerical test, if ϵ_F is slightly below ϵ_{top} , all masses are equal.

The optical mass of the hole pocket at $T = 0$ defined as

$$\frac{1}{m_{\text{opt}}} = \left\langle \frac{\partial^2 \epsilon_{\mathbf{p}}}{\partial P_x^2} \right\rangle \quad (47)$$

is an important ingredient of the Kubo single band sum rule [70] for the frequency dependent real part of the conductivity $\sigma_{xx}(\omega)$ we have [71, 72, 73]

$$\frac{q_e^2 n_h}{2m_{\text{opt}}} = \int_{-\infty}^{\infty} \sigma_{xx}(\omega) \frac{d\omega}{2\pi}. \quad (48)$$

Let c_0^{-1} be the density of CuO_2 planes in the c -direction, then the volume density of the holes reads

$$n_h = \frac{2f_h}{c_0 a_0^2}. \quad (49)$$

For $T \ll T_c$ all charge carriers are superconducting, $n_s = n_h$, and for the in-plane penetration depth we obtain

$$\frac{1}{\lambda_{ab}^2(0)} = \frac{q_e^2}{\varepsilon_0 c^2} \frac{a_0^2}{\hbar^2} \langle v^2 \rangle \nu_F, \quad \nu_F \equiv \frac{\rho_F}{a_0^2 c_0}. \quad (50)$$

To derive a general formula for finite temperatures $\lambda(0) \rightarrow \lambda(T)$ we have to regularize the Fermi surface averaging as follows [13]

$$\langle v^2 \rangle \rightarrow \left\langle v^2 r_d \left(\frac{\Delta_{\mathbf{p}}}{2T} \right) \right\rangle, \quad (51)$$

where

$$r_d(y) \equiv \left(\frac{y}{\pi} \right)^2 \sum_{n=0}^{\infty} \left[\left(\frac{y}{\pi} \right)^2 + \left(n + \frac{1}{2} \right)^2 \right]^{-3/2}. \quad (52)$$

Asymptotically we have

$$r_d(y) \approx 7\zeta(3) \left(\frac{y}{\pi} \right)^2 \quad \text{for } y \ll 1, \quad r_d(\infty) = 1.$$

In such a way we reveal how the results of the LCAO s - d approximation are incorporated into the standard theory of anisotropic gap BCS superconductors. The general formula for the tensor of the reciprocal squares of penetration depths reads [74]

$$\left(\frac{1}{\lambda^2(T)} \right)_{i,j} = \frac{q_e^2}{\varepsilon_0 c^2} 2\nu_F \langle V_i V_j r_d \rangle, \quad (53)$$

where ε_0^{-1} is an eccentric manner to write 4π in the good old system and $i, j = 1, 2, 3$. For clean superconductors and low temperatures $T \ll T_c$, $2m_{\text{opt}}$ is the effective mass of Cooper pairs, say m_{opt} is the mass of the superfluid charge carrier (per particle). This important for the physics of CuO_2 superconductors parameter is experimentally accessible by electrostatic charge modulation of thin superconducting films [75]. For such significant energy reduction unexplained broad maximum of mid infrared (MIR) absorption of CuO_2 plane finds natural interpretation as direct inter-band transition between the conduction $\text{Cu}3d_{x^2-y^2}$ band and the completely empty $\text{Cu}4s$ band. For more details on optical conductivity and spatial inhomogeneity of cuprate superconductors see e.g. the review Ref. [76].

For comparison of the results for the optical mass and penetration depth here we also give the conductivity $\sigma_{i,j}$ tensor in $\tau_{\mathbf{p}}$ approximation [50, 47]

$$\sigma_{i,j} = 2q_e^2 \nu_F \langle V_i V_j \tau_{\mathbf{p}} \rangle. \quad (54)$$

Here we wish to emphasize the significant discrepancy between optical mass of the conduction CuO_2 plane according to Table 2 and Ref. [75]. We do not exclude that all energy scales of the electron bands have to be re-examined. Another weak point of all electron band calculations is the very high position of the $\text{Cu}4s$ level. We consider $\epsilon_s \simeq 4\text{ eV}$ to be unusually high as the energy difference between the ground state level of the Cu atom $3d^{10}4s^1$ and the first excited level $3d^9 4s^2$ is (after multiplet fine structure averaging) $\Delta E \approx 1.5\text{ eV}$ is much smaller than all values of ϵ_s , which describe the energy difference between $\text{Cu}3d$ and $\text{Cu}4s$ levels; for atomic data see Ref. [77]. This difference is unlikely to be ascribed to influence of oxygen on the ligands.

After this long introduction of notions and notations, we calculate the matrix elements of the exchange interaction in the next section.

2.2 Influence of strong s - d correlation on Cu site

A reliable theory of CuO_2 plane must incorporate strong electron correlations. Two fermion terms describe self-consistent single particle motion. Strong correlations are fast processes which in the effective low-frequency Hamiltonians give four-fermion terms. Heitler-London 2-electron correlations in two atom molecules are perhaps the most famous example. Two electrons are newer in one at the same atom and in the second-quantization language we write down the 4-fermion Hamiltonian of the valence bound. However, magneto-chemistry, the physics of magnetism and perhaps the exchange mediated superconductivity is based on the proximity of $4s$ and $3d$ levels. There are no interesting magnetic properties for light elements before the group of iron. Shubin-Kondo-Zener s - d exchange interaction (or c - l exchange in the general case) is actually the most usual s - d exchange is described practically in all textbooks on condensed matter physics and physics of magnetism. It was introduced in the physics long time before the BCS theory. We write it in the lattice representation

$$\hat{H}_{sd} = -J_{sd} \sum_{\mathbf{n}, \alpha, \beta} \hat{S}_{\mathbf{n}\beta}^\dagger \hat{D}_{\mathbf{n}\alpha}^\dagger \hat{S}_{\mathbf{n}\alpha} \hat{D}_{\mathbf{n}\beta}; \quad (55)$$

one $\text{Cu}4s$ electron with spin α is annihilated in the lattice cell \mathbf{n} and resurrected with the same spin in the $\text{Cu}3d_{x^2-y^2}$ orbital. Simultaneously, one $\text{Cu}3d_{x^2-y^2}$ electron with spin β jumps without spin flip in the $\text{Cu}4s$ orbital. There is no charge transfer for this exchange process which we sum on all elementary cells \mathbf{n} .

The substitution here of the representation by momentum space operators Eq. (32) using the explicit eigenfunctions Eq. (20), the exchange Hamiltonian for the conduction band

$$\hat{H}_{sd} = -\frac{J_{sd}}{N} \sum_{\substack{\mathbf{p}' + \mathbf{q}' = \mathbf{p} + \mathbf{q} \\ \alpha, \beta}} S_{\mathbf{q}'} D_{\mathbf{p}'} \hat{c}_{\mathbf{q}'\beta}^\dagger \hat{c}_{\mathbf{p}'\alpha}^\dagger \hat{c}_{\mathbf{p}\alpha} \hat{c}_{\mathbf{q}\beta} S_{\mathbf{p}} D_{\mathbf{q}} \quad (56)$$

Let us remind that the band index $b = 3$ is omitted and we keep further only the conduction d -band. Next we perform a BCS reduction of this exchange Hamiltonian and after the success of the analysis of the description of the superconducting properties we later carry out a Fermi liquid reduction.

2.3 BCS reduction

If we wish to obtain a homogeneous in space order parameter with zero momentum in Hamiltonian (56), we have to perform the BCS reduction

$$\mathbf{p}' + \mathbf{q}' = \mathbf{p} + \mathbf{q} = 0, \quad \beta = -\alpha. \quad (57)$$

In other words, we create singlet Cooper pairs: creation of an electron with momentum \mathbf{p} and spin α with simultaneous creation of another electron with momentum $-\mathbf{p}$ and opposite spin

projection $\beta = -\alpha$, i.e. in the sum in the r.h.s of Eq. (56) we have to take into account only the terms with $\mathbf{q} = -\mathbf{p}$ and $\beta = -\alpha$. Analogously for creation without spin flip we have to take only terms with $\mathbf{q}' = -\mathbf{p}'$. Formally this initial reduction can be represented by insertion of δ -functions in the summand in Eq. (56), i.e.

$$\begin{aligned}\hat{c}_{\mathbf{q}'\beta}^\dagger \hat{c}_{\mathbf{p}'\alpha}^\dagger \hat{c}_{\mathbf{p}\alpha} \hat{c}_{\mathbf{q}\beta} &\rightarrow \delta_{\mathbf{q}'+\mathbf{p}',0} \delta_{\mathbf{q}+\mathbf{p},0} \delta_{\beta,\bar{\alpha}} \hat{c}_{\mathbf{q}'\beta}^\dagger \hat{c}_{\mathbf{p}'\alpha}^\dagger \hat{c}_{\mathbf{p}\alpha} \hat{c}_{\mathbf{q}\beta} \\ &\rightarrow \delta_{\mathbf{q}',-\mathbf{p}'} \delta_{\mathbf{q},-\mathbf{p}} \delta_{\beta,\bar{\alpha}} \left(\delta_{\alpha,+} \hat{B}_{\mathbf{p}'} \hat{B}_{\mathbf{p}} + \delta_{\alpha,-} \hat{B}_{-\mathbf{p}'} \hat{B}_{-\mathbf{p}} \right),\end{aligned}$$

where

$$\hat{B}_{\mathbf{p}} \equiv \hat{c}_{-\mathbf{p},-} \hat{c}_{\mathbf{p},+}.$$

Whence, the reduced BCS Hamiltonian can be written as

$$\hat{H}_{\text{BCS}} = \frac{1}{N} \sum_{\mathbf{p},\mathbf{p}'} \hat{B}_{\mathbf{p}'}^\dagger f(\mathbf{p}, \mathbf{p}') \hat{B}_{\mathbf{p}}, \quad (58)$$

with

$$f(\mathbf{p}, \mathbf{p}') \equiv -2J_{sd}\chi_{\mathbf{p}}\chi_{\mathbf{p}'}. \quad (59)$$

The multiplier 2 stems from the summation on α . We partially follow the notations from 9-th volume of Landau Lifshitz course of theoretical physics [55] in order to emphasize that the only difference is the χ factors in the reduced Hamiltonian.

Using the Bogolyubov transformation

$$\begin{aligned}\hat{c}_{\mathbf{p}+} &= u_{\mathbf{p}} \hat{b}_{\mathbf{p}+} + v_{\mathbf{p}} \hat{b}_{-\mathbf{p},-}^\dagger, & u_{-\mathbf{p}} &= u_{\mathbf{p}}, \\ \hat{c}_{\mathbf{p}-} &= u_{\mathbf{p}} \hat{b}_{\mathbf{p}-} - v_{\mathbf{p}} \hat{b}_{-\mathbf{p},+}^\dagger, & v_{-\mathbf{p}} &= v_{\mathbf{p}},\end{aligned}$$

with $u_{\mathbf{p}}$ and $v_{\mathbf{p}}$ the parameters the Bogolyubov rotation $u_{\mathbf{p}}^2 + v_{\mathbf{p}}^2 = 1$ and the new Fermi operators $\hat{b}_{\mathbf{p}}$. The BCS self-consistent approximation yields

$$\langle B_{\mathbf{p}}^\dagger \hat{B}_{\mathbf{p}'} \rangle \approx \langle B_{\mathbf{p}}^\dagger \rangle \langle \hat{B}_{\mathbf{p}'} \rangle,$$

thus using

$$n_{\mathbf{p}+} = n_{\mathbf{p}-} \equiv n_{\mathbf{p}} = \langle \hat{b}_{\mathbf{p}-}^\dagger \hat{b}_{\mathbf{p}-} \rangle = \langle \hat{b}_{\mathbf{p}+}^\dagger \hat{b}_{\mathbf{p}+} \rangle,$$

we get

$$\langle B_{\mathbf{p}}^\dagger \rangle = \langle B_{\mathbf{p}} \rangle = u_{\mathbf{p}} v_{\mathbf{p}} (1 - n_{\mathbf{p}+} - n_{\mathbf{p}-}).$$

Finally, for the averaged interaction energy we have the standard functional $E_{\text{BCS}}(\{u_{\mathbf{p}}\}, \{n_{\mathbf{p}}\}) = \langle \hat{H}_{\text{BCS}} \rangle$. The non-interacting part of the Hamiltonian $\langle \hat{H}^{(0)} \rangle$ has the same form as in Ref. [55].

Minimization of the variational energy first with respect of $u_{\mathbf{p}}$ and taking into account that

$$n_{\mathbf{p}} = \frac{1}{\exp(E_{\mathbf{p}}/T) + 1}, \quad (60)$$

the Fermi distribution gives the standard equation for the superconducting gap $\Delta_{\mathbf{p}}$ in cuprates, i.e.

$$2J_{sd} \frac{\chi_{\mathbf{p}}^2}{2E_{\mathbf{p}}} \tanh\left(\frac{E_{\mathbf{p}}}{2T}\right) = 1, \quad (61)$$

where

$$E_{\mathbf{p}} = \sqrt{\eta_{\mathbf{p}}^2 + \Delta_{\mathbf{p}}^2}, \quad \eta_{\mathbf{p}} = \epsilon_{\mathbf{p}} - \epsilon_F, \quad \Delta_{\mathbf{p}} = \Xi(T) \chi_{\mathbf{p}}.$$

The occurrence of the BCS spectrum for cuprates was analyzed in the review [78]. In the next section we recall the main results of the Pokrovsky theory [79, 80] for the thermodynamics of anisotropic gap superconductors.

2.4 Pokrovsky theory of anisotropic gap superconductors

The s - d exchange interaction is localized in a single transition ion in elementary cell which automatically gives separable kernel of the BSC gap equation

$$V_{\mathbf{q},\mathbf{p}} \equiv f(\mathbf{q}, \mathbf{p}) = -2J_{sd}\chi_{\mathbf{q}}\chi_{\mathbf{p}}. \quad (62)$$

At the Fermi surface we have

$$\langle V_{\mathbf{q},\mathbf{p}}\chi_{\mathbf{p}} \rangle_{\mathbf{p}} = -V_0\chi_{\mathbf{q}}, \quad (63)$$

where $V_0 = 2J_{sd}\langle\chi^2\rangle$ is the eigenvalue of the interaction kernel. In the general case the BCS gap equation reads

$$\Delta_{\mathbf{q}} = \overline{V_{\mathbf{q},\mathbf{p}} \frac{\Delta_{\mathbf{p}}}{E_{\mathbf{p}}} \tanh\left(\frac{E_{\mathbf{p}}}{2T}\right)}. \quad (64)$$

Yet the separability of the kernel reduces the equation above to the problem described by Eq. (61).

The general consideration by Pokrovsky reveals that in the BCS weak coupling limit we have to solve the corresponding eigenvalue problem and to use the maximal in modulus eigenvalue V_0 . The LCAO s - d approximation simply gives us a text-book example of the Pokrovsky theory for the anisotropic gap superconductors.

Inspired by Euler and Mascheroni definition for the popular constant we introduce a new notion, namely the Euler-Mascheroni energy of the gap anisotropy

$$E_C \equiv \lim_{\epsilon \rightarrow 0} \left[\epsilon \exp \left\{ \frac{\theta(|\eta_{\mathbf{p}}| - \epsilon) \chi_{\mathbf{p}}^2 / |\eta_{\mathbf{p}}|}{2\langle\chi^2\rangle\rho_F} \right\} \right]. \quad (65)$$

Introduced in such a way the Euler-Mascheroni energy is a convenient notion to describe the BCS properties of superconductors with 4-fermion (two particle) interaction. Within the so introduced notations we use the well-known BCS formulas for the critical temperature

$$T_c = \frac{2\gamma}{\pi} E_C \exp\left(-\frac{1}{\lambda}\right), \quad (66)$$

where the BCS coupling parameter

$$\lambda \equiv V_0 \rho_F = 2J_{sd} \langle \chi^2 \rangle \rho_F, \quad V_0 \equiv 2J_{sd} \langle \chi^2 \rangle, \quad (67)$$

the order parameter at zero temperature

$$\tilde{\Xi}(0) = 2E_C \exp\left(-\frac{1}{\lambda}\right), \quad \frac{2\tilde{\Xi}(0)}{T_c} = \frac{2\pi}{\gamma} \approx 3.53, \quad (68)$$

and the superconducting gap

$$\Delta_{\mathbf{p}}(T) = \tilde{\Xi}(T) \tilde{\chi}_{\mathbf{p}} = \Xi(T) \chi_{\mathbf{p}}. \quad (69)$$

that is factorizable function of the temperature and momentum.

In the original works by Pokrovsky [79, 80] the factorizable order parameter and separable approximation of the pairing kernel are results of the weak coupling BCS approximation, but for our Hamiltonian it is an immanent property. Then for the maximal gap at zero temperature and the jump of the [heat capacity](#) at the critical temperature the result by Pokrovsky reads [13]

$$\frac{2\Delta_{\max}}{T_c} = \frac{2\pi}{\gamma} \frac{|\chi|_{\max}}{\chi_{\text{av}}}, \quad \frac{\Delta C}{C_n(T_c)} = \frac{12}{7\zeta(3)} \frac{\langle \chi_{\mathbf{p}}^2 \rangle^2}{\langle \chi_{\mathbf{p}}^4 \rangle}. \quad (70)$$

Perhaps the most important ingredient for the thermodynamics is the Pokrovsky equation for the temperature dependence of the order parameter

$$\ln \frac{\tilde{\Xi}(0)}{\tilde{\Xi}(T)} = 2 \langle \tilde{\chi}_{\mathbf{p}}^2 I(\tilde{\Xi}(T) \tilde{\chi}_{\mathbf{p}}/T) \rangle, \quad (71)$$

with

$$I(u) \equiv \int_0^\infty \frac{dx}{\sqrt{u^2 + x^2} [\exp(\sqrt{u^2 + x^2}) + 1]}.$$

The brackets $\langle \dots \rangle_{\text{F}}$ here denote averaging on the Fermi contour. Note that the only difference between the isotropic BCS model is given by the χ -factors.

The result for the temperature dependence of the superconducting gap Eq. (71) for anisotropic superconductors is derived by Pokrovsky [79, 80] in the early BCS epoch. The CuO₂ plane

gives a simple analytical example of the gap anisotropy which for qualitative purposes can be approximated by

$$\chi_{\mathbf{p}} \simeq \frac{t_{sp}t_{pd}}{(\epsilon_s - \epsilon_d)(\epsilon_d - \epsilon_p)} \cos(2\theta), \quad \epsilon_F \approx \epsilon_d, \quad (72)$$

where θ is the angle along the Fermi contour. The sequence of the perturbation theory denominators reveals that in first order the d -electron becomes p -one and only in the second order perturbation theory p -electron obtain s -amplitude necessary to be involved in the s - d interaction. In short we follow the $3d$ -to- $4s$ -by- $2p$ highway to superconductivity [81] where the s - d interaction was proposed as pairing

Finally, as a test example of the used approach we rewrite $\chi_{\mathbf{p}}$ for the phonon model

$$\chi_{\mathbf{p}} = \theta(E_C - |\eta_{\mathbf{p}}|), \quad E_C = \hbar\omega_D, \quad \omega_D = \sqrt{\frac{K}{M}} \quad (73)$$

for which the Euler-Mascheroni E_c energy is nothing but the Debye energy $\hbar\omega_D$. This statement reveals the applicability criterion of the BCS theory $\exp(-1/\lambda) \ll 1$ which gives the condition $T_c/E_C \ll 1$ which is perfectly satisfied according to the results presented in Table 2. For the exchange mediated superconductors the reader may consult Ref. [82].

Now we can continue with technical details for application of the Pokrovsky theory for anisotropic superconductors for LCAO s - d approximation applied to the CuO_2 plane.

2.5 Calculation of T_c of CuO_2 plane

Our first task is to calculate the exchange amplitude J_{sd} supposing that for a 90 K superconductor LCAO electron band parameters are determined by the fit to band calculations, for example. According to Eq. (61) the reciprocal exchange integral can be expressed by momentum integration

$$\frac{1}{J_{sd}} = I_{\text{sum}} \equiv \overline{\frac{\chi_{\mathbf{p}}^2}{\eta_{\mathbf{p}}} \tanh\left(\frac{\eta_{\mathbf{p}}}{2T_c}\right)}. \quad (74)$$

The behavior of the integrand is depicted in Fig. 4 at higher temperature $T = 300$ K in order for a sharp function to be visible. To evaluate the integral in Eq. (74), we split the integration interval into three sections. The narrow first domain corresponds to $\epsilon_a \gg T_c$ (with $\epsilon_a = 5 T_c$), where the density of states can be taken as constant. Simultaneously, we suppose that $\epsilon_a \ll \epsilon_b \sim (\epsilon_F - \epsilon_{\text{Van Hove}})/2$, i.e. the energy parameter is much smaller than the typical band energies, for example, the distance between the Fermi level and the energy of the Van Hove $\epsilon_{\text{Van Hove}} \equiv \epsilon_M \epsilon_0, \pi$. The second energy parameter ϵ_b ensures that topology will not be changed in the intermediate energy interval. In short, the integral in Eq. (74) can be represented by a sum of three integrals, i.e. $I_{\text{sum}} = I_a + I_{ab} + I_b$.

For the first integral assuming that density of states is almost equal, using the well known integral limit

$$\lim_{M \rightarrow \infty} \left(\int_0^M \frac{\tanh x}{x} dx - \ln M \right) = \ln \left(\frac{4\gamma}{\pi} \right) \quad (75)$$

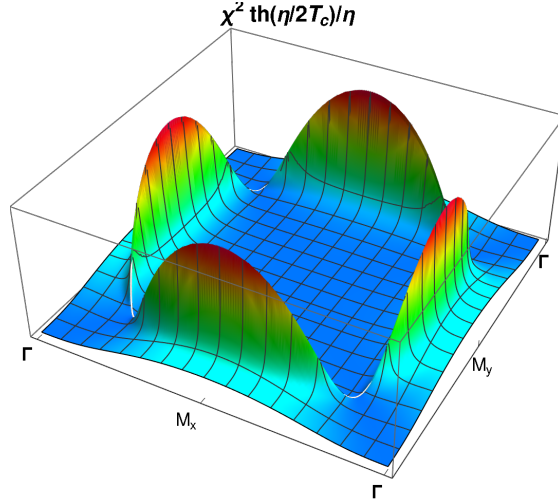


Figure 4: The integrand of the equation Eq. (74) for the critical temperature drawn at 300 K.

Table 2: Output parameters of our numerical calculation, the extra numbers are only for a numerical test. The new quantities are the values of the s - d exchange amplitude J_{sd} and the effective masses derived from the parameters of electron band calculations [16]. The value of $\tilde{\chi}_{\max} = 1.167$ is within 10% accuracy of its theoretical value for a pure d -wave gap with isotropic Fermi velocity $2/\sqrt{e} = 1.213$.

$E_C = 1.928$ eV	$\lambda = 0.177$	$m_{\text{top}} = 0.839$
$\epsilon_F = 1.851$ eV	$\tilde{\chi}_{\max} = 1.167$	$m_c = 0.931$
$\epsilon_M = 1.167$ eV	$\langle \chi^2 \rangle = 0.065$	$m_{\text{opt}} = 0.890$
$\epsilon_X = 4.193$ eV	$\langle \chi^2 \rangle^2 / \langle \chi^4 \rangle = 0.737$	$r = 0.365$ eV
$E_0 = 0.528$ eV	$\rho_F = 0.281$ eV $^{-1}$	$2/\sqrt{e} = 1.213$
$J_{sd} = 7.230$ eV	$2\Delta_{\max}/T_c = 4.116$	$V_0 = 0.940$ eV

we obtain after energy integration

$$I_a = \theta(\epsilon_a - |\eta_p|) \frac{\chi_p^2}{\eta_p} \tanh\left(\frac{\eta_p}{2T_c}\right) \approx 2\langle \chi^2 \rangle \rho_F \ln\left(\frac{2\gamma\epsilon_a}{\pi T_c}\right). \quad (76)$$

For the rest of the momentum space when $\epsilon_a \gg 2T_c$ we use the $\tanh(\epsilon_a/2T_c) \approx 1$ approximation and for the second integral we obtain

$$I_{ab} = \theta(\epsilon_a < |\eta_p| < \epsilon_b) \frac{\chi_p^2}{\eta_p} \tanh\left(\frac{\eta_p}{2T_c}\right) \approx \int_{\epsilon_a}^{\epsilon_b} \left[\langle \chi^2 \rangle \rho|_{(\epsilon_F - \eta)} + \langle \chi^2 \rangle \rho|_{(\epsilon_F + \eta)} \right] \frac{d\eta}{\eta} \approx 2 \ln\left(\frac{\epsilon_b}{\epsilon_a}\right) \langle \chi^2 \rangle \rho_F, \quad (77)$$

where for the last approximation we suppose constant density of states. If $\epsilon_b = \epsilon_a$ this second integral is annulled. The third integral

$$I_b = \theta(|\eta_p| - \epsilon_b) \frac{\chi_p^2}{|\eta_p|} \quad (78)$$

is simply an energy integration far from the Fermi energy. Supposing that ϵ_a is almost zero i.e. much smaller than the band parameters, we recognize the Euler-Mascheroni energy Eq. (65)

$$\ln \epsilon_a + \theta(|\eta_p| - \epsilon_a) \frac{\chi_p^2}{\eta_p} (2\langle\chi^2\rangle\rho_F)^{-1} \approx \ln E_C. \quad (79)$$

The numerical integration here can be performed by a Riemann sum of the bi-linear approximation of the integrand functions. As a result the summary integral can be expressed as

$$I_{\text{sum}} \approx 2\langle\chi^2\rangle\rho_F \left[\ln \left(\frac{2\gamma}{\pi T_c} \right) + \ln E_C \right]$$

and finally after substitution in Eq. (74) we arrive at Eq. (66).

The most important ingredient of the BCS formula for the critical temperature T_c is the BCS coupling constant λ defined by Eq. (67). On the other hand, Pavarini *et al.* [16] observed a remarkable correlation between their range parameter $r(\epsilon_F)$ defined by Eq. (29) and the critical temperature T_c . What is hidden in this band trend correlation? Emphasizing the importance of this empirical correlation Patrick Lee pointed out that it is not a simple task for the theory [59, *t-J* Model and Gauge Theory Description of Underdoped Cuprates]. For the application of *t-J* model in the physics of high- T_c cuprates see also the reviews by Spalek [5], P. Lee [83] and Livelong [84].

The range parameter $r(\epsilon_F)$ defined by Eq. (29) is also almost linear function of the ratio t'/t Eq. (28) as shown in Fig. 5.

On the other hand, the dimensionless BCS coupling constant defined in the present article by Eq. (67) is exactly linear function of the t'/t Eq. (28) ratio depicted in Fig. 6. In such a way the Pavarini *et al.* [16] T_c - r correlation we redraw in Fig. 7, reveals correlation between the critical temperature T_c and the BCS coupling constant λ according the well-known BCS formula Eq. (66). In short, Pavarini *et al.* [16] empirically discovered the BCS correlation between the coupling constant and the critical temperature. We express our respect of this indirect confirmation of the BCS theory obtained by observation of correlations between the shape of the Fermi contours and critical temperatures of hole doped cuprates. This is a result of a huge volume of electron band calculations. In the next section we try qualitatively to interpret this result.

2.6 Why the exchange amplitude J_{sd} can have antiferromagnetic sign

In our work the exchange amplitude J_{sd} is just a parameter of the theory which can be determined to fit to one experiment and then to be used to predict the results of many others. Actually the *s-d*

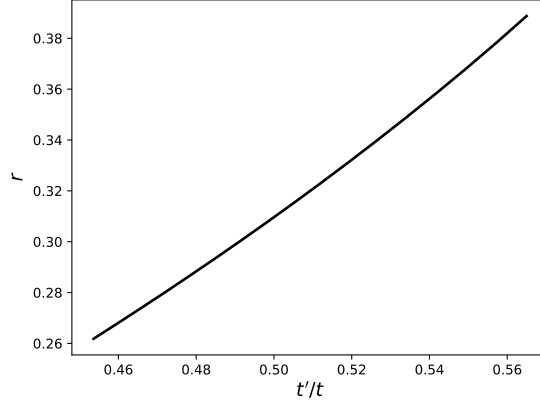


Figure 5: Almost linear dependence between range parameter $r(\epsilon_F)$ Eq. (29) and the ratio t'/t Eq. (28). These parameters are introduced in Ref. [16].

interaction was introduced by Schubin and Wonsovsky and later by Zener long time before some *ab initio* calculations to give even a small chance for reliable calculation. However, the Kondo effect gave the proof that in many cases J_{sd} can have antiferromagnetic sign. Let suppose for a while that we have Coulomb repulsion only in one Cu ion. In this case we have a single impurity Anderson model [85]. Let us try to adapt a well-known from the textbooks formula by White and Geballe [86, Eq. (7.17)] for CuO_2 plane. Starting from the notations from these books we try to trace an analogy making the replacement

$$J = 2 |V_{0\mathbf{k}_F}|^2 \frac{U}{E_0(E_0 + U)} \quad (80)$$

$$\rightarrow -J_{sd} \simeq 2 |t_{pd}|^2 \frac{U_{dd}}{(\epsilon_d - \epsilon_F)[(\epsilon_d - \epsilon_F) + U_{dd}]}.$$

Even for infinite Hubbard repulsion in $\text{Cu}_3d_{x^2-y^2}$ we have finite antiferromagnetic sign for the Kondo interaction. Then we should admit that for an array or lattice of transition Cu ions the result could be qualitatively the same. The theory of Kondo arrays and lattices is an intensive topic of contemporary researches [87, 88, 89, 90] and we are just waiting a CuO_2 oriented study to be performed. There is perhaps no need of more apology. As in mathematical physics many theorists consider negative U Hubbard model, we following Kondo do have antiferromagnetic J_{sd} . If the phenomenology is successful, *ab initio* consideration will not come with substantial delay.

Up to now we can only conclude that LCAO projection of electron degree of freedom works successfully and we put the calculation of J_{sd} in the agenda of condensed matter physics. First considerations of the J_{sd} calculations from first principles will be only qualitative, the development of the atomic physics is an excellent example for such a scenario. The only one reliably

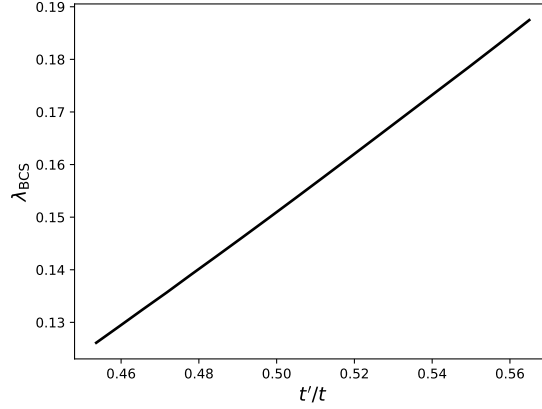


Figure 6: This non-interesting straight line (within the accuracy of the numerical calculation) represents the relation between the BCS coupling constant λ defined in Eq. (67) admitting common J_{sd} given in Table 2 for all cuprates and the ratio of the tight binding parameters t'/t calculated in Eq. (28) where Eq. (22) is substituted. It is well-known according to Eq. (66) that λ has the main influence on the critical temperature T_c . The complicated integral representing $\langle \chi^2 \rangle \rho_F$ with analytical expression Eq. (36) substituted in Fermi contour averaging gives little hope for an analytical solution. In such a way we have only the graphical solution that BCS coupling constant λ is in good approximation linear function of the t'/t parameter determining the shape of the Fermi surface; for both variables we derived complicated explicit expressions Eq. (28) and Eq. (66) exact in the used LCAO approximation for electronic the band structure.

calculated single electron hopping is between

$$t = 2 \frac{\hbar^2}{m_e a_B^2} R \exp(-R - 1), \quad R = \frac{r}{a_B} \quad (81)$$

between 2 protons in the H_2^+ ion [91], where r is the distance between protons and a_B is the Bohr radius, and m_e is the mass of the free electron. This is the well-known result by Landau [91, Sec.61] and Herring [92] The second one is the two-electron exchange in the Hydrogen quasi-molecule considered by Herring and Flicker [93]

$$J = 1.64 \frac{\hbar^2}{m_e a_B^2} R^{5/2} \exp(-R). \quad (82)$$

Before these two old problems to become a part of the solid state physics, it is premature to calculate quantitatively exchange parameters but qualitative consideration is one indispensable first step.

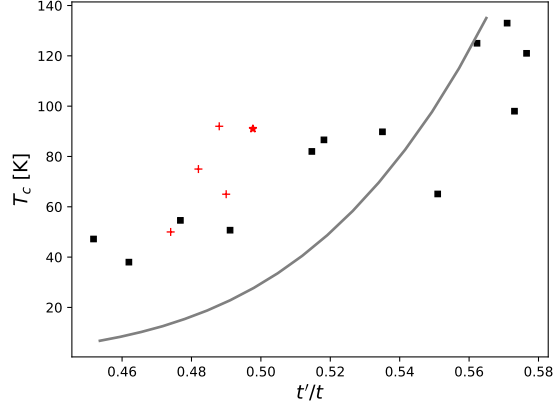


Figure 7: Pavarini *et al.* [16] (■) correlation between the critical temperature T_c and t'/t which is almost linear function of their range parameter $r(\epsilon_F)$ drawn in Fig. 5, The t'/t parameter itself is exactly a linear function of the BCS coupling parameter λ supposing constant J_{sd} in Fig. 6. According to our traditional BCS interpretation (solid line) this band-structure trend describes T_c - λ correlation for the s - d exchange amplitude J_{sd} approximately equal for all cuprates. With (★) we have included ARPES data by Zonno *et al.* [32, Fig. 5c] and Ref. [24] for which $p_c = 0.589$ rad, and $p_d = 1.155$ rad and with (+) ARPES data from Vishik *et al.* [26] for underdoped Bi-2212.

2.7 Short consideration of the unique properties CuO_2 plane

Close to the winter solstice or two moons later *Homo sapiens* exchange season greetings. But in the spring there is another, even bigger occasion for season greetings related to triple coincidence which we are going to consider qualitatively.

The conduction band in the cuprate plane CuO_2 can be considered as the energy of atomic $\text{Cu}3d_{x^2-y^2}$ level smeared by the transition amplitudes between neighboring ions. In this sense we can say that the single conduction band is a $\text{Cu}3d$ band. However, the pairing exchange interaction is between $\text{Cu}3d$ and $\text{Cu}4s$ states in every Cu ion. But what is necessary for the band electron function with momentum \mathbf{p} to have significant $\text{Cu}4s$ component $S_{\mathbf{p}}$ according to Eq. (20)? The qualitative analysis is transparent in the model case if all inter-ionic transfer amplitudes are much smaller than the differences between the atomic levels. In this case the Fermi energy of the almost half filled $\text{Cu}3d$ band is approximately equal to the atomic level $\epsilon_F \approx \epsilon_d$ and $D_{\mathbf{p}} \approx 1$. In the same approximation

$$S_{\mathbf{p}} \approx -\frac{t_{sp}t_{dp}}{(\epsilon_s - \epsilon_d)(\epsilon_d - \epsilon_p)} (s_x^2 - s_y^2).$$

Taking into account

$$s_x^2 - s_y^2 = -2(\cos p_x - \cos p_y),$$

we obtain

$$S_{\mathbf{p}} \approx \frac{2t_{sp}t_{dp}}{(\epsilon_s - \epsilon_d)(\epsilon_d - \epsilon_p)} (\cos p_x - \cos p_y). \quad (83)$$

As the hopping between planes is going through the big radius Cu4s orbital, the inter-layer hopping is proportional to S_p^2 , i.e.

$$t_{\perp}(\mathbf{p}) = t_{ss}S_p^2 = \frac{t_0}{4}(\cos p_x - \cos p_y)^2, \quad (84)$$

with $t_0 \approx 150$ meV for $\text{Bi}_2\text{Sr}_2\text{CaCu}_2\text{O}_8$ [34]. This behavior of inter-layer hopping and corresponding S_p amplitude is in agreement with many band-structure calculations [14, 15] and further LCAO analysis [51].

Now following the perturbative formula Eq. (83), we can better understand the causes of the high- T_c in cuprates. The perturbative formula has transfer amplitudes in the numerator and energy denominators. For example, O2p amplitudes X_p and Y_p have multiplier $t_{pd}/(\epsilon_d - \epsilon_p)$ describing hopping between Cu4d and O2p with corresponding energy denominator. Continuing from X_p to Cu4s we obtain an additional factor $t_{sp}/(\epsilon_s - \epsilon_d)$. Finally for the Cu4s amplitude we have dimensionless energy factor

$$\mathcal{Q} = \frac{t_{sp}t_{dp}}{(\epsilon_s - \epsilon_d)(\epsilon_d - \epsilon_p)} \ll 1,$$

which together with the angular dependence participates in the BCS gap equation Eq. (61). As

$$\chi_p \simeq \mathcal{Q}(\cos p_x - \cos p_y)$$

in order to have maximal T_c , the dimensionless BCS-coupling constant (here we omit the $\langle \chi^2 \rangle$ factor in the exact definition for λ)

$$G_0 \equiv J_{sd}\rho_F\mathcal{Q}^2 \ll 1$$

has to be as big as possible. Typically $\rho_F J_{sd} \lesssim 1$ but simultaneously $\mathcal{Q} \lesssim 1$ and as a result the product of those three factors are small enough in order weak coupling BCS theory to be in its habitat of applicability. On the other hand, the exchange integral J_{sd} is much bigger than the Debye frequency and it is not necessary to take into account Eliashberg type corrections for the ratio $2\Delta(0)/T_c$, for example. In this sense the CuO_2 plane is closer to the original BCS weak coupling theory than strong coupling conventional superconductors like Sn and Pb.

Perhaps for the CuO_2 plane we have the closest triple coincidence of the 3 levels of the transition metal and the chalcogenide $\epsilon_p < \epsilon_d < \epsilon_s$. Like after the spring equinox we wait for the full moon and next weekend in order to have a Great holiday – happy Easter to the CuO_2 plane: from 3d to 4s by 2p the highway of high- T_c superconductivity [81].

It is remarkable that the correlation between the band parameters

$$s(\epsilon_F) = \frac{(\epsilon_s - \epsilon_F)(\epsilon_F - \epsilon_p)}{2t_{sp}^2}, \quad r = \frac{1}{2(1+s)}, \quad (85)$$

and maximal critical temperature $T_{c,\text{max}}$ at optimal doping was observed by Pavarini *et al.* [16] analyzing the band structure of many hole doped cuprates. This band structure trend is a strong hint that cuprate superconductivity is the modern face of the ancestral two-electron exchange [94, 95].

The band theory has proven to be successful in deriving parameters for an effective Hamiltonian, and in capable hands can explain the trends in various members of the cuprate family. Nevertheless, this is only the starting point for achieving a deeper understanding of a strongly correlated problem, and the game is by no means over.

Before we begin the description of the normal state properties we had to recall and complete the superconducting ones. It is challenging to try to use one and the same Hamiltonian to explain simultaneously normal and superconducting properties of the high- T_c cuprates which is the main purpose of the present work. Next we analyze the s - d exchange Hamiltonian in the spirit of Fermi liquid theory.

FERMI LIQUIDS

3.1 Fermi liquid reduction and inter-layers electric field fluctuations

Let us consider what is necessary to be supposed in order the “cold spot” concept to be derived sequentially from the *s-d* Shubin-Kondo-Zener Hamiltonian Eq. (56) which we write again in the momentum representation

$$\hat{H}_{sd} = -\frac{J_{sd}}{N} \sum_{\substack{\mathbf{p}'+\mathbf{q}'=\mathbf{p}+\mathbf{q} \\ \alpha, \beta}} S_{\mathbf{q}'} D_{\mathbf{p}'} \hat{c}_{\mathbf{q}'\beta}^\dagger \hat{c}_{\mathbf{p}'\alpha}^\dagger \hat{c}_{\mathbf{p}\alpha} \hat{c}_{\mathbf{q}\beta} S_{\mathbf{p}} D_{\mathbf{q}}. \quad (86)$$

Now we perform Landau-Fermi liquid reduction taking from the sum above only the terms with $\mathbf{p}' = \mathbf{p}$ and $\mathbf{q}' = \mathbf{q}$, and introducing standard operators for the electron numbers $\hat{n}_{\mathbf{p},\alpha} = \hat{c}_{\mathbf{p}\alpha}^\dagger \hat{c}_{\mathbf{p}\alpha}$ in the conduction $\text{Cu}3d_{x^2-y^2}$ band of cuprates. For comparison with Eq. (58) now we have to insert different δ -function multipliers, formally

$$\begin{aligned} \hat{c}_{\mathbf{q}'\beta}^\dagger \hat{c}_{\mathbf{p}'\alpha}^\dagger \hat{c}_{\mathbf{p}\alpha} \hat{c}_{\mathbf{q}\beta} &\rightarrow \delta_{\mathbf{q}',\mathbf{q}} \delta_{\mathbf{p}',\mathbf{p}} \hat{c}_{\mathbf{q}\beta}^\dagger \hat{c}_{\mathbf{p}\alpha}^\dagger \hat{c}_{\mathbf{p}\alpha} \hat{c}_{\mathbf{q}\beta} \\ &= \delta_{\mathbf{q}',\mathbf{q}} \delta_{\mathbf{p}',\mathbf{p}} (\hat{n}_{\mathbf{p},\alpha} \hat{n}_{\mathbf{q},\beta} + \delta_{\mathbf{p},\mathbf{q}} \delta_{\alpha,\beta} \hat{n}_{\mathbf{p},\alpha}). \end{aligned} \quad (87)$$

The last term with $\delta_{\mathbf{p},\mathbf{q}}$ is irrelevant for the interaction and we omit it in the further considerations. In such a way we obtain a separable Fermi liquid Hamiltonian

$$\hat{H}_{\text{FL}} = \frac{1}{2N} \sum_{\mathbf{p}, \mathbf{q}, \alpha, \beta} \hat{n}_{\mathbf{p},\alpha} f(\mathbf{p}, \mathbf{q}) \hat{n}_{\mathbf{q},\beta} \quad (88)$$

for which we are going to use the self-consistent approximation

$$\langle \hat{n}_{\mathbf{p}\alpha} \hat{n}_{\mathbf{q}\beta} \rangle \approx \langle \hat{n}_{\mathbf{p}\alpha} \rangle \langle \hat{n}_{\mathbf{q}\beta} \rangle \quad (89)$$

and when necessary apply thermal averaging and spin summation $n_{\mathbf{p}} = \sum_{\alpha} \langle \hat{n}_{\mathbf{p},\alpha} \rangle$.

We wish to emphasize that in Eq. (88) we again arrives at the same separable kernel $f(\mathbf{p}, \mathbf{q}) = -2J_{sd}\chi_{\mathbf{p}}\chi_{\mathbf{q}}$ as for the BCS reduction and gap anisotropy Eq. (59) and Eq. (62).

According to the Landau idea Eq. (2.2) and Eq. (39.20) of Ref. [55] the influenced by the interaction electron band spectrum we express by the functional derivative

$$\varepsilon(\mathbf{p}, \mathbf{r}) = \epsilon_{\mathbf{p}} + \frac{\partial \hat{H}_{\text{FL}}}{\partial \hat{n}_{\mathbf{p},\alpha}} \rightarrow \epsilon_{\mathbf{p}} + \frac{1}{N} \sum_{\mathbf{q},\beta} f(\mathbf{p}, \mathbf{q}) \hat{n}_{\mathbf{q},\beta}(\mathbf{r}). \quad (90)$$

In the spirit of BCS averaged variational energy we can use Fermi liquid averaged energy

$$E(\{n_{\mathbf{p}}\}) = \langle \hat{H}_{\text{FL}} \rangle$$

and single particle spectrum

$$\varepsilon(\mathbf{p}, \mathbf{r}) = \epsilon_{\mathbf{p}} + \frac{(-2J_{sd})}{N} \chi_{\mathbf{p}} \sum_{\mathbf{q}} \chi_{\mathbf{q}} n_{\mathbf{q}}(\mathbf{r}, t) \quad (91)$$

in which space argument \mathbf{r} can be introduced only in the quasi-classical WKB approximation. Considering here the second \mathbf{r} -dependent term as perturbative scattering potential the perturbative scattering amplitude is $\propto \chi_{\mathbf{p}}$, and for the scattering rate we have

$$1/\tau_{\mathbf{p}} \propto |\chi_{\mathbf{p}}|^2. \quad (92)$$

This way, after a long chain of approximations, we arrive at the conclusion that strong anisotropy of the lifetime is a consequence of the s - d interaction and the specific d -type symmetry $S_{\mathbf{p}}$ of the empty $4s$ band.

In a qualitative consideration we can extend the WKB concept in order to analyze even short wavelength thermal fluctuations of the electron density. For the dispersion of this random variable, the χ factor is of order of one and can be omitted in the qualitative considerations. Summation on the momentum \mathbf{p} gives simply the local fluctuations of the electron density $\delta n(\mathbf{r})$ around space point $\mathbf{r} = a_0 \mathbf{n}$ or CuO_2 plaquette \mathbf{n} . The local thermal fluctuations of the electron density $\delta n(\mathbf{n})$ are related to the thermally excited random charge Q in the plane capacitor model [51]

$$\frac{1}{N} \sum_{\mathbf{q}} \chi_{\mathbf{q}} \delta n_{\mathbf{q}}(\mathbf{r}, t) \simeq \frac{Q}{e} \propto T. \quad (93)$$

Here we repeat the qualitative arguments related to the physics of the linear resistivity. Layered cuprates are metals in the ab -plane CuO_2 but in the perpendicular c -direction in the normal phase there is no coherent electron transport. Along this “dielectric” c -direction or z -direction,

indispensably there are thermal fluctuations of the electric field E_z electrostatically connected to the 2D charge density of single or doubled CuO_2 planes. In such a way local thermal fluctuations of the electron density Q substituted in the WKB formula Eq. (91) give a random potential $U(\mathbf{r}) = \varepsilon(\mathbf{p}, \mathbf{r})$ on which charge carriers scatter. The scattering rate $1/\tau_p$ in the WKB approximation in Born approximation is proportional to the matrix elements of the random potential $1/\tau_p \propto |U_p|^2 \propto \chi_p^2$. In such a way our qualitative model consideration leads that the scattering rate is proportional to the square of the s - d hybridization amplitude and temperature. Calculating in the Born approximation the scattering amplitude we have in Eq. (91) χ_p , giving for the scattering rate $\propto \chi_p^2$ and explaining Ioffe and Millis [34] “cold spots” simply as zeros of the χ_p factor in the separable interaction kernel general for BCS pairing and FL approach. In Eq. (91) χ_p is momentum dependent while the sum depends on the space vector \mathbf{r} and thermally activated number of quasi-particles $\langle n_q(\mathbf{r}, t) \rangle \propto T$ are proportional to the temperature and this is simple consequence of the classical fluctuations of the electric field perpendicular to the planes of the layered conductor.

On the Fermi contour a hole pocket around (π, π) point has shape of a rounded square but conserving topology (in the spherical cow approximation) can be approximated by a circle. Making Fourier analysis in acceptable approximation d -wave gap anisotropy function can be approximated by d -wave with $l = 2$ giving $\chi_p \propto \cos(2\theta)$. In this model approximation for the separable kernel, we obtain exactly the angular dependence of Ioffe and Millis [34]

$$f(\mathbf{p}, \mathbf{q}) = I \cos(2\theta) \cos(2\theta'), \quad (94)$$

where

$$I \simeq (-J_{sd}) \left(\frac{t_{sp} t_{pd}}{(\epsilon_s - \epsilon_d)(\epsilon_d - \epsilon_p)} \right)^2, \quad (95)$$

where the authors take into account angles from the BZ diagonal $\tilde{\theta} = \theta - \frac{\pi}{4}$ which converts $\cos(2\theta) = \sin(2\tilde{\theta})$. In such a way the electron scattering rate $\Gamma_p = 1/\tau_p$ proportional to the imaginary part of the energy according second Fermi golden rule take the “cold spot” angular form speculated by Ioffe and Millis in Ref. [34]

$$-\text{Im}(\epsilon_p) \propto \Gamma_p = \frac{\Gamma_0}{4} \sin^2(2\tilde{\theta}) + \frac{1}{\tau_0} \approx \Gamma_0 \tilde{\theta}^2 + \frac{1}{\tau_0}, \quad (96)$$

where $\Gamma_0 = k_1 T + k_2 T^2$. The exact scattering rate $\Gamma_p \propto \chi_p^2$ is represented in Fig. 8. The small constant $1/\tau_0 = \Gamma_C$ describes the scattering rates in cold spot direction which could have Coulomb scattering origin described in the beginning of the present work, i.e. $\tau_0 \equiv \tau_{\text{cold}}$. The coefficient k_1 describes classical fluctuations of the electric field perpendicular to the CuO_2 plane when k_2 is negligible. If however, for overdoped cuprates we have significant conductivity in the c -direction and small fluctuations of the electric field, we have the condition of applicability of the most conventional Landau-Fermi liquid theory with $k_1 = 0$ and k_2 calculated according to 4-fermion s - d Hamiltonian using the general scheme described in Sec. 76 “Absorption of sound in Fermi liquid” of the textbook by Lifshitz and Pitaevskii (X-th volume of the Landau-Lifshitz

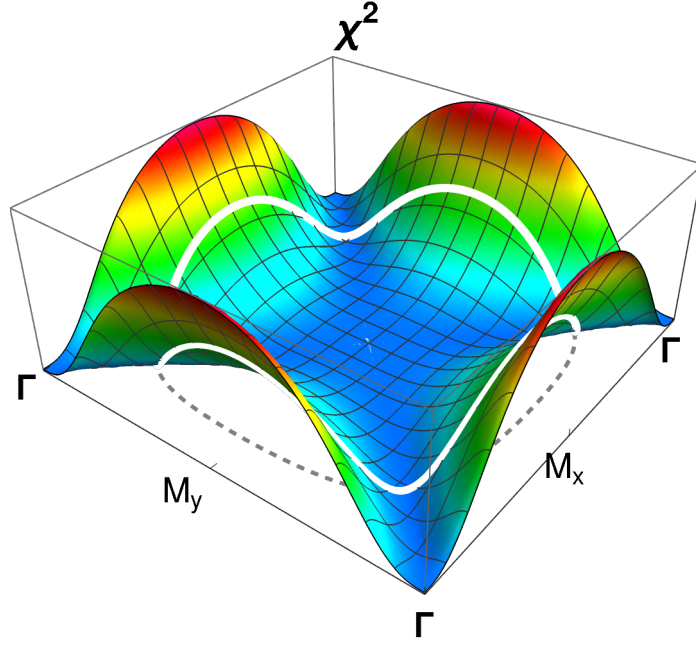


Figure 8: The hybridization probability $\chi_p^2 = S_p^2 D_p^2$ which participates in the BCS gap equation Eq. (61) and scattering rate of the normal charge carriers by exchange interaction Eq. (96). The heights correspond hot spots while navigation channels in the deep blue sea correspond to cold spots in $(0, 0) - (\pi, \pi)$ direction. The Fermi contour (dashed line) projected on this χ_p^2 surface and this is curve is important detail of scattering rate theory; after [Fig. 2.3.c] [13].

course) [47]. In other words having strongly anisotropic scattering rate we have to average the momentum dependent relaxation time τ_p along the Fermi contour and with this intuitively clear notion we can use the Drude formula again. Thus using the relation

$$\frac{1}{\tau(\theta)} = \frac{1}{\tau_{\text{hot}}} \cos^2(2\theta) + \frac{1}{\tau_{\text{cold}}}. \quad (97)$$

The Drude relaxation time is given by

$$\tau_{\text{Drude}} = \langle \tau(\theta) \rangle \approx \sqrt{\tau_{\text{cold}} \tau_{\text{hot}}} \gg \tau_{\text{hot}} \equiv \frac{4}{\Gamma_0}, \quad (98)$$

and the scattering rate yields

$$\sigma_{ab} = q_e^2 n_e \tau_{\text{Drude}} / m_c. \quad (99)$$

Inequality (98) reveals that pure Coulomb scattering considered in Ref. [51] is only the first step in a correct direction. We use the Fermi liquid approach and Fermi liquid notions but for superconductors with anti-ferromagnetic exchange amplitude J_{sd} the zero sound is only a thermally activated dissipative mode, as velocity of a Brownian particle. Real zero sound is however possible to be observed in layered perovskites with ferromagnetic J_{sd} .

In order to trace a path to the derivation of hot and cold spots along the Fermi contour we perform a qualitative analysis in the spirit of the Migdal [96, “Qualitative methods in quantum mechanics”] or de Gennes[“ Simple views on condensed matter physics”] [97]. The natural explanations gives a hint that we are on a correct path and it is worthwhile to apply the methods of statistical physics giving the possibility to analyze every kinetic problem.

Another hint for the correctness of our research is the qualitative agreement between our scattering rate calculation from Fig. 8 and the published ARPES data[22] shown in Fig. 9. We

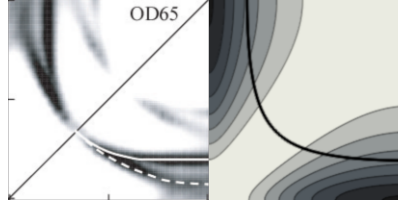


Figure 9: Comparison of: (Left) ARPES data for spectral intensity for overdoped $\text{Bi}_2\text{Sr}_2\text{CaCu}_2\text{O}_{8+\delta}$ (Bi2212) for $T_c = 65$ K OD65 from Ref. [22]; the figure is taken from the arXiv version. (Right) Scattering rate calculated in the framework of the s - d exchange according to Eq. (92) depicted in Fig. 8. Continuous line in this theoretical calculation denotes the Fermi contour according to Eq. (27).

have reached this coherence in kinetics using the one and same Hamiltonian which describes the pairing and the T_c -Cu $4s$ energy correlation. Broadening of the qualitative agreement of viable descriptions of variety of phenomena is an essential initial step towards the creation of the detailed theory.

But if we are on a correct path, we have to obtain more than we invest. At least one new phenomenon has to be predicted if we have a general picture for superconducting pairing and anisotropic scattering rate in the normal phase. The pendentive of the Landau-Fermi liquid theory is the prediction of zero sound which is a property of a Fermi gas with repulsion. The superconductivity is created by the attraction of the electrons and in this case the zero sound is only a dissipation mode which can be only thermally activated. In this section we have only touched to the normal state transport properties of the high- T_c superconductors, for an introduction in the problem see the excellent reviews [59, 98]. If we are on a correct track the exchange interaction scattering can be taken in state-in-the-art way together with electromagnetic fluctuations in infinite media which are well-described in the textbooks [48, 55]

In the next section we consider whether nevertheless it is possible to observe zero sound in layered transition metal perovskites.

3.2 Zero sound for ferromagnetic sign of s - d exchange interaction

The cuprates are high- T_c superconductors because J_{sd} has antiferromagnetic sign and we have almost triple coincidence of the transition metal levels $3d$ and $4s$ and oxygen $2p$. But what

will happen if in some perovskite the s - d exchange integral has ferromagnetic sign with positive ($-J_{sd} > 0$)? This leads to a repulsion between electrons which prevents superconducting condensation and opens the possibility for propagation of zero sound. This topic is slightly lateral to our present study, but the developed system of notion and notations can be useful to study propagation of zero sound in similar compounds of layered perovskites with transition metal ions.

Following the textbook by Lifshitz and Pitaevskii (IX volume of the Landau and Lifshitz course) [55] we introduce notations and recall some basic notions of Landau-Fermi liquid theory.

The zero sound can be described as a collective degree of freedom related to local deformation of the Fermi surface considering in momentum space local change of the Fermi energy $\epsilon_F \rightarrow \epsilon_F + \nu_{\mathbf{p}}$. We repeat that quasi-momentum is represented by the dimensionless phases \mathbf{p} in the BZ, and around the center of the hole pocket of CuO_2 plane we can introduce polar coordinates $\mathbf{p} = p(\cos \theta, \sin \theta)$. In WKB wavelengths approximation we can consider distribution of quasi-electrons per fixed spin projection in the phase space $n(\mathbf{p}, \mathbf{r}, t)$ by small linear deviation $\delta n(\mathbf{p}, \mathbf{r}, t)$ from equilibrium Fermi step $\theta(\epsilon_F - \epsilon_{\mathbf{p}})$ described by the Heavyside θ -function. Differentiating $\theta(\epsilon_F + \nu_{\mathbf{p}} - \epsilon_{\mathbf{p}})$ we obtain

$$n(\mathbf{p}, \mathbf{r}, t) = n_{\mathbf{p}}^{(0)} + \delta n(\mathbf{p}, \mathbf{r}, t), \quad n_{\mathbf{p}}^{(0)} = \theta(\epsilon_F - \epsilon_{\mathbf{p}}) \quad (100)$$

$$\delta n(\mathbf{p}, \mathbf{r}, t) = \delta(\epsilon_F - \epsilon_{\mathbf{p}}) \nu_{\mathbf{p}} \exp(i(\mathbf{K} \cdot \mathbf{r} - \omega t)), \quad (101)$$

$$n = \theta(\epsilon_F - \epsilon_{\mathbf{p}}) + \delta(\epsilon_F - \epsilon_{\mathbf{p}}) \nu_{\mathbf{p}} \exp(i(\mathbf{K} \cdot \mathbf{r} - \omega t)), \quad (102)$$

where plane wave amplitude $\nu_{\mathbf{p}} \exp(i(\mathbf{K} \cdot \mathbf{r} - \omega t))$ with wave-vector \mathbf{K} and frequency ω can be inserted in quasi-classical approximation $a_0 K \ll 1$ and $\hbar \omega \ll \epsilon_F$.

The evolution of $n(\mathbf{p}, \mathbf{r}, t)$ quasi-particle distribution we analyze in the initial collision approximation with zero substantial derivative in the phase space

$$0 = d_t n = \partial_t n + \partial_{\mathbf{p}} n \cdot \dot{\mathbf{P}} + \partial_{\mathbf{r}} n \cdot \dot{\mathbf{r}}, \quad (103)$$

where we apply standard time and space derivatives

$$\begin{aligned} \partial_{\mathbf{r}} \delta n &= i\mathbf{K} \delta n, \quad \mathbf{K} = K(\cos \beta, \sin \beta), \quad \partial_t \delta n = -i\omega \delta n, \\ \dot{\mathbf{r}} &= \mathbf{V}_{\mathbf{p}}, \quad \mathbf{V}_{\mathbf{p}} = \partial_{\mathbf{p}} \epsilon_{\mathbf{p}} = \frac{a_0}{\hbar} \mathbf{v}_{\mathbf{p}}, \quad v_{F, \mathbf{p}} = v(\mathbf{p})|_{\epsilon_{\mathbf{p}} = \epsilon_F}, \end{aligned}$$

where $\epsilon_{\mathbf{p}}$ and $\mathbf{v}_{\mathbf{p}}$ have dimension energy, $\mathbf{V}_{\mathbf{p}}$ has dimension velocity, \mathbf{r} distance, \mathbf{P} momentum, and $\mathbf{k} \equiv a_0 \mathbf{K}$ is the dimensionless wave-vector. The force acting on quasi-particles we calculate as space derivative of the Fermi liquid single particle Hamiltonian Eq. (90) which gives

$$\dot{\mathbf{P}} = \mathbf{F} = -\partial_{\mathbf{r}} \varepsilon(\mathbf{p}, \mathbf{r}) = -i\mathbf{K} \int_{\text{BZ}} f(\mathbf{p}, \mathbf{p}') \delta n_{\mathbf{p}'} \frac{dp'_x dp'_y}{(2\pi)^2}. \quad (104)$$

See also the well-known textbook by Nozieres [99]. The plasma waves effects are negligible only for charge neutral oscillations with zero amplitude oscillations of 2D charge density $\rho_{\text{el}}(\mathbf{r}, t)$ and

current

$$\rho_{\text{el}}(\mathbf{r}, t) = \frac{e}{Na_0^2} \sum_{\mathbf{p}} \delta n(\mathbf{p}, \mathbf{r}, t), \quad (105)$$

$$\mathbf{j}(\mathbf{r}, t) = \int_{\text{BZ}} e \mathbf{V}_{\mathbf{p}} \delta n(\mathbf{p}, \mathbf{r}, t) \frac{dp_x dp_y}{(2\pi a_0)^2}. \quad (106)$$

In other words we can forget the electric force $e\mathbf{E}$ if we use only solutions of the kinetic equation with $\langle \nu_{\mathbf{p}} \rangle_{\text{F}} = 0$ and $\langle \mathbf{k} \cdot \mathbf{v}_{\mathbf{p}} \nu_{\mathbf{p}} \rangle_{\text{F}} = 0$. The last condition in polar coordinates gives $\langle \cos(\beta - \theta) \nu_{\mathbf{p}} \rangle_{\text{F}} = 0$.

After substitution of the described details in the Boltzmann kinetic equation Eq. (103) we obtain the dispersion relation

$$[\omega - \mathbf{K} \cdot \mathbf{V}_{\text{F}}(\mathbf{p})] \nu_{\mathbf{p}} = \frac{\mathbf{K} \cdot \mathbf{V}_{\text{F}}(\mathbf{p})}{(2\pi)^2} \oint_{\text{FC}} f(\mathbf{p}, \mathbf{p}') \nu_{\mathbf{p}'} \frac{dp'_l}{v_{\text{F}}(p'_l)} \quad (107)$$

giving $\omega(\mathbf{K})$ dependence [48, 55]. The separable kernel Eq. (94) with positive I and ferromagnetic sign of the exchange integral $(-J_{sd}) > 0$ trivializes the calculation of the above integral. For model evaluation here we ignore the relatively weak Fermi velocity anisotropy and use parabolic dispersion $\epsilon \approx E_0 p^2 / 2m_{\text{eff}}$; *i.e.* in spherical cow approximation. Following the standard substitutions, we easily obtain for the deformation of the Fermi circle with amplitude a

$$\nu(\theta; \beta) = a \frac{\cos(\theta - \beta)}{\tilde{s} - \cos(\theta - \beta)} \cos(2\theta) \quad (108)$$

and the dispersion relation for the zero sound takes the form

$$F_0 \left\langle \frac{\tilde{\chi}^2(\theta - \beta)}{\tilde{s} - \cos(\theta)} \right\rangle_{\text{F}} = 1, \quad \tilde{s} = \frac{\omega/K}{v_{\text{F}}}, \quad F_0 = \rho_{\text{F}} I, \quad (109)$$

similar to the well-known results [49, 55]. In linear approximation the zero-sound amplitude a is arbitrary. The solution of the elementary integrals for the circular Fermi surface and d -type interaction Eq. (94) is

$$-\frac{1}{2} + \frac{\tilde{s}}{2\varsigma} \{1 + 4\tilde{s}\varsigma [1 - 2s(\tilde{s} - \varsigma)]\} \cos(4\beta) = \frac{1}{F_0} \quad (110)$$

where $\varsigma \equiv \sqrt{\tilde{s}^2 - 1}$. The solution for the dimensionless zero sound velocity \tilde{s} as a function of the angle along the Fermi circle is depicted in Fig. 10. However, this illustration has only conditional sense because of charge and current neutrality conditions

$$\int_0^{2\pi} \nu(\theta, \pi/4) d\theta = 0, \\ \int_0^{2\pi} \cos(\theta - \pi/4) \nu(\theta, \pi/4) d\theta = 0$$

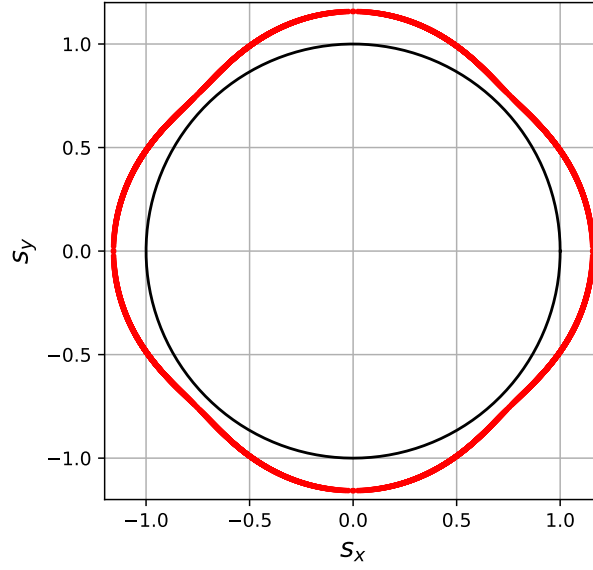


Figure 10: Two dimensional velocity space in units v_F . The unit circle is filled by electrons. The zero sound phase velocity $\tilde{s} = (\tilde{s}_x, \tilde{s}_y) = \tilde{s}(\cos \beta, \sin \beta)$ has several percent anisotropy with maxima along the pairing directions and minima along the cold spots diagonals and zeros of the interaction function χ . No surfing electrons in all directions $\tilde{s} = \omega/kv_F > 1$. This is a model calculation with negligible plasmon effects which could be acceptable approximation when oscillations in neighboring planes are in anti-phase.

give the restrictions $\beta = \frac{\pi}{4}$ and $\cos \beta = -1$, which means that low frequency zero sound oscillations can propagate only along the BZ diagonals of the layered transition metal oxides with basic elementary cell TO_2 . The deformation ν_p of the FC for such charge neutral oscillations is shown in Fig. 11.

One can speculate how strict the charge neutrality conditions are close to the “cold spot” diagonals. Theoretically Coulomb interaction can be easily taken into account, moreover we consider zero sound at the wave-vector $K_x = \pi/c_0$ when neighboring transition metal planes TO_2 have charge and current oscillations with opposite sign in c -direction so that zero sound oscillations are charge neutral only if averaged in small volumes. However, these conditions are not universal and require consideration of the properties for every compound separately.

Here we wish to point out some contemporary studies on similar topics: zero sound in two dimensions [35], shear zero sound [37] and zero sound for p -type interaction [38]. We suppose that except liquid ^3He layered structures with large ferromagnetic exchange interaction could become interesting systems for implementation of old idea by Landau [39, 40, 103]. Returning to superconducting cuprates with antiferromagnetic sign of J_{sd} we have to point out that in the normal phase the zero sound modes are dissipative modes. The thermal excitation of those modes creates only fluctuations of the electron density. Finally the scattering of normal charge carriers by these density fluctuations creates the Ohmic resistivity. In the next section we continue with

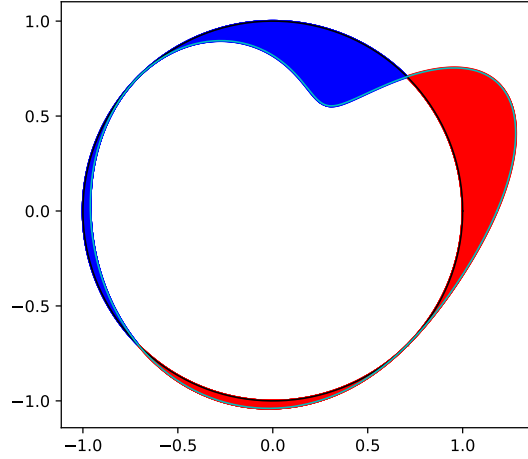


Figure 11: Deformation of the Fermi contour in two dimensional momentum space \mathbf{p} for zero sound propagating along cold spots diagonal $\beta = \pi/4$ in layered perovskites. For this special case according to Eq. (108) electric charge and current oscillations are zero. For some appropriate wave-amplitude a are given two contours $\varepsilon_{\mathbf{p}} = \varepsilon_{\mathbf{F}}$ and $\varepsilon_{\mathbf{p}} = \varepsilon_{\mathbf{F}} + \nu_{\mathbf{p}}$. For wave-vector in general direction it is necessary to take into account Coulomb interaction and plasmon effects as it is done in works on kinetic theories for the electrodynamic response of Fermi liquids and anisotropic metals [100, 101, 102].

general considerations of the non-resolved problems.

3.3 Fermi liquid behavior of overdoped cuprates

Our qualitative consideration of the electron scattering rate Eq. (92) can be precised in we consider state-of-the-art consideration of electromagnetic fluctuations in a layered metal of CuO_2 plane following [55, Chap. VIII] followed by consideration of Stoss-integral in plasmas [47, Chap. IV] with incorporated exchange interaction. However linear behaviour of the resistivity demonstrated at least qualitatively that even in gaseous approximation electrons are scattered by electron density fluctuations. We suppose however that these fluctuations of density and perpendicular to the CuO_2 layers electric field E_z are gradually frozen with increasing of doping.

As it was emphasized by P. Lee [83] with increasing of the doping *sanity gradually returns*. In this section we consider the case of strong inter-layer hybridization when the plasma frequency is higher than the temperature and the electric field E_z fluctuations and related with them 2-dimensional density fluctuations are frozen. In this case we have usual Baber [104] and Landau-Pomeranchuk [105] scattering qualitatively described in the monograph by Mott [46, Chap 2, Sec 6, Eq (18)]. For the calculation of the Stoss-integral of the scattering in cuprates we apply the second Fermi golden rule for the transition rate [106, Chap. 7, Sec. 46, Eq. (39)], [107, Eq. (23.13)], [91, Eq. (42.5)] applied to the s - d exchange interaction Eq. (55) or rather Eq. (56)

where only conduction band $b = 3$ is taken into account

$$\text{St}[n](\mathbf{p}) = \frac{2\pi}{\hbar} \sum \overline{\left| \langle f | \hat{H}_{sd} | i \rangle \right|^2} \delta(E_f - E_i - \hbar\omega). \quad (111)$$

In the initial state we have 2 charge carriers with momenta \mathbf{p}' and \mathbf{p}'_1 which after scattering have momenta \mathbf{p} and \mathbf{p}_1 , cf. Ref. [47, Eq. (38)]

$$|i\rangle = (\mathbf{p}', \alpha; \mathbf{p}'_1, \beta), \quad |f\rangle = (\mathbf{p}, \alpha; \mathbf{p}_1, \beta). \quad (112)$$

The Stoss-integral is a functional of the momentum distribution $[n]$ and a function of the fixed momentum \mathbf{p} , i.e. we should not sum over the index \mathbf{p} . Additionally as we precise later, \mathbf{p}'_1 is fixed from the momentum conservation included in the s - d interaction in momentum representation.

In our model calculation we omit umklapp processes which can be easily taken into account when necessary. There is no summation over momentum \mathbf{p} in Eq. (111), the summation is over \mathbf{p}_1 , \mathbf{p}' , and \mathbf{p}'_1 . In this paper we analyze static Ohmic resistivity with zero frequency $\omega = 0$. The initial and final energies are just the band energies of the charge carriers scattered by exchange interaction

$$E_i = \varepsilon_{\mathbf{p}'} + \varepsilon_{\mathbf{p}'_1}, \quad E_f = \varepsilon_{\mathbf{p}} + \varepsilon_{\mathbf{p}_1}. \quad (113)$$

The over-line in the Fermi golden rule Eq. (111) denotes the square average of the modulus of the matrix element. For the electron number operators we have

$$\hat{n}_{\mathbf{p},\alpha} = \hat{c}_{\mathbf{p},\alpha}^\dagger \hat{c}_{\mathbf{p},\alpha}, \quad 1 - \hat{n}_{\mathbf{p},\alpha} = \hat{c}_{\mathbf{p},\alpha} \hat{c}_{\mathbf{p},\alpha}^\dagger. \quad (114)$$

This averaging we perform with matrix element of the conduction band Hamiltonian Eq. (56). In the averaged squares denoted by over-line in Eq. (111) of the modulus we now recognize the averaged momentum distribution of electrons

$$\overline{|\hat{c}_{\mathbf{p},\alpha}|^2} = n_{\mathbf{p},\alpha} \in (0, 1), \quad \overline{|\hat{c}_{\mathbf{p},\alpha}^\dagger|^2} = 1 - n_{\mathbf{p},\alpha}. \quad (115)$$

More precisely, in this averaging we take into account creation and annihilation operators with coinciding momenta

$$\overline{\hat{c}_{\mathbf{q},\beta}^\dagger \hat{c}_{\mathbf{p},\alpha}} = \delta_{\mathbf{qp}} \delta_{\alpha\beta} n_{\mathbf{p},\alpha}. \quad (116)$$

In Eq. (56) we suppose that all momenta are different and in this case commutation relation between Fermi operators are irrelevant.

For electron in equilibrium we have the Fermi distribution

$$n_{\mathbf{p},\alpha}^{(0)} = \frac{1}{\exp((\varepsilon_{\mathbf{p}} - \epsilon_F)/T) + 1} \quad (117)$$

with zero temperature limit

$$n_{\mathbf{p},\alpha}^{(0)} = \theta(\epsilon_F - \varepsilon_{\mathbf{p}}), \quad \text{at } T = 0. \quad (118)$$

The substitution of the exchange Hamiltonian in Fermi II golden rule Eq. (111) gives

$$\begin{aligned} \text{St}(\mathbf{p}) &= \frac{2\pi}{\hbar} \frac{J_{sd}^2}{N^2} \sum_{\mathbf{p}_1, \mathbf{p}', \mathbf{p}'_1} \delta(\varepsilon + \varepsilon_1 - \varepsilon' - \varepsilon'_1) \delta_{\mathbf{p}+\mathbf{p}_1, \mathbf{p}'+\mathbf{p}'_1} \\ &\times [(1-n)(1-n_1)n'n'_1 - (1-n')(1-n'_1)nn_1] \\ &\times [(SD_1S'D'_1)^2 + (DS_1D'S'_1)^2], \end{aligned} \quad (119)$$

where for brevity momentum and spin indices are omitted

$$\begin{aligned} n &= n_{\mathbf{p}, \alpha}, & n_1 &= n_{\mathbf{p}_1, \alpha}, & n' &= n_{\mathbf{p}', \alpha}, & n'_1 &= n_{\mathbf{p}'_1, \alpha}, \\ \varepsilon &= \varepsilon_{\mathbf{p}}, & \varepsilon_1 &= \varepsilon_{\mathbf{p}_1}, & \varepsilon' &= \varepsilon_{\mathbf{p}'}, & \varepsilon'_1 &= \varepsilon_{\mathbf{p}'_1}, \\ S &= S_{\mathbf{p}}, & S_1 &= S_{\mathbf{p}_1}, & S' &= S_{\mathbf{p}'}, & S'_1 &= S_{\mathbf{p}'_1}, \\ D &= D_{\mathbf{p}}, & D_1 &= D_{\mathbf{p}_1}, & D' &= D_{\mathbf{p}'}, & D'_1 &= D_{\mathbf{p}'_1}. \end{aligned} \quad (120)$$

The Kronecker symbol coming from the Hamiltonian Eq. (56) removes the summation on \mathbf{p}'_1 giving the condition $\mathbf{p}'_1 = \mathbf{p} + \mathbf{p}_1 - \mathbf{p}'$. The energy conservation is embedded in Eq. (111) while the momentum conservation is embedded in Eq. (56). The first (income) term in brackets [...] arises from creation $\hat{c}_{\mathbf{p}, \alpha}^\dagger$ operator while in the second (outgo) term with minus sign corresponds to the process in which initial $|i\rangle$ and final states $|f\rangle$ are exchanged. According to our system of notations \mathbf{p} are dimensionless momenta with components in $(0, 2\pi)$ interval for which we have

$$\frac{1}{N} \sum_{\mathbf{q}} \dots = \int_0^{2\pi} \int_0^{2\pi} \frac{dq_x dq_y}{(2\pi)^2} \dots \quad (121)$$

In such a way the Stoss-integral is in agreement with standard Landau theory for Fermi liquids [47, Eq. (74.5)] applied to our two dimensional CuO_2 plane with s - d exchange interaction

$$\begin{aligned} \text{St}[n](\mathbf{p}) &= \int_{\mathbf{p}_1, \mathbf{p}'} w(\mathbf{p}, \mathbf{p}_1; \mathbf{p}', \mathbf{p}'_1) \delta(\varepsilon + \varepsilon_1 - \varepsilon' - \varepsilon'_1) \\ &\times [(1-n)(1-n_1)n'n'_1 - (1-n')(1-n'_1)nn_1] \\ &\times \frac{d^D p_1 d^D p'}{[(2\pi)^D]^2}, \quad \text{with } \mathbf{p}'_1 = \mathbf{p} + \mathbf{p}_1 - \mathbf{p}', \end{aligned} \quad (122)$$

where for the scattering rate with dimension of frequency we obtain

$$w(\mathbf{p}, \mathbf{p}_1; \mathbf{p}', \mathbf{p}'_1) = \frac{2\pi}{\hbar} J_{sd}^2 [(SD_1S'D'_1)^2 + (DS_1D'S'_1)^2], \quad (123)$$

and notations in the integrant are introduced in Eq. (120). The collision frequencies w have dimension energy times frequency. It is instructive to compare the so derived Stoss-integral for classical gases [47, Eq. (3.8)], electron-phonon interaction [47, Eq. (79.3)], plasmas [47, Eq. (46.7)] impurity scattering of phonons [47, Eq. (70.1)], electron impurity scattering [47, Eq. (78.14)], *etc.*

This form for the Stoss-integral exactly coincides with the standard Landau one [47, Eq. (74.5)] for the Fermi liquids applied in our case for the two dimensional space $D = 2$, $p_x, p_y \in (0, 2\pi)$ for which [47, Eq. (74.30)] and in our case

$$\int \dots \delta(\varepsilon_{\mathbf{p}} - \epsilon_F) d^2p = \oint_{\varepsilon_{\mathbf{p}}=\epsilon_F} \dots \frac{dp_l}{v_F(\mathbf{p})}. \quad (124)$$

In such a way we arrive at the standard Landau Stoss-integral for Fermi liquids and for the function

$$w(\mathbf{p}, \mathbf{p}_1; \mathbf{p}', \mathbf{p}'_1) = w(\mathbf{p}', \mathbf{p}'_1; \mathbf{p}, \mathbf{p}_1) = w(\mathbf{p}_1, \mathbf{p}; \mathbf{p}', \mathbf{p}'_1). \quad (125)$$

we derive the explicit expression in the framework of LCAO method applied to the standard s - d interaction.

SOLUTION OF THE KINETIC EQUATION AND DERIVATION OF THE CONDUCTIVITY

According to the original Landau consideration the explicit form of the transition rate w is irrelevant for the final conclusion that at low temperatures in case of negligible impurity scattering the electron-electron interaction leads to $\varrho_\Omega = A_\Omega T^2$ and the *sanity* returns by the freezing of E_z and the related two dimensional density fluctuations [55, Sec. 1, Eqs. (1.11-12)]. Scattering rate determined by Drude fit of conductivity can demonstrate significant temperature dependence [59, 108, Bonn and Hardy, Fig. 4.24]. For a nice review of normal state properties of high- T_c cuprates see [59, Hussey, Chap. 10]. For a qualitative description of mean free path $l = V_F \tau_{\text{Drude}} \propto T^{-2}$ see [55, Sec. 1, Eqs. (1.11-12)] and [47, Eq. (75.1)].

Now following the original we perform detailed calculation in order to solve the kinetic equation

$$d_t n(t, \mathbf{p}) = \text{St}[n](\mathbf{p}), \quad d_t = \frac{\partial}{\partial t} + e\mathbf{E} \cdot \frac{\partial}{\partial \mathbf{p}} \quad (126)$$

in the case of small homogeneous in-plane electric field $\mathbf{E} = E\mathbf{e}_x$.

The momentum distribution n we represent as small correction to the equilibrium distribution $n^{(0)}$

$$\begin{aligned} n(t, \mathbf{p}) &= n^{(0)}(\mathbf{p}) + \delta n(t, \mathbf{p}) = \bar{n} + \Delta, \\ n &= n(t, \mathbf{p}), \quad \delta n(t, \mathbf{p}) \equiv \Delta(t, \mathbf{p}), \\ \bar{n} \equiv n^{(0)}(\mathbf{p}) &= n^{(0)}(\varepsilon_{\mathbf{p}}) = \frac{1}{\exp((\varepsilon_{\mathbf{p}} - \epsilon_F)/T) + 1}. \end{aligned} \quad (127)$$

For brevity we omit the arguments and keep only the superscripts and indices denoting the complete notation for $\Delta, \Delta_1, \Delta', \Delta'_1$.

The term in brackets in Eq. (122) we rewrite as

$$\begin{aligned} \mathcal{Z} \equiv & (1-n)(1-n_1)(1-n')(1-n'_1) \\ & \times \left[\frac{n'n'_1}{(1-n')(1-n'_1)} - \frac{nn_1}{(1-n)(1-n_1)} \right]. \end{aligned} \quad (128)$$

Taking into account the conservation of energy

$$\varepsilon + \varepsilon_1 = \varepsilon' + \varepsilon'_1 \quad (129)$$

and that in equilibrium

$$\frac{n_{\mathbf{p}}^{(0)}}{1-n_{\mathbf{p}}^{(0)}} = \frac{\bar{n}}{1-\bar{n}} = \exp\left(-\frac{\varepsilon_{\mathbf{p}} - \epsilon_F}{T}\right) \quad (130)$$

in Eq. (122) we have

$$\begin{aligned} \overline{\mathcal{Z}} = & (1-\bar{n})(1-\bar{n}_1)(1-\bar{n}')(1-\bar{n}'_1) \\ & \times [\exp((\varepsilon + \varepsilon_1)/T) - \exp((\varepsilon' + \varepsilon'_1)/T)] = 0, \end{aligned} \quad (131)$$

i.e. in equilibrium the Stoss-integral is zero. The current in equilibrium is of course also zero because $\varepsilon_{\mathbf{p}} = \varepsilon_{-\mathbf{p}}$ and $\bar{n}_{\mathbf{p}} = \bar{n}_{-\mathbf{p}}$.

In order to calculate the two dimensional current density

$$\mathbf{j} = \frac{e}{a_0^2 N} \sum_{\mathbf{p}} \mathbf{V}_{\mathbf{p}} n_{\mathbf{p}} = \sigma \mathbf{E} \quad (132)$$

at an evanescent electric field $\mathbf{E} = E\mathbf{e}_x \rightarrow 0$ we have to calculate the small deviation of the momentum distribution. In 2D the current \mathbf{j} has dimension A/m.

Following Enskog 1917 cf. [47, Eq. (6.1) and Eq. (74.15)] we represent

$$\begin{aligned} n \approx \bar{n} + \Delta = & n^{(0)}(\varepsilon(\mathbf{p} - \mathbf{q}_{\mathbf{p}})) = n^{(0)} - \mathbf{q}_{\mathbf{p}} \cdot \frac{\partial n^{(0)}}{\partial \mathbf{p}} \\ \approx & n^{(0)}(\varepsilon_{\mathbf{p}} - \varphi_{\mathbf{p}}) = n^{(0)} - \varphi_{\mathbf{p}} \frac{\partial n^{(0)}}{\partial \varepsilon}. \end{aligned} \quad (133)$$

As $n^{(0)} = n^{(0)}(\varepsilon(\mathbf{p}))$

$$\frac{\partial n^{(0)}}{\partial \mathbf{p}} = \frac{\partial n^{(0)}}{\partial \varepsilon} \mathbf{v}_{\mathbf{p}}, \quad \mathbf{v}_{\mathbf{p}} = \frac{\partial \varepsilon}{\partial \mathbf{p}} \quad (134)$$

we have

$$\varphi_{\mathbf{p}} = \mathbf{v}_{\mathbf{p}} \cdot \mathbf{q}_{\mathbf{p}}, \quad \Delta = -\frac{\partial \bar{n}}{\partial \varepsilon} \varphi_{\mathbf{p}} = -\mathbf{q}_{\mathbf{p}} \cdot \frac{\partial \bar{n}}{\partial \mathbf{p}} \quad (135)$$

For the energy derivative we have

$$-\frac{d\bar{n}}{d\varepsilon} = \frac{(1-\bar{n})\bar{n}}{T} \rightarrow \delta(\varepsilon - \epsilon_F), \quad \text{at } T \rightarrow 0, \quad (136)$$

see [47, Eq. (74.16)]. Analogously we have

$$-\frac{\partial n^{(0)}}{\partial \mathbf{p}} = \frac{(1 - \bar{n}) \bar{n}}{T} \mathbf{v}_{\mathbf{p}} \rightarrow \delta(\varepsilon - \varepsilon_{\mathbf{F}}) \mathbf{v}_{\mathbf{p}}. \quad (137)$$

In order to understand the meaning of the energy φ or momentum shift \mathbf{Q} we analyse the kinetic equation in τ approximation. This is actually independent mode approximation [109, Eq. (13.3)]

$$\text{St} = -\frac{n(\mathbf{P}, t) - \bar{n}(\mathbf{P})}{\tau}, \quad n(\mathbf{P}, t) \approx \bar{n}(\mathbf{P} - \mathbf{Q}_{\mathbf{P}}(t)). \quad (138)$$

Supposing small deviations from equilibrium

$$\Delta_{\mathbf{P}} \approx -\mathbf{Q}_{\mathbf{P}} \cdot \frac{\partial \bar{n}}{\partial \mathbf{P}}, \quad \text{St}(\mathbf{P}) \approx \frac{\mathbf{Q}_{\mathbf{P}}}{\tau} \cdot \frac{\partial \bar{n}}{\partial \mathbf{P}}. \quad (139)$$

For the time derivative we have

$$\frac{\partial n}{\partial t} = -\frac{\partial \bar{n}}{\partial \mathbf{P}} \cdot \frac{\partial \mathbf{Q}_{\mathbf{P}}}{\partial t}. \quad (140)$$

And for the term with electric field in Eq. (126) we use the gradient from the non-perturbed distribution

$$\mathbf{E}(t) \cdot \frac{\partial \bar{n}}{\partial \mathbf{P}}. \quad (141)$$

We substitute all those terms in Eq. (126) and omit the common multiplier $\frac{\partial \bar{n}}{\partial \mathbf{P}}$ we arrive at the Newton equation for a fictitious particle moving in a viscous fluid

$$\frac{d\mathbf{Q}}{dt} = e\mathbf{E} - \mathbf{Q}/\tau. \quad (142)$$

In the model case of parabolic dispersion $\varepsilon = P^2/2m$ with $\mathbf{V}_{\mathbf{P}} = \mathbf{P}/m$ and constant electric field \mathbf{E} the whole Fermi surface, as a rigid object, is shifted in velocity space at distance $\Delta \mathbf{V} = e\mathbf{E}\tau/m$. And for the current we obtain the Drude formula

$$\mathbf{j} = \sigma \mathbf{E}, \quad \sigma = e^2 n_D \tau / m, \quad (143)$$

where n_D is the electron volume density in D dimensional space.

The motivation of the Enskog ansatz is that \mathcal{Q} and φ are smooth functions of energy and momentum and sharp dependence is concentrated in the energy and momentum derivatives.

$$\Delta = \delta n \approx -\varphi \frac{d\bar{n}}{d\varepsilon} = \frac{(1 - \bar{n}) \bar{n}}{T} \varphi. \quad (144)$$

Using these variables we have

$$\frac{n_{\mathbf{p}}}{1 - n_{\mathbf{p}}} = \exp(-(\varepsilon_{\mathbf{p}} - \varphi_{\mathbf{p}} - \varepsilon_{\mathbf{F}})/T) \quad (145)$$

and for its variation

$$\delta \frac{n_{\mathbf{p}}}{1 - n_{\mathbf{p}}} = \frac{\varphi_{\mathbf{p}}}{T} \exp(-(\varepsilon_{\mathbf{p}} - \epsilon_{\mathbf{F}})/T) = \frac{\bar{n}}{1 - \bar{n}} \frac{\varphi_{\mathbf{p}}}{T}. \quad (146)$$

Taking into account that term in brackets [...] in Eq. (128) is in equilibrium zero, for calculation of variation $\delta \bar{\mathcal{Z}}$ we have to calculate only his variations. In such a way using additionally Eq. (130) we obtain

$$\begin{aligned} \delta \mathcal{Z} = & (1 - n)(1 - n_1)(1 - n')(1 - n'_1) \\ & \times \frac{1}{T} \left[e^{-(\varepsilon' - \epsilon_{\mathbf{F}})/T} (\varphi' + \varphi'_1) e^{-(\varepsilon'_1 - \epsilon_{\mathbf{F}})/T} \right. \\ & \left. - e^{-(\varepsilon - \epsilon_{\mathbf{F}})/T} (\varphi + \varphi_1) e^{-(\varepsilon_1 - \epsilon_{\mathbf{F}})/T} \right]. \end{aligned} \quad (147)$$

For this variation on the energy surface $\varepsilon' + \varepsilon'_1 = \varepsilon + \varepsilon_1$ we have

$$\begin{aligned} \delta \mathcal{Z} = & \frac{1}{T} e^{-(\varepsilon - \epsilon_{\mathbf{F}})/T} (1 - n) e^{-(\varepsilon_1 - \epsilon_{\mathbf{F}})/T} (1 - n_1) \\ & \times (1 - n')(1 - n'_1) [\varphi' + \varphi'_1 - \varphi - \varphi_1]. \end{aligned} \quad (148)$$

Using again Eq. (130) we finally arrive in linearized approximation

$$\delta \mathcal{Z} = \frac{1}{T} \bar{n} \bar{n}_1 (1 - \bar{n}') (1 - \bar{n}'_1) (\varphi' + \varphi'_1 - \varphi - \varphi_1). \quad (149)$$

And linearized Stoss-integral [47, Eq. (74.24)]

$$\begin{aligned} \text{St}(\mathbf{p}) = & \frac{1}{T} \int w \bar{n} \bar{n}_1 (1 - \bar{n}') (1 - \bar{n}'_1) (\varphi' + \varphi'_1 - \varphi - \varphi_1) \\ & \times \delta(\varepsilon' + \varepsilon'_1 - \varepsilon - \varepsilon_1) \frac{d^D p_1 d^D p'}{(2\pi)^{2D}}. \end{aligned} \quad (150)$$

Where argument of the Stoss-integral \mathbf{p} is fixed and $\bar{n} = n^{(0)}(\varepsilon_{\mathbf{p}})$ can be written before the integral. According momentum conservation in Eq. (122) $\mathbf{p}'_1 = \mathbf{p} + \mathbf{p}_1 - \mathbf{p}'$ and $n'_1 = n^{(0)}(\varepsilon_{\mathbf{p} + \mathbf{p}_1 - \mathbf{p}'})$ Integration on two dimensional momentum space we will perform as integration on the Constant Energy Curves (CEC) followed by the energy integration

$$\int_{\mathbf{p}} \dots d^2 p = \int d\varepsilon \oint_{\varepsilon_{\mathbf{p}} = \varepsilon} \dots \frac{dl}{v(\mathbf{p})}, \quad dl = dp_l, \quad (151)$$

where $l \equiv p_l$ is the length in \mathbf{p} -space along the CEC. We will apply this formula for the integration with respect of \mathbf{p}_1 and \mathbf{p}' . Starting with $d^2 p_1 = dl_1 d\varepsilon_1 / v_1$ the integration of δ -function in the integrant of Eq. (150) gives with respect of ε_1 gives

$$\begin{aligned} \varepsilon_1 = & \varepsilon' + \varepsilon'_1 - \varepsilon, \\ \bar{n}_1 = & n^{(0)}(\varepsilon' + \varepsilon'_1 - \varepsilon) = \frac{1}{\exp((\varepsilon' + \varepsilon'_1 - \varepsilon - \epsilon_{\mathbf{F}})/T) + 1}. \end{aligned} \quad (152)$$

and this energy argument is supposed in the next representation of the Stoss-integral

$$\text{St}(\mathbf{p}) = \frac{\bar{n}(\varepsilon(\mathbf{p}))}{T} \oint_{l_1} \int_{\varepsilon'} \oint_{l'} w \bar{n}_1 (1 - \bar{n}') (1 - \bar{n}'_1) \times [\varphi' + \varphi'_1 - \varphi - \varphi_1] \frac{dl_1 d\varepsilon' dl'}{(2\pi)^4 v_1 v'}.$$
(153)

For numerical implementation we need to use the function $\mathbf{p}' = \mathbf{p}'(\varepsilon', l')$ and $\mathbf{p}_1 = \mathbf{p}_1(\varepsilon_1, l_1)$ which express the momentum (p_x, p_y) as function of the energy of CEC ε and the length p_l along it. Then in the integrant we calculate

$$\mathbf{p}'_1 = \mathbf{p} + \mathbf{p}_1 - \mathbf{p}', \quad v_1 = v_F(\mathbf{p}_1), \quad v' = v_F(\mathbf{p}'),$$
(154)

$$\varepsilon'_1 = \varepsilon(\mathbf{p}'_1), \quad \varepsilon_1 = \varepsilon(\mathbf{p}_1), \quad \varepsilon' = \varepsilon(\mathbf{p}'),$$
(155)

equilibrium distributions from Eq. (127) and w from Eq. (123).

For the static homogeneous electric field the kinetic equation Eq. (126) writes

$$-\mathbf{F} \cdot \mathbf{v}_\mathbf{p} = T \text{St}(\mathbf{p}), \quad \mathbf{F} \equiv \frac{ea_0 \mathbf{E}}{\hbar} (1 - \bar{n}) \bar{n}.$$
(156)

So introduced variable \mathbf{F} has dimension of frequency and $\mathbf{v}_\mathbf{p}$ has dimension of energy; $\mathbf{V}_\mathbf{p} = a_0 \mathbf{v}_\mathbf{p} / \hbar$ has dimension of velocity. For the energy shift $\varphi(\mathbf{p})$ the kinetic equation is actually a system of in-homogeneous linear equations. For this system we apply a relaxation scheme

$$\varphi = \frac{\mathbf{F} \cdot \mathbf{v}_\mathbf{p} + \bar{n} \int w \bar{n}_1 (1 - \bar{n}') (1 - \bar{n}'_1) [\varphi' + \varphi'_1 - \varphi_1] \mathcal{D}}{\bar{n} \int w \bar{n}_1 (1 - \bar{n}') (1 - \bar{n}'_1) \mathcal{D}},$$

$$\mathcal{D} \equiv \frac{dl_1 d\varepsilon' dl'}{(2\pi)^4 v_1 v'}, \quad \int \equiv \oint_{l_1} \int_{\varepsilon'} \oint_{l'}.$$
(157)

As $p_x, p_y \in (0, 2\pi)$ are actually dimensionless phases, \mathcal{D} has dimension of 1/energy; the vector $\mathbf{P} = \hbar \mathbf{p} / a_0$ has dimension of momentum.

In the right side of Eq. (157) we apply the old iteration and explicitly we obtain the new one $\varphi^{(\text{new})}$. It is also possible to apply successive over-relaxation

$$\varphi^{(\text{sor})} = \varphi + (\varphi^{(\text{new})} - \varphi) \omega^{(\text{sor})}, \quad 1 < \omega^{(\text{sor})} < 2.$$
(158)

We can take say $N_\varepsilon = 101$ CEC in the energy interval $(\epsilon_F - 5T, \epsilon_F + 5T)$ and $N_p = 100$ points along every CEC. Having this solution we can express the current Eq. (132) as

$$\mathbf{j} = 2e \int \left(\frac{a_0}{\hbar} \mathbf{v}_\mathbf{p} \right) \left[(1 - \bar{n}) \bar{n} \frac{\varphi}{T} \right] \frac{d^2 p}{(2\pi a_0)^2},$$
(159)

where in parentheses and brackets we recognize sequentially \mathbf{V}_p and δn and multiplier 2 comes from spin summation. At low temperatures according Eq. (136) and Eq. (136) we have

$$\mathbf{j} = 2e \oint_{\epsilon_p = \epsilon_F} \left(\frac{a_0}{\hbar} \frac{\mathbf{v}_p}{v_p} \right) \varphi \frac{dl}{(2\pi a_0)^2}, \quad \varphi = \mathbf{v}_p \cdot \mathbf{Q}. \quad (160)$$

The conductivity can be determined as ratio $\sigma = j/E$ and due to symmetry of the quadratic lattice the orientation of \mathbf{E} is irrelevant. Finally linear regression $\varrho_\Omega = 1/\sigma$ versus T^2 gives the searched coefficient A_Ω which is the fingerprint of the applicability of the usual Landau Fermi liquid theory. The numerical implementation is described in the next sub-section. Where for illustration we neglect consideration of the real energy of the quasi-particles, cf. Ref. [47, Eqs. (74.17) and (74.21)]. The application of so derived kinetic equation to derivation of kinetics coefficient will be subject of a different study.

4.1 Re-scaling of energy

Roughly speaking, the science begins with simplicity and perhaps linear dependence is the simplest possibility. In Fig. 12 is depicted a correlation between the experimentally measured $\ln T_c$ and the theoretically calculated reciprocal coupling constant $1/\lambda$. In spite of many approxima-

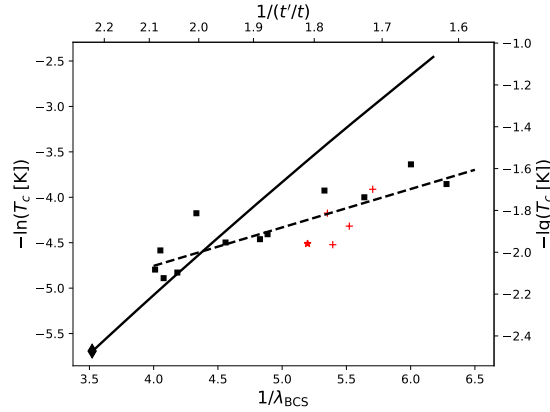


Figure 12: BCS correlation between the critical temperature $-\ln(T_c)$ and coupling constant λ . According to Eq. (66) this should be in initial approximation a straight line. The high correlation coefficient $\rho > 0.82$ is a hint that nature wishes to tell us something. The straight line is derived supposing that for different cuprates only position of $4s$ level it is ϵ_s is different and all other parameters of the Hamiltonian are constant, and $J_{sd} = 2776$ meV. Within this approximation the coupling constant λ is a linear function of t'/t . The slope of the linear regression of the experimental data (dashed line) from Pavarini *et al.* [16] (\blacksquare), Kaminski *et. al.* [24] for underdoped Bi-2212 (+) and ARPES data [26] (\star) (same as in Fig. 5) is lower than the $1/\lambda$ line (continuous) line. We interpret this difference as a linear dependence of $1/J_{sd}$ as function of ϵ_s .

tions the LCAO method for the band theory and common value of the exchange integral J_{sd} for

all cuprates we arrive to the conclusion that linear regression can be used for prediction of the critical temperature T_c of some new cuprate. In our opinion it is a good step in our quantitative description of the theory of high- T_c superconductivity which starts with calculation of T_c . In our LCAO analysis we follow the detailed works by Andersen *et al.* [14, 15, 16]. However, it is well known that electron band calculations give significantly broader conductivity band than observed by photoemission data. In order to solve this contradiction we make a compromise re-normalizing all energy parameters given by the group of Andersen by a common energy denominator: energy/ $=Z_\epsilon$. We choose $Z_\epsilon = 3.34$ in order for the Fermi velocity V_F for optimally doped $\text{Bi}_2\text{Sr}_2\text{Ca}_1\text{Cu}_2\text{O}_8$ to be close to the ARPES data by Zhou *et al.* [59, 110, Chap. 3, Fig. 3.21 and Fig. 1] $V_F = 37$ km/s. See also [59, 111, Fig. 1.1, K. A. Müller]. We use Fermi velocity V_F for $\epsilon_F - \epsilon > \hbar\omega_D$, for energy difference lower than the Debye frequency $\hbar\omega_D$ due to polaronic effects the slope of energy dispersion is smaller [55, Eqs. (65.12-13)]

$$V_F^{(0)} = \left. \frac{\partial \epsilon}{\partial P} \right|_{(\epsilon_F - \epsilon) < \hbar\omega_D}. \quad (161)$$

This change of the slope is evident in the ARPES data we use not only for Bi2212 but for all studied materials [59, 110, Chap. 3, Fig. 3.21 and Fig. 1].

The corresponding re-normalized parameters are represented in Table 3. The re-normalized optical mass $m_{\text{opt}} \approx 3$ is already an acceptable 3% agreement with the effective mass of Cooper pairs (per particle) $m_{\text{eff}} \approx 5.1 \times 0.6 = 3.06$ if we take into account that 40% of the mass can be attributed to the grain boundaries [75].

ϵ_s	ϵ_p	ϵ_d	t_{sp}	t_{pp} [69]	t_{pd}
1.2	-0.27	0.0	0.6	0.06	0.45

Table 3: Re-normalized single site energies ϵ , hopping amplitudes t in eV and effective masses from Table 1 taken from Refs. [14, 16] with the energy denominator $Z_\epsilon = 3.34$; $m_{\text{opt}}^{(\text{ren})} = Z_\epsilon m_{\text{opt}} = 3.34 \times 0.89 = 2.97 \approx 3$ (from Table 2).

Now J_{sd} has the more acceptable value of 2.776 eV, too. The re-scaling of the energy is somehow in agreement with atomic and ionic spectra because for all atoms and single charge ions the energies of $4s^2 3d^n \leftrightarrow 4s^1 3d^{n+1}$ never exceed 3 eV. Another hint for significant energy re-scaling gives the infrared absorption of cuprates in energy ~ 1 eV, for a reference if IR spectra see the monograph by Plakida [45]. The simplest possible explanation is that we observe absorption between filled $3d$ conduction band and completely empty $4s$ band. The corresponding theory is too simple to attract attention for article publication.

The high correlation coefficient $\rho > 0.82$ reveals that less 20% deviation from the straight line can be ascribed to the material science of accessories related to the specific properties of the crystal structure.

No doubts Pavarini *et al.* [16] T_c - r correlation is perhaps the most significant hint revealing the mechanism of high- T_c superconductivity; this article received more than 555 citations for the

last 20 years. Alas we do not find theoretical attempts to explain this remarkable correlation. Moreover it is proclaimed as *empirical correlation* [59, P. A. Lee, Chap. 14, Page 531]. and *Who is afraid of Virginia Woolf* the authors of Ref. [16] are reluctant to consider the fundamental grounds. According to our traditional interpretation we are witnesses of standard BCS correlation $-\ln T_c$ versus $1/\lambda$ for which we have to apply Pokrovsky theory [79, 80] for anisotropic superconductors. It is a property of LCAO model applied to s - d exchange interaction that BCS coupling constant λ is linear function of the ratio t'/t parameterizing the shape of the Fermi contour at optimal doping. Using $t'/t = 0.3$ in their numerical calculation [59, 112, K. A. Müller, Fig. 1.7] have shown that $\Delta_{\max} \propto T_c$. See also the study by Kugler *et al.* [113] reproduced by Kirtley and Tafuri [59, Fig. 2.31] where $2\Delta_{\max}/T_c \approx 4.3$ which is in acceptable 5% agreement with the BCS value of 4.116 from Table 2 according to Pokrovsky's theory [79], calculated as

$$\frac{2\Delta_{\max}}{T_c} = \frac{2\pi}{\gamma} \frac{\max |\Delta_{\mathbf{p}}|}{\exp \left\{ \frac{\langle \Delta_{\mathbf{p}}^2 \ln |\Delta_{\mathbf{p}}| \rangle}{\langle \Delta_{\mathbf{p}}^2 \rangle} \right\}}, \quad \Delta_{\mathbf{p}}(T) = \tilde{\Xi}(T) \tilde{\chi}_{\mathbf{p}} \quad (162)$$

or

$$\frac{2}{T_c} \exp \left(\langle \Delta_{\mathbf{p}}^2 \ln |\Delta_{\mathbf{p}}| \rangle / \langle \Delta_{\mathbf{p}}^2 \rangle \right) \Big|_{T=0} = \frac{2\pi}{\gamma} \approx 3.53. \quad (163)$$

We have applied a 60 years old theory to a 30 years old experimental problem and have obtained acceptable understanding of the thermodynamics of high- T_c cuprates. The shape of the Fermi contour and the s - d hybridization of the conduction band are determined by the position of Cu4s level with respect to Cu3d level. Here we have to give an indispensable credit to the intuition of Roehler [11, 12] who has emphasized the importance of Cu4s long time ago. We have to repeat the banal phrase that physics is an experimental science because in the early attempts to build the foundation of the theory of high- T_c superconductivity the Cu4s state has been ignored in the sophisticated lattice models [114, 2, 115, 83] and initial set of dogmas [116]. According to the best of our knowledge the Cu4s state was never incorporated as an indispensable ingredient of the mechanism of high- T_c superconductivity.

Last but not least, we wish to explain why so simple ingredients of the theory have to wait quarter of century to be incorporated in a text-book compilation explaining main properties of high- T_c superconductivity. As a simple example we have to consider how stubborn was one of the authors of the present study (TMM): Long time ago the late E.H. Brand explained that in his MPI there is a guy who only looking on the Fermi surface can immediately guess whether the cuprate T_c is high or low. The stupid contra-argument that it is impossible was base on the conclusion that T_c is determined by particle-particle interaction and the Fermi surface “*Thou comest in such a questionable shape*” [117, Shakespeare, Hamlet, Act. 1, Scene 4, motto of Chap. 9] is irrelevant. However for cuprates Cu4s state determines simultaneously s - d hybridization with corresponding coupling constant and the shape of the Fermi contour. As a training for the eye we draw in Fig. 13 the Fermi contours for the cuprates with 3 different critical temperatures. Analyzing the subtle difference in the shape we can evaluate the professionalism of the colleagues working in the electron-band calculation.

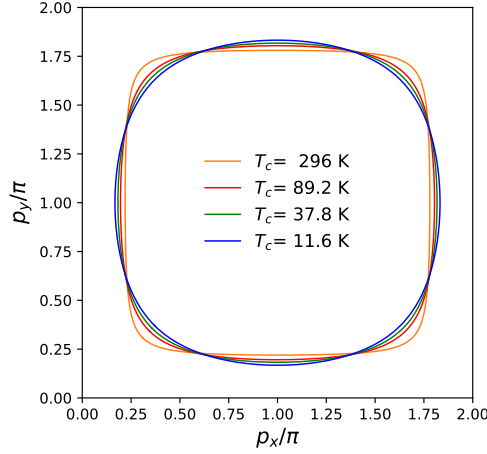


Figure 13: Three rounded-square Fermi contours for optimally doped concentration $f = 0.58$ with different critical temperatures T_c . In the used LCAO approximation the shape of the contours is determined by the equation $-2t [\cos(p_x) + \cos(p_y)] + 4t' \cos(p_x) \cos(p_y) = \text{const.}$ The contour with lowest T_c is the most rounded one, while the highest T_c contour with higher t'/t ratio according to Fig. 6 and Fig. 12 corresponds to maximal curvature at the Brillouin zone diagonals. The difference in the shape is subtle, but subtle is the Lord. In order to reach room T_c (blue dream of physicists) by a meta-stable cuprate layer according to our linear extrapolation in Fig. 12, it is necessary the $\text{Cu}4s$ level ϵ_s to be only slightly above the Fermi level ϵ_F using an appropriate apex structure ($\epsilon_s - \epsilon_F > 2T_c$). *Raffiniert ist der Her Got aber boshafft is er nicht* – it is a doable task for MBE (Molecular Beam Epitaxy) technologists. The basic parameters corresponding to these Fermi contours are given in Table 4.

Considering *why high temperature superconductivity is difficult* Kivelson and Fradkin in Ref. [59, Chap. 15] cited the well known article *more is different* (quantity is itself a quality :-)) but an *enemy of working class* was a great trivialisator. We repeat that linear temperature dependence of resistivity and strong anisotropy of the lifetime can be understand not in Fermi liquid but in gaseous approach. Simultaneous experimentally confirmed relation between gap anisotropy and critical temperature Eq. (163) are hints for conventional behavior of cuprates. *We fools of nature* (Act. 1, Scene 4) have only to put in the agenda calculation of J_{sd} and to explain the antiferromagnetic sign of the exchange interaction between itinerant electrons in the conduction band. The spin-singlet pairing is most likely to arise on the border of antiferromagnetism, cf. [59, Sec. 16.5].

Let us repeat and clarify the basic idea. For cuprate superconductors the most typical Kondo interaction substitutes the electron-phonon interaction as pairing mechanism. The applicability of the standard BCS scheme is checked by the fit of parameters. The comparison with the experiment convincingly demonstrates that ratio of critical temperature and exchange amplitude T_c/J_{sd} see Table 2, is so small that Eliashberg type corrections taking into account retardation effects are negligible. Real interaction amplitude is actually not J_{sd} but the eigenvalue of the

ϵ_s [eV]	ϵ_F [eV]	t'/t	λ	T_c [K]
0.569	0.493	0.623	0.284	296.75
1.237	0.557	0.542	0.224	89.22
1.619	0.582	0.500	0.194	37.81
2.096	0.607	0.454	0.162	11.65

Table 4: Parameters of the Fermi contours drawn in Fig. 13. The energy of Cu4s level ϵ_s (the first column) and the Fermi level ϵ_F (the second column) are taken into account from Cu3d_{x²-y²} atomic level. These energies are re-scaled by a multiplier $Z_\epsilon = 3.34$ chosen to describe the Fermi velocity according to ARPES data. The BCS coupling constant λ is calculated supposing that the exchange integral $J_{sd} = 2.776$ eV has almost one and the same value for all CuO₂ planes. The dimensionless t'/t parameter is widely used in many studies. The critical temperature, actually its logarithm is well described by the linear correlation in Fig. 12 and its high correlation coefficient encourages us to represent in the first row of the table a linear extrapolation of 15% difference for the t'/t , from 0.542 to 0.623 for 50% decrease of ϵ_s . This extrapolation is marked by \blacklozenge in the lower left corner of Fig. 12. Whether chemistry allows existence of such metastable structure – this is the question.

pairing kernel V_0 Eq. (63), for which T_c/V_0 is also small enough. One can say the same for the Euler-Mascheroni energy E_C which substitutes the Debye frequency in the formula for the critical temperature Eq. (66). Here we have to emphasize one important difference between phonon superconductors and the exchange mediated cuprates. For phonon superconductors the applicability of the Pokrovsky theory is a consequence of the weak coupling limit. However for s - d exchange superconductors with a single transition atom in the elementary cell the pairing interaction is separable. This property of the Hamiltonian can be checked by one A4 sheet of handwriting pen calculation. In other words the weak coupling Pokrovsky approximation is an exact result for the s - d exchange applied to LCAO electron band functions. In this sense cuprate superconductivity mediated by s - d exchange interaction is more conventional than the phonon superconductivity. We can use BCS trial function even in the case when BCS coupling constant λ is scarcely small Table 2, simply because the pairing is exactly separable and we do not need to take into account any corrections. That is why for cuprates calculated within s - d LCAO approximation Δ_{\max}/T_c , see Eq. (163), is within high precision of 5% agreement with weak coupling Pokrovsky theory for the anisotropic superconductors; the ARPES data are not directly involved in this agreement; see also model calculations [118] for parabolic dispersion where by chance we have numerical coincidence with the tunneling experiment. Here we have to mention that for MgB₂ we can see the the same good work for the week coupling approximation [119]. In other words the separability of the pairing interaction extends the applicability of the weak coupling theory. It is not necessary for the coupling itself to be small.

Our final remark is that for the relative jump of heat capacity for cuprates [118] and MgB₂ [119] we can see the same good agreement with the Pokrovsky theory for anisotropic BCS super-

conductors

$$\frac{\Delta C}{C_N(T_c)} = \frac{12}{7\zeta(3)} \frac{\langle \Delta_{\mathbf{p}}^2 \rangle^2}{\langle \Delta_{\mathbf{p}}^4 \rangle}. \quad (164)$$

This result can be easily re-derived by minimization of the free energy [120]; for applications see also the comments [121, 122].

DISCUSSION AND CONCLUSIONS

5.1 Psychoanalysis of the phenomenology

Analyzing the zone-diagonal-dominated transport in high- T_c cuprates Ioffe and Millis [34] pointed out that angular dependence of the Fermi-liquid scattering rate is reminiscent of $d_{x^2-y^2}$ superconducting gap and proposed that the life time is caused by interaction of electrons with nearly singular $d_{x^2-y^2}$ pairing fluctuations. Led by religious arguments, here we have to insert only a minor correction to their consideration: both the pairing fluctuations and the scattering rate in the normal phase has to be derived from one and the same interaction Hamiltonian.

5.2 “In the beginning was the Hamiltonian, and the \hat{H} was by the God, and \hat{H} was the God.” Saint John (citation by memory)

When Allah wrote the Hamiltonian the Universe blew up; something are so serious that about them we can speak only by joke; *Nota bene* by Niels Bohr. Popularizing this idea, St. John emphasized (citing by memory) that in the beginning was the Hamiltonian. We conclude that one and the same Shubin-Kondo-Zener s - d exchange Hamiltonian creates the pairing in the superconducting phase of CuO_2 high- T_c superconductors and the scattering rate of the charge carriers in the normal phase. In such a way the best investigated high- T_c materials have a common basic Hamiltonian single electron hopping between $\text{Cu}3d_{x^2-y^2}$, $\text{O}2p_x$, $\text{O}2p_y$, and $\text{Cu}4s$, and the electron exchange with antiferromagnetic sign between $\text{Cu}4s$ and $\text{Cu}3d_{x^2-y^2}$ orbitals. For every cuprate to this generic Hamiltonian, accessories describing double planes, chains, apex oxygen etc. have to be added. In the present work we demonstrate that the main phenomenological properties of the

normal charge carriers scattering time can be at least qualitatively derived from the s - d pairing exchange Hamiltonian. That is why the s - d exchange Hamiltonian can be put into the agenda to be treated by standard methods of the statistical mechanics which can explain the complete set of phenomena of the normal state of high- T_c cuprates. Definitely high- T_c is not a mystery – all details of its theory can be found in the textbooks written long time ago before Bednorz and Mueller to discover superconductivity in cuprates. We strongly believe that the approach we use interaction projected on LCAO basis is applicable for other transition metal perovskites and zero-sound propagating along the cold spot direction is a new phenomenon which we can predict if the s - d interaction has ferromagnetic sign. We suppose that charge neutral zero sound oscillations can be detected when they are converted in Tera-Hertz hyper-sound in the opposite sing of the transition metal perovskite. Excitation can be made by nonspecific rough impulse in the exciting side of the layered perovskite crystal. The sample has to be cut in $[110]$ plane.

Returning to the consideration of cuprates the Pavarini *et al.* [16] relation reveals also that exchange amplitude J_{sd} is a common constant for all cuprates and the difference in $T_{c, \max}$ is related to different band structure. Band structure calculations have low social rank, the specialists in these numerical calculations are not considered as theorists midst high level science fiction authors. But honest work is nevertheless *modus vivendi* at least at surviving level. Band calculators have to be proud that their noble efforts revealed which parameter is most important for determination of T_c which reveals the mechanism of high- T_c .

The band calculations can give a reliable set of LCAO parameters: transfer integrals and single site energies which together with s - d exchange integral completely determine the lattice Hamiltonian. Then calculation of kinetic properties is already a technical task of the statistical physics without the freedom to change the Hamiltonian and the rule of the game.

In the present work we qualitatively trace only the initial path which can be extended to the high-way of layered cuprate physics. And the developed methods can be useful for many other materials for which the exchange interaction is essential.

5.3 Small quantum of history

Analyzing only plane dimpling in $\text{YBa}_2\text{Cu}_3\text{O}_{7-\delta}$ even in 2000 Röhler [11, 12] emphasized that the $\text{Cu}4s\text{-}3d_{x^2-y^2}$ hybridization seems to be the crucial quantum chemical parameter controlling related electronic degree of freedom. We appreciate this early insight which becomes the precursor of the detailed electron band studies and microscopic investigation of the influence of s - d exchange originally suggested by Shubin [8] on the statistical properties of the cuprates.

Few words we have to add also to the history of 2-electron correlations. Soon after discovery of the electron J. J. Thompson [123] suggested that electric current is created by *electron doublets*. Later on in the beginning of quantum physics N. Bohr [124] considered that two electrons in helium are moving with opposite momenta $\mathbf{P}_1 = -\mathbf{P}_2$, this possibility for two s -electrons was experimentally observed in double Rydberg states of noble gas atoms, see the review by Read [125]. In this strongly correlated states two electrons with zero angular momentum fall simultaneously to the nucleus like resurrecting kamikaze.

The history of self-consistent approximation starts from 19th century and the first work on collective phenomena is the consideration by J.-C. Maxwell [126] that Saturn rings cannot be rigid discs but consist of self-consistent motion of gravitating particles. This idea was developed in the atomic physics by Hartree and Fock, and works by Bardeen, Cooper and Schrieffer [127] and Bogolyubov [128] develop for the physics of superconductivity the same idea of free particles moving in a self-consistent field created by the interaction Hamiltonian. We consider that Hubbard U_d , U_s and U_p have to be taken into a self-consistent way in the single site energies ϵ_d , ϵ_s and ϵ_p while the Schubin [8] s - d exchange is considered as the pairing interaction in the standard BCS scheme. The s - d exchange parameter J_{sd} is actually the main amplitude determining many phenomena with transition ion compounds; for a review of strong correlations and exchange phenomena see the monograph by Anisimov and Izyumov [129].

Having an unified scenario is indispensable, we open the Pandora box of the necessity of making compromises between researches in different areas. For example, an optical mass calculated according to *ab initio* band calculation exceeds almost 2π times the same determined by electrostatic modulation of the kinetic inductance. With such energy reduction the unexplained maximum of the mid infrared absorption can be explained as a direct inter-band absorption caused by electron transitions between conduction band and completely empty Cu4s band. This is however only an example which type of disagreement can create a trial for unified description of the electron properties of the CuO₂ plane.

We finish with one unresolved problem. What is the explanation of the anti-ferromagnetic sign of the Kondo s - d exchange in Cu transition ion J_{sd} ? The two electron exchange is a correlation, and words “strongly correlated” is repeated as mantra already 33 years (the age of Jesus Christ) in the physics of high- T_c superconductivity. The present work is not an exception. This anti-ferromagnetic sign is against the Hund rule from the atomic physics and indispensably requires consideration of strong correlations in the simplest cluster CuO₂ which plays an important fundamental role in the physics of cuprates. Multiplet splitting of energy levels of a transition ion surrounded by non-innocent ligands has been a fundamental problem of the quantum chemistry for decades. We hope that the development of the physics cuprates can stimulate the satisfactory solution of this old problem.

5.4 Results

This investigation of the electronic properties of a generic CuO₂ plane in the framework of the Shubin-Kondo-Zener s - d exchange interaction simultaneously describes two phenomena in cuprates. Using the Pokrovsky theory for the anisotropic gap BCS superconductors and a microscopic model to calculate a separable interaction, the following phenomena in the superconducting regime are quantitatively explained: 1) The dependency between the superconducting critical temperature T_c and the Cu4s energy level; 2) The scattering rate and the superconducting gap anisotropy, as our theoretical approach reproduces the phenomenological analysis Refs. [33, 34] performed to describe data from ARPES experiments on cuprates. Simply stated the hot/cold spots phenomenology is derived from a microscopic Hamiltonian describing the superconducting

spectrum of optimally doped and overdoped cuprates. Moreover, this theory is also applicable to underdoped cuprates if additional features like glassy nematicity is included as accomplished by Lee, Kivelson and Kim [41]. We can conclude that the electric charge fluctuations should be analyzed in the framework of the standard theory of electromagnetic fluctuations in continuous media [55, Chap. 8] and [48, Chap. 6].

Another result of this study is the prediction for propagation of zero sound in non-superconducting cuprates. For anti-ferromagnetic sign of the s - d interaction $J_{sd} > 0$ we have tendency for superconductivity, while for ferromagnetic sign, $J_{sd} < 0$, we expect zero sound to be observed. Superconductivity via the s - d exchange interaction can be reached only for anti-ferromagnetic sign meaning that in the normal phase of high- T_c cuprates propagation of zero sound is impossible, it is a dissipation mode. The thermal excitation of charge density fluctuation modes creates Ohmic resistivity and intensive scattering, and the strong angular dependence of this scattering rate causes the so called “hot spots” phenomenologically postulated for the interpretation of the experimental data [33]. In addition, it should be also noted that the thermal fluctuations of plasmons could contribute to the hot spots along the Fermi contour [130].

Now it is difficult to determine the zero sound propagation for different layered compounds; which material is more or less technologically appropriate for production of a clean ac -surface. This theoretical study is just the beginning, now it is turn for the experiments. As it seems the most probable solution would be provided by a thin layer geometry.

Let us repeat the main results obtained in our short study. We have derived a well-known and working phenomenology of the hot/cold spots along the Fermi contour of layered high- T_c cuprates. We use the most typical Kondo-Zener exchange interaction incorporated in the LCAO approach. Then we perform two standard reductions of one and the same Hamiltonian. The BCS one describes the well-known properties of the superconducting phase of the overdoped cuprates, while the Fermi liquid reduction explains the hot/cold spots phenomenology, which is our main result belonging to the physics of normal metals.

The next step will be the derivation of these result within some alternative approach and the main problem we set in the agenda is the derivation of J_{sd} exchange amplitude starting with LCAO approximation and Coulomb repulsion.

To summarize, our main result is a qualitative physical explanation rather than some technical details related to derivation of the necessary formulae. The new result is that the kernel of the Landau zero sound theory coincides with the kernel of the BCS coupling. This is a property of the s - d exchange interaction and is also a hint of the importance of this interaction.

Acknowledgments

Authors are thankful to Patrick Lee for pointing out significant works on T -linearity of conductivity. The authors are also thankful to Davide Valentinis for the interest to the present study and pointing out for recently appeared related works on kinetic theories for the electrodynamic response of Fermi liquids and anisotropic metals [100, 101, 102]. Critical remarks by Valery Pokrovsky are also highly appreciated. Considerations with Mihail Mishonov and Evgeni Penev in the early stages of this study are highly appreciated. This work is supported by grant KP-06-N58/1 from 15.11.2021 of the Bulgarian National Science Fund.

Eleven years ago a preliminary fragment of the present work was represented at the conference in memoriam of Matey Mateev. When proximity of the three levels in CuO_2 plane was juxtaposed to the sequence of three holidays in the spring Alvaro De Rujula said – you are right, congratulations happy Easter to the CuO_2 plane. One of the authors of the present work (TMM) received big impetus to finalize the initial idea.

The authors are also thankful to Hassan Chamati for the interest to the present study, creative atmosphere in ISSP, BAS, critical reading of the manuscript, stimulating discussions and many suggested amendments and references. The initial version of this work was presented in a conference devoted to the 90th anniversary of VLP. Different our results from this manuscript were reported in conferences on physics of superconductivity and magnetism in Bodrum and Madrid. We are thankful to colleagues for the comments and reviews.

BIBLIOGRAPHY

- [1] B. Keimer, S. A. Kivelson, M. R. Norman, S. Uchida, and J. Zaanen. From quantum matter to high-temperature superconductivity in copper oxides. *Nature*, 518(7538):179–186, Feb 2015. doi:[10.1038/nature14165](https://doi.org/10.1038/nature14165).
- [2] V. J. Emery. Theory of High- T_c Superconductivity in Oxides. *Phys. Rev. Lett.*, 58:2794–2797, Jun 1987. URL: <https://link.aps.org/doi/10.1103/PhysRevLett.58.2794>, doi:[10.1103/PhysRevLett.58.2794](https://doi.org/10.1103/PhysRevLett.58.2794).
- [3] F. C. Zhang and T. M. Rice. Effective Hamiltonian for the superconducting Cu oxides. *Phys. Rev. B*, 37:3759–3761, Mar 1988. URL: <https://link.aps.org/doi/10.1103/PhysRevB.37.3759>, doi:[10.1103/PhysRevB.37.3759](https://doi.org/10.1103/PhysRevB.37.3759).
- [4] Daniel P. Arovas, Erez Berg, Steven A. Kivelson, and Srinivas Raghu. The Hubbard Model. *Ann. Rev. Condens. Matter Phys.*, 13(1):239–274, Mar 2022. doi:[10.1146/annurev-conmatphys-031620-102024](https://doi.org/10.1146/annurev-conmatphys-031620-102024).
- [5] J. Spałek. t - J Model Then and Now: a Personal Perspective from the Pioneering Times. *Acta Phys. Pol. A*, 111(4):409, Apr 2007. arXiv:[0706.4236](https://arxiv.org/abs/0706.4236), doi:[10.12693/APhysPolA.111.409](https://doi.org/10.12693/APhysPolA.111.409).
- [6] Józef Spałek, Michał Żegrodnik, and Jan Kaczmarczyk. Universal properties of high-temperature superconductors from real-space pairing: $t - J - U$ model and its quantitative comparison with experiment. *Phys. Rev. B*, 95:024506, Jan 2017. URL: <https://link.aps.org/doi/10.1103/PhysRevB.95.024506>, doi:[10.1103/PhysRevB.95.024506](https://doi.org/10.1103/PhysRevB.95.024506).
- [7] J. Spałek, M. Fidrysiak, M. Żegrodnik, and A. Biborski. Superconductivity in high- T_c and related strongly correlated systems from variational perspective: Beyond mean field theory. *Phys. Rep.*, 959:1–117, 2022. URL: <https://www.sciencedirect.com/science/article/pii/S0370157322000503>, doi:<https://doi.org/10.1016/j.physrep.2022.02.003>.
- [8] S. Schubin and S. Wonsowsky. On the electron theory of metals. *Proc. R. Soc. London, Ser. A*, 145(854):159–180, 1934. doi:[10.1098/rspa.1934.0089](https://doi.org/10.1098/rspa.1934.0089).

- [9] C. Zener. Interaction Between the d Shells in the Transition Metals. *Phys. Rev.*, 81:440–444, Feb 1951. doi:[10.1103/PhysRev.81.440](https://doi.org/10.1103/PhysRev.81.440).
- [10] Jun Kondo. Anomalous Scattering Due to s-d Interaction. *J. Appl. Phys.*, 37(3):1177–1180, 1966. doi:[10.1063/1.1708385](https://doi.org/10.1063/1.1708385).
- [11] J. Röhler. Plane dimpling and Cu4s hybridization in YBa₂Cu₃O_x. *Physica B: Cond. Matter*, 284-288:1041–1042, 2000. doi:[10.1016/S0921-4526\(99\)02386-8](https://doi.org/10.1016/S0921-4526(99)02386-8).
- [12] Jürgen Röhler. The underdoped-overdoped transition in YBa₂Cu₃O_x. *Physica C: Supercond. and Appl.*, 341-348:2151–2152, 2000. URL: <https://www.sciencedirect.com/science/article/pii/S0921453400011345>, doi: [https://doi.org/10.1016/S0921-4534\(00\)01134-5](https://doi.org/10.1016/S0921-4534(00)01134-5).
- [13] T. M. Mishonov and E. S. Penev. *Theory of High Temperature Superconductivity. A Conventional Approach*. World Scientific, New Jersey, 2010. doi:[10.1142/8104](https://doi.org/10.1142/8104).
- [14] O. K. Andersen, A. I. Liechtenstein, O. Jepsen, and F. Paulsen. LDA energy bands, low-energy hamiltonians, t' , t'' , $t_{\perp}(\mathbf{k})$, and J_{\perp} . *J. Phys. Chem. Solids*, 56(12):1573–1591, 1995. Procs. Conf. Spectroscopies in Novel Superconductors. doi:[https://doi.org/10.1016/0022-3697\(95\)00269-3](https://doi.org/10.1016/0022-3697(95)00269-3).
- [15] O. K. Andersen, S. Y. Savrasov, O. Jepsen, and A. I. Liechtenstein. Out-of-plane instability and electron-phonon contribution to s- and d-wave pairing in high-temperature superconductors; LDA linear-response calculation for doped CaCuO₂ and a generic tight-binding model. *J. Low Temp. Phys.*, 105(3-4):285–304, Nov 1996. doi:[10.1007/BF00768402](https://doi.org/10.1007/BF00768402).
- [16] E. Pavarini, I. Dasgupta, T. Saha-Dasgupta, O. Jepsen, and O. K. Andersen. Band-Structure Trend in Hole-Doped Cuprates and Correlation with $T_{c\text{max}}$. *Phys. Rev. Lett.*, 87:047003, Jul 2001. doi:[10.1103/PhysRevLett.87.047003](https://doi.org/10.1103/PhysRevLett.87.047003).
- [17] Z.-X. Shen and D. S. Dessau. Electronic structure and photoemission studies of late transition-metal oxides - Mott insulators and high-temperature superconductors. *Phys. Rep.*, 253(1):1–162, 1995. doi:[https://doi.org/10.1016/0370-1573\(95\)80001-A](https://doi.org/10.1016/0370-1573(95)80001-A).
- [18] M. Randeria. High- T_c superconductors: New insights from angle-resolved photoemission. *J. Supercond.*, 9:471–474, 1996. arXiv:[cond-mat/9709107](https://arxiv.org/abs/cond-mat/9709107), doi:[10.1007/BF00727299](https://doi.org/10.1007/BF00727299).
- [19] D. L. Feng, N. P. Armitage, D. H. Lu, A. Damascelli, J. P. Hu, P. Bogdanov, A. Lanzara, F. Armita Ronning, K. M. Shen, H. Eisaki, C. Kim, Z.-X. Shen, J.-i. Shimoyama, and K. Kishio. Bilayer Splitting in the Electronic Structure of Heavily Overdoped Bi₂Sr₂CaCu₂O_{8+δ}. *Phys. Rev. Lett.*, 86:5550–5553, Jun 2001. URL: <https://>

link.aps.org/doi/10.1103/PhysRevLett.86.5550, [arXiv:cond-mat/0102385](https://arxiv.org/abs/cond-mat/0102385), [doi:10.1103/PhysRevLett.86.5550](https://doi.org/10.1103/PhysRevLett.86.5550).

- [20] T. Takeuchi, T. Yokoya, S. Shin, K. Jinno, M. Matsuura, T. Kondo, H. Ikuta, and U. Mizutani. Topology of the Fermi surface and band structure near the Fermi level in the Pb-doped $\text{Bi}_2\text{Sr}_2\text{CuO}_{6+\delta}$ superconductor. *J. Electron Spectrosc.*, 114-116:629–634, 2001. Procs. Eight Int. Conf. on Electronic Spectroscopy and Structure. [doi:10.1016/S0368-2048\(00\)00354-6](https://doi.org/10.1016/S0368-2048(00)00354-6).
- [21] N. P. Armitage, F. Ronning, D. H. Lu, C. Kim, A. Damascelli, K. M. Shen, D. L. Feng, H. Eisaki, Z.-X. Shen, P. K. Mang, N. Kaneko, M. Greven, Y. Onose, Y. Taguchi, and Y. Tokura. Doping Dependence of an n -Type Cuprate Superconductor Investigated by Angle-Resolved Photoemission Spectroscopy. *Phys. Rev. Lett.*, 88:257001, Jun 2002. [arXiv:cond-mat/0201119](https://arxiv.org/abs/cond-mat/0201119), [doi:10.1103/PhysRevLett.88.257001](https://doi.org/10.1103/PhysRevLett.88.257001).
- [22] D. L. Feng, C. Kim, H. Eisaki, D. H. Lu, A. Damascelli, K. M. Shen, F. Ronning, N. P. Armitage, N. Kaneko, M. Greven, J.-i. Shimoyama, K. Kishio, R. Yoshizaki, G. D. Gu, and Z.-X. Shen. Electronic excitations near the Brillouin zone boundary of $\text{Bi}_2\text{Sr}_2\text{CaCu}_2\text{O}_{8+\delta}$. *Phys. Rev. B*, 65:220501, May 2002. URL: <https://link.aps.org/doi/10.1103/PhysRevB.65.220501>, [arXiv:cond-mat/0107073](https://arxiv.org/abs/cond-mat/0107073), [doi:10.1103/PhysRevB.65.220501](https://doi.org/10.1103/PhysRevB.65.220501).
- [23] Andrea Damascelli, Zahid Hussain, and Zhi-Xun Shen. Angle-resolved photoemission studies of the cuprate superconductors. *Rev. Mod. Phys.*, 75:473–541, Apr 2003. [doi:10.1103/RevModPhys.75.473](https://doi.org/10.1103/RevModPhys.75.473).
- [24] A. Kaminski, H. M. Fretwell, M. R. Norman, M. Randeria, S. Rosenkranz, U. Chatterjee, J. C. Campuzano, J. Mesot, T. Sato, T. Takahashi, T. Terashima, M. Takano, K. Kad-owaki, Z. Z. Li, and H. Raffy. Momentum anisotropy of the scattering rate in cuprate superconductors. *Phys. Rev. B*, 71:014517, Jan 2005. [arXiv:cond-mat/0404385](https://arxiv.org/abs/cond-mat/0404385), [doi:10.1103/PhysRevB.71.014517](https://doi.org/10.1103/PhysRevB.71.014517).
- [25] D. S. Inosov, J. Fink, A. A. Kordyuk, S. V. Borisenko, V. B. Zabolotnyy, R. Schuster, M. Knupfer, B. Büchner, R. Follath, H. A. Dürr, W. Eberhardt, V. Hinkov, B. Keimer, and H. Berger. Momentum and Energy Dependence of the Anomalous High-Energy Dispersion in the Electronic Structure of High Temperature Superconductors. *Phys. Rev. Lett.*, 99:237002, Dec 2007. URL: <https://link.aps.org/doi/10.1103/PhysRevLett.99.237002>, [doi:10.1103/PhysRevLett.99.237002](https://doi.org/10.1103/PhysRevLett.99.237002).
- [26] I M Vishik, W S Lee, R-H He, M Hashimoto, Z Hussain, T P Devereaux, and Z-X Shen. ARPES studies of cuprate Fermiology: superconductivity, pseudogap and quasiparticle dynamics. *New J. Phys.*, 12(10):105008, Oct 2010. [doi:10.1088/1367-2630/12/10/105008](https://doi.org/10.1088/1367-2630/12/10/105008).

- [27] Rui-Hua He, M. Hashimoto, H. Karapetyan, J. D. Koralek, J. P. Hinton, J. P. Testaud, V. Nathan, Y. Yoshida, Hong Yao, K. Tanaka, W. Meevasana, R. G. Moore, D. H. Lu, S.-K. Mo, M. Ishikado, H. Eisaki, Z. Hussain, T. P. Devereaux, S. A. Kivelson, J. Orenstein, A. Kapitulnik, and Z.-X. Shen. From a Single-Band Metal to a High-Temperature Superconductor via Two Thermal Phase Transitions. *Science*, 331(6024):1579–1583, Mar 2011. URL: <http://dx.doi.org/10.1126/science.1198415>, [arXiv:1103.2329](https://arxiv.org/abs/1103.2329), [doi:10.1126/science.1198415](https://doi.org/10.1126/science.1198415).
- [28] H. Jang, S. Asano, M. Fujita, M. Hashimoto, D. H. Lu, C. A. Burns, C.-C. Kao, and J.-S. Lee. Superconductivity-Insensitive Order at $q \sim 1/4$ in Electron-Doped Cuprates. *Phys. Rev. X*, 7:041066, Dec 2017. [doi:10.1103/PhysRevX.7.041066](https://doi.org/10.1103/PhysRevX.7.041066).
- [29] Tianlun Yu, Christian E. Matt, Federico Bisti, Xiaoqiang Wang, Thorsten Schmitt, Johan Chang, Hiroshi Eisaki, Donglai Feng, and Vladimir N. Strocov. The relevance of ARPES to high- T_c superconductivity in cuprates. *npj Quantum Mater.*, 5:46, 2020. [doi:10.1038/s41535-020-0251-3](https://doi.org/10.1038/s41535-020-0251-3).
- [30] Yu He, Su-Di Chen, Zi-Xiang Li, Dan Zhao, Dongjoon Song, Yoshiyuki Yoshida, Hiroshi Eisaki, Tao Wu, Xian-Hui Chen, Dong-Hui Lu, Christoph Meingast, Thomas P. Devereaux, Robert J. Birgeneau, Makoto Hashimoto, Dung-Hai Lee, and Zhi-Xun Shen. Superconducting Fluctuations in Overdoped $\text{Bi}_2\text{Sr}_2\text{CaCu}_2\text{O}_{8+\delta}$. *Phys. Rev. X*, 11:031068, Sep 2021. URL: <https://link.aps.org/doi/10.1103/PhysRevX.11.031068>, [doi:10.1103/PhysRevX.11.031068](https://doi.org/10.1103/PhysRevX.11.031068).
- [31] Jonathan A. Sobota, Yu He, and Zhi-Xun Shen. Angle-resolved photoemission studies of quantum materials. *Rev. Mod. Phys.*, 93:025006, May 2021. [doi:10.1103/RevModPhys.93.025006](https://doi.org/10.1103/RevModPhys.93.025006).
- [32] M. Zonno, F. Boschini, and A. Damascelli. Time-resolved ARPES on cuprates: Tracking the low-energy electrodynamics in the time domain. *J. Electron Spectrosc.*, 251:147091, 2021. [arXiv:2106.11316](https://arxiv.org/abs/2106.11316), [doi:https://doi.org/10.1016/j.elspec.2021.147091](https://doi.org/10.1016/j.elspec.2021.147091).
- [33] R. Hlubina and T. M. Rice. Resistivity as a function of temperature for models with hot spots on the Fermi surface. *Phys. Rev. B*, 51:9253–9260, Apr 1995. [doi:10.1103/PhysRevB.51.9253](https://doi.org/10.1103/PhysRevB.51.9253).
- [34] L. B. Ioffe and A. J. Millis. Zone-diagonal-dominated transport in high- T_c cuprates. *Phys. Rev. B*, 58(17):11631–11637, Nov 1998. [doi:10.1103/PhysRevB.58.11631](https://doi.org/10.1103/PhysRevB.58.11631).
- [35] Jun Yong Khoo and Inti Sodemann Villadiego. Shear sound of two-dimensional Fermi liquids. *Phys. Rev. B*, 99(7):075434, Feb 2019. [arXiv:1806.04157](https://arxiv.org/abs/1806.04157), [doi:10.1103/PhysRevB.99.075434](https://doi.org/10.1103/PhysRevB.99.075434).

- [36] M P Gochan, J T Heath, and K S Bedell. Atypical behavior of collective modes in two-dimensional Fermi liquids. *J. Phys.: Condens. Matter*, 32(34):345602, May 2020. doi:[10.1088/1361-648x/ab8aa1](https://doi.org/10.1088/1361-648x/ab8aa1).
- [37] D. Valentinis, J. Zaanen, and D. van der Marel. Propagation of shear stress in strongly interacting metallic Fermi liquids enhances transmission of terahertz radiation. *Sci. Rep.*, 11(1):7105:13, 2021. doi:[10.1038/s41598-021-86356-2](https://doi.org/10.1038/s41598-021-86356-2).
- [38] Shanshan Ding and Shizhong Zhang. Fermi-Liquid Description of a Single-Component Fermi Gas with p -Wave Interactions. *Phys. Rev. Lett.*, 123:070404, Aug 2019. doi:[10.1103/PhysRevLett.123.070404](https://doi.org/10.1103/PhysRevLett.123.070404).
- [39] L. D. Landau. The Theory of a Fermi Liquid. *Sov. Phys. JETP*, 3:920–925, 1956. ZhETF **30**(6), 1058 Dec (1956), <http://www.jetp.ras.ru/cgi-bin/r/index/r/30/6/p1058?a=list>, (in Russian). URL: <http://jetp.ras.ru/cgi-bin/e/index/e/3/6/p920?a=list>.
- [40] L. D. Landau. Oscillations in a Fermi Liquid. *Sov. Phys. JETP*, 5:101–108, 1957. ZhETF **32**(1), 59 Dec (1957), <http://www.jetp.ras.ru/cgi-bin/r/index/r/32/1/p59?a=list>, (in Russian). URL: <http://jetp.ras.ru/cgi-bin/e/index/e/5/1/p101?a=list>.
- [41] Kyungmin Lee, Steven A. Kivelson, and Eun-Ah Kim. Cold-spots and glassy nematicity in underdoped cuprates. *Phys. Rev. B*, 94:014204, Jul 2016. doi:[10.1103/PhysRevB.94.014204](https://doi.org/10.1103/PhysRevB.94.014204).
- [42] Zi-Xiang Li, Steven A. Kivelson, and Dung-Hai Lee. Superconductor to metal transition in overdoped cuprates. *npj Quantum Mater.*, 6:36, 2021. URL: <https://www.nature.com/articles/s41535-021-00335-4>, arXiv:<https://arxiv.org/abs/2010.06091>, doi:[10.1038/s41535-021-00335-4](https://doi.org/10.1038/s41535-021-00335-4).
- [43] T. M. Mishonov, N. I. Zahariev, H. Chamati, and A. M. Varonov. Hot spots along the Fermi contour of high- T_c cuprates explained by s - d exchange interaction. *SN Appl. Sci.*, 4:242, 2022. arXiv:[2208.00936](https://arxiv.org/abs/2208.00936), doi:[10.1007/s42452-022-05106-9](https://doi.org/10.1007/s42452-022-05106-9).
- [44] T. M. Mishonov, N. I. Zahariev, H. Chamati, and A. M. Varonov. Possible zero sound in layered perovskites with ferromagnetic s - d exchange interaction. *SN Appl. Sci.*, 4:228, 2022. arXiv:[2208.00938](https://arxiv.org/abs/2208.00938), doi:[10.1007/s42452-022-05107-8](https://doi.org/10.1007/s42452-022-05107-8).
- [45] N. Plakida. *High-Temperature Cuprate Superconductors*. Springer, New York, 2010. doi:[10.1007/978-3-642-12633-8](https://doi.org/10.1007/978-3-642-12633-8).
- [46] N. F. Mott. *Metal-Insulator Transitions*. Taylor & Francis, London, 2 edition, 1990.
- [47] E. M. Lifshitz and L. P. Pitaevskii. *Physical Kinetics*, volume 10 of *Landau-Lifshitz course of theoretical physics*. Pergamon, New York, 1980.

- [48] A. A. Abrikosov, L. P. Gor'kov, and I. Ye. Dzyaloshinskii. *Methods of quantum field theory in statistical physics*. Prentice Hall, Englewood Cliffs, N.J., 1963.
- [49] A. A. Abrikosov. *Fundamentals of the Theory of Metals*. North Holland, Amsterdam, 1988.
- [50] I. M. Lifshits, M. Ya. Azbel, and M. I. Kaganov. *Electron Theory of Metals*. Consultants Bureau, New York, 1973.
- [51] Todor M. Mishonov and Mihail T. Mishonov. Simple model for the linear temperature dependence of the electrical resistivity of layered cuprates. *Physica A*, 278(3):553–562, Apr 2000. [arXiv:cond-mat/0001031](https://arxiv.org/abs/cond-mat/0001031), [doi:10.1016/S0378-4371\(99\)00568-3](https://doi.org/10.1016/S0378-4371(99)00568-3).
- [52] J. Herapath. A Mathematical Inquiry into the Causes, Laws, and principal Phenomena of Heat, Gases, Gravitation. *Ann. Phil. New Series*, 1:273, 1821. URL: <https://www.biodiversitylibrary.org/item/20041>.
- [53] J. J. Waterston and Francis Beaufort. On the Physics of media that are composed of free and perfectly elastic molecules in a state of motion. *Proc. R. Soc. Lond.*, 5:604–604, 1851. [doi:10.1098/rspl.1843.0077](https://doi.org/10.1098/rspl.1843.0077).
- [54] J. J. Waterston, Francis Beaufort, and John William Strutt. I. On the physics of media that are composed of free and perfectly elastic molecules in a state of motion. *Phil. Trans. R. Soc. Lond. A*, 183:1–79, 1892. [doi:10.1098/rsta.1892.0001](https://doi.org/10.1098/rsta.1892.0001).
- [55] E. M. Lifshitz and L. P. Pitaevskii. *Statistical Physics. Part 2*, volume 9 of *Landau-Lifshitz course of theoretical physics*. Pergamon, New York, 1980.
- [56] Lino Reggiani and Eleonora Alfinito. Fluctuation Dissipation Theorem and Electrical Noise Revisited. *Fluct. Noise Lett.*, 18(01):1930001, 2019. [doi:10.1142/S0219477519300015](https://doi.org/10.1142/S0219477519300015).
- [57] T. M. Mishonov, I. M. Dimitrova, and A. M. Varonov. Callen–Welton fluctuation dissipation theorem and Nyquist theorem as a consequence of detailed balance principle applied to an oscillator. *Physica A*, 530:121577, 2019. [arXiv:1811.06944](https://arxiv.org/abs/1811.06944), [doi:10.1016/j.physa.2019.121577](https://doi.org/10.1016/j.physa.2019.121577).
- [58] Lino Reggiani and Eleonora Alfinito. Beyond the Formulations of the Fluctuation Dissipation Theorem Given by Callen and Welton (1951) and Expanded by Kubo (1966). *Front. Phys.*, 8:238:4, 2020. [doi:10.3389/fphy.2020.00238](https://doi.org/10.3389/fphy.2020.00238).
- [59] J. R. Schrieffer, editor. *Handbook of High-Temperature Superconductivity: Theory and Experiment*. Springer-Verlag, New York, 2007. [doi:10.1007/978-0-387-68734-6](https://doi.org/10.1007/978-0-387-68734-6).

- [60] A. Carrington, A. P. Mackenzie, C. T. Lin, and J. R. Cooper. Temperature dependence of the Hall angle in single-crystal $\text{YBa}_2(\text{Cu}_{1-x}\text{Co}_x)_3\text{O}_{7-\delta}$. *Phys. Rev. Lett.*, 69:2855–2858, Nov 1992. doi:[10.1103/PhysRevLett.69.2855](https://doi.org/10.1103/PhysRevLett.69.2855).
- [61] Branko P. Stojkovic and David Pines. Theory of the longitudinal and Hall conductivities of the cuprate superconductors. *Phys. Rev. B*, 55:8576–8595, Apr 1997. doi:[10.1103/PhysRevB.55.8576](https://doi.org/10.1103/PhysRevB.55.8576).
- [62] Chandra M. Varma. Colloquium: Linear in temperature resistivity and associated mysteries including high temperature superconductivity. *Rev. Mod. Phys.*, 92(3):031001, Jul 2020. doi:[10.1103/RevModPhys.92.031001](https://doi.org/10.1103/RevModPhys.92.031001).
- [63] Z.-X. Shen and J. R. Schrieffer. Momentum, Temperature, and Doping Dependence of Photoemission Lineshape and Implications for the Nature of the Pairing Potential in High- T_c Superconducting Materials. *Phys. Rev. Lett.*, 78:1771–1774, Mar 1997. doi:[10.1103/PhysRevLett.78.1771](https://doi.org/10.1103/PhysRevLett.78.1771).
- [64] T. Valla, A. V. Fedorov, P. D. Johnson, Q. Li, G. D. Gu, and N. Koshizuka. Temperature Dependent Scattering Rates at the Fermi Surface of Optimally Doped $\text{Bi}_2\text{Sr}_2\text{CaCu}_2\text{O}_{8+\delta}$. *Phys. Rev. Lett.*, 85:828–831, Jul 2000. doi:[10.1103/PhysRevLett.85.828](https://doi.org/10.1103/PhysRevLett.85.828).
- [65] J. Fink, J. Nayak, E. D. L. Rienks, J. Bannies, S. Wurmehl, S. Aswartham, I. Morozov, R. Kappenberger, M. A. ElGhazali, L. Craco, H. Rosner, C. Felser, and B. Büchner. Evidence of hot and cold spots on the Fermi surface of LiFeAs . *Phys. Rev. B*, 99:245156, Jun 2019. doi:[10.1103/PhysRevB.99.245156](https://doi.org/10.1103/PhysRevB.99.245156).
- [66] Xingjiang Zhou, Wei-Sheng Lee, Masatoshi Imada, Nandini Trivedi, Philip Phillips, Hae-Young Kee, Päivi Törmä, and Mikhail Erements. High-temperature superconductivity. *Nat. Rev. Phys.*, 3(7):462–465, Jan 2021. doi:[10.1038/s42254-021-00324-3](https://doi.org/10.1038/s42254-021-00324-3).
- [67] Warren E. Pickett. Electronic structure of the high-temperature oxide superconductors. *Rev. Mod. Phys.*, 61:433–512, Apr 1989. doi:[10.1103/RevModPhys.61.433](https://doi.org/10.1103/RevModPhys.61.433).
- [68] A. A. Abrikosov. Metal–insulator transition in layered cuprates (SDW model). *Physica C: Supercond. and Appl.*, 391(2):147–159, 2003. doi:[https://doi.org/10.1016/S0921-4534\(03\)00888-8](https://doi.org/10.1016/S0921-4534(03)00888-8).
- [69] Todor M. Mishonov, R. K. Koleva, Ivan N. Genchev, and Evgeni S. Penev. Quantum chemical calculation of oxygen-oxygen electron hopping amplitude - first principles evaluation of conduction bandwidth in layered cuprates. *Czech J. Phys.*, 46:2645–2646, 1996. doi:[10.1007/BF02570309](https://doi.org/10.1007/BF02570309).
- [70] Ryogo Kubo. Statistical-Mechanical Theory of Irreversible Processes. I. General Theory and Simple Applications to Magnetic and Conduction Problems. *J. Phys. Soc. Jpn.*, 12(6):570–586, 1957. doi:[10.1143/JPSJ.12.570](https://doi.org/10.1143/JPSJ.12.570).

- [71] M. R. Norman and C. Pépin. Quasiparticle formation and optical sum rule violation in cuprate superconductors. *Phys. Rev. B*, 66:100506, Sep 2002. [arXiv:cond-mat/0201415](#), [doi:10.1103/PhysRevB.66.100506](#).
- [72] M R Norman and C Pépin. The electronic nature of high temperature cuprate superconductors. *Rep. Prog. Phys.*, 66(10):1547–1610, Sep 2003. [arXiv:cond-mat/0302347](#), [doi:10.1088/0034-4885/66/10/r01](#).
- [73] Guy Deutscher, Andrés Felipe Santander-Syro, and Nicole Bontemps. Kinetic energy change with doping upon superfluid condensation in high-temperature superconductors. *Phys. Rev. B*, 72:092504, Sep 2005. URL: <https://link.aps.org/doi/10.1103/PhysRevB.72.092504>, [doi:10.1103/PhysRevB.72.092504](#).
- [74] V. G. Kogan. Free Energy and Torque for Superconductors with Different Anisotropies of H_{c2} and λ . *Phys. Rev. Lett.*, 89:237005, Nov 2002. [doi:10.1103/PhysRevLett.89.237005](#).
- [75] A. T. Fiory, A. F. Hebard, R. H. Eick, P. M. Mankiewich, R. E. Howard, and M. L. O'Malley. Fiory et al. reply. *Phys. Rev. Lett.*, 67:3196, 1991. [doi:10.1103/PhysRevLett.67.3196](#).
- [76] J. Orenstein. Optical Conductivity and Spatial Inhomogeneity in Cuprate Superconductors. In J. Robert Schrieffer and James S. Brooks, editors, *Handbook of High-Temperature Superconductivity: Theory and Experiment*, pages 299–324. Springer, New York, NY, 2007. [doi:10.1007/978-0-387-68734-6_7](#).
- [77] A. Kramida, Yu. Ralchenko, J. Reader, and and NIST ASD Team. NIST Atomic Spectra Database (ver. 5.8), [Online]. Available: <https://physics.nist.gov/asd> [2021, October 11]. National Institute of Standards and Technology, Gaithersburg, MD., 2020. [doi:10.18434/T4W30F](#).
- [78] Juan Carlos Campuzano. Abrikosov and the path to understanding high- T_c superconductivity. *Low Temp. Phys.*, 44(6):506–509, 2018. [doi:10.1063/1.5037552](#).
- [79] V. L. Pokrovskii. Thermodynamics of Anisotropic Superconductors. *J. Exp. Theor. Phys.*, 13(2):447–450, 1961. *ZhETF* **40**(2), 641 Aug (1961), <http://www.jetp.ras.ru/cgi-bin/r/index/r/40/2/p641?a=list> (in Russian). URL: <http://jetp.ras.ru/cgi-bin/e/index/e/13/2/p447?a=list>.
- [80] V. L. Pokrovskii and M. S. Ryvkin. Thermodynamics of Anisotropic Superconductors. *J. Exp. Theor. Phys.*, 16(1):67–75, 1961. *ZhETF* **43**(1), 92 Jan (1963), <http://www.jetp.ras.ru/cgi-bin/r/index/r/43/1/p92?a=list>, (in Russian). URL: <http://jetp.ras.ru/cgi-bin/e/index/e/16/1/p67?a=list>.

- [81] Todor M. Mishonov, Joseph O. Indekeu, and Evgeni S. Penev. The $3d$ -to- $4s$ -by- $2p$ highway to superconductivity in cuprates. *Int. J. Mod. Phys. B*, 16(30):4577–4585, 2002. [arXiv:cond-mat/0206350](#), [doi:10.1142/S0217979202014991](#).
- [82] Dirk Manske. *Theory of Unconventional Superconductors*. Springer-Verlag, Berlin, 2004. [doi:10.1007/b13050](#).
- [83] Patrick A. Lee, Naoto Nagaosa, and Xiao-Gang Wen. Doping a Mott insulator: Physics of high-temperature superconductivity. *Rev. Mod. Phys.*, 78:17–85, Jan 2006. [arXiv:cond-mat/0410445](#), [doi:10.1103/RevModPhys.78.17](#).
- [84] S. A. Kivelson, I. P. Bindloss, E. Fradkin, V. Oganesyan, J. M. Tranquada, A. Kapitulnik, and C. Howald. How to detect fluctuating stripes in the high-temperature superconductors. *Rev. Mod. Phys.*, 75:1201–1241, Oct 2003. [doi:10.1103/RevModPhys.75.1201](#).
- [85] Frithjof Anders. The Kondo Effect. In Eva Pavarini, editor, *Correlated electrons: from models to materials*, volume 2, chapter 11. Forschungszentrum Jülich GmbH Zentralbibliothek, Verlag, Jülich, 2012. URL: <https://juser.fz-juelich.de/record/136393>.
- [86] R. M. White and T. H. Geballe. *Long-Range Order in Solids*. Solid State Physics. Academic Press, New York, 1979.
- [87] Fabian Eickhoff, Benedikt Lechtenberg, and Frithjof B. Anders. Effective low-energy description of the two-impurity Anderson model: RKKY interaction and quantum criticality. *Phys. Rev. B*, 98:115103, Sep 2018. [doi:10.1103/PhysRevB.98.115103](#).
- [88] Fabian Eickhoff and Frithjof B. Anders. Strongly correlated multi-impurity models: The crossover from a single-impurity problem to lattice models. *Phys. Rev. B*, 102:205132, Nov 2020. [doi:10.1103/PhysRevB.102.205132](#).
- [89] Fabian Eickhoff and Frithjof B. Anders. Kondo holes in strongly correlated impurity arrays: RKKY-driven Kondo screening and hole-hole interactions. *Phys. Rev. B*, 104:045115, Jul 2021. [doi:10.1103/PhysRevB.104.045115](#).
- [90] Fabian Eickhoff and Frithjof B. Anders. Spectral properties of strongly correlated multi-impurity models in the Kondo insulator regime: Emergent coherence, metallic surface states, and quantum phase transitions. *Phys. Rev. B*, 104:165105, Oct 2021. [doi:10.1103/PhysRevB.104.165105](#).
- [91] L. D. Landau and E. M. Lifshitz. *Quantum Mechanics: Non-Relativistic Theory*, volume 3 of *Landau-Lifshitz Course of Theoretical Physics*. Pergamon, New York, 3 edition, 1977.
- [92] Conyers Herring. Critique of the Heitler-London Method of Calculating Spin Couplings at Large Distances. *Rev. Mod. Phys.*, 34:631–645, Oct 1962. [doi:10.1103/RevModPhys.34.631](#).

- [93] Conyers Herring and Michael Flicker. Asymptotic Exchange Coupling of Two Hydrogen Atoms. *Phys. Rev.*, 134:A362–A366, Apr 1964. doi:[10.1103/PhysRev.134.A362](https://doi.org/10.1103/PhysRev.134.A362).
- [94] T. M. Mishonov, J. O. Indekeu, and E. S. Penev. Superconductivity of overdoped cuprates: The modern face of the ancestral two-electron exchange. *J. Phys. Cond. Matter*, 15(25):4429–4456, 2003. arXiv:[cond-mat/0209191](https://arxiv.org/abs/cond-mat/0209191), doi:[10.1088/0953-8984/15/25/312](https://doi.org/10.1088/0953-8984/15/25/312).
- [95] Z. D. Dimitrov, S. K. Varbev, K. J. Omar, A. A. Stefanov, E. S. Penev, and T. M. Mishonov. Correlation between T_c and the Cu4s Level Reveals the Mechanism of High-Temperature Superconductivity. *Bulg. J. Phys.*, 38(1):106–112, 2011. URL: <https://www.bjp-bg.com/paper1.php?id=573>, arXiv:[1103.2966](https://arxiv.org/abs/1103.2966).
- [96] A. B. Migdal. *Qualitative methods in quantum theory*. CRC Press, Boca Raton, 1977.
- [97] Pierre-Gilles de Gennes. *Simple Views on Condensed Matter (Expanded Edition)*. World Scientific, Singapore, 1998. doi:[10.1142/3601](https://doi.org/10.1142/3601).
- [98] N. E. Hussey. Low-energy quasiparticles in high- T_c cuprates. *Adv. Phys.*, 51(8):1685–1771, 2002. doi:[10.1080/00018730210164638](https://doi.org/10.1080/00018730210164638).
- [99] P. Nozières and D. Pines. *The Theory of Quantum Liquids*. CRC Press, Boca Raton, 1 edition, 1966. doi:[10.4324/9780429492662](https://doi.org/10.4324/9780429492662).
- [100] D. Valentinis. Optical signatures of shear collective modes in strongly interacting Fermi liquids. *Phys. Rev. Research*, 3:023076, Apr 2021. URL: <https://link.aps.org/doi/10.1103/PhysRevResearch.3.023076>, doi:[10.1103/PhysRevResearch.3.023076](https://doi.org/10.1103/PhysRevResearch.3.023076).
- [101] Davide Valentinis, Graham Baker, Douglas A. Bonn, and Jörg Schmalian. Kinetic theory of the non-local electrodynamic response in anisotropic metals: skin effect in 2D systems, 2022. arXiv:[2204.13344](https://arxiv.org/abs/2204.13344).
- [102] Graham Baker, Timothy W. Branch, James Day, Davide Valentinis, Mohamed Oudah, Philippa McGuinness, Seunghyun Khim, Piotr Surówka, Roderich Moessner, Jörg Schmalian, Andrew P. Mackenzie, and D. A. Bonn. Non-local microwave electrodynamics in ultra-pure PdCoO₂, 2022. arXiv:[2204.14239](https://arxiv.org/abs/2204.14239).
- [103] L. D. Landau. On the Theory of the Fermi Liquid. *Sov. Phys. JETP*, 8:70–74, 1959. URL: <http://jetp.ras.ru/cgi-bin/e/index/e/8/1/p70?a=list>.
- [104] W. G. Baber. The contribution to the electrical resistance of metals from collisions between electrons. *Proc. R. Soc. London, Ser. A*, 158(894):383–396, 1937. doi:[10.1098/rspa.1937.0027](https://doi.org/10.1098/rspa.1937.0027).

- [105] L. Landau and I. Pomeranchuk. Über die Eigenschaften der Metalle bei sehr niedrigen Temperaturen. *Phys. Z. Sowjetunion*, 10:649–665, 1936. (in German). URL: <https://www.zbmath.org/?q=an%3A0016.09603>.
- [106] P. A. M. Dirac. *The Principles of Quantum Mechanics*. Oxford Univeristy Press, Oxford, 3 edition, 1947.
- [107] E. Fermi. *Notes on quantum mechanics*. Univeristy of Chicago Press, Chicago, 1954. See Eq. (23.13) for rate of transition.
- [108] R. Harris, P. J. Turner, Saeid Kamal, A. R. Hosseini, P. Dosanjh, G. K. Mullins, J. S. Bobowski, C. P. Bidinosti, D. M. Broun, Ruixing Liang, W. N. Hardy, and D. A. Bonn. Phenomenology of \hat{a} -axis and \hat{b} -axis charge dynamics from microwave spectroscopy of highly ordered $\text{YBa}_2\text{Cu}_3\text{O}_{6.50}$ and $\text{YBa}_2\text{Cu}_3\text{O}_{6.993}$. *Phys. Rev. B*, 74:104508, Sep 2006. doi:10.1103/PhysRevB.74.104508.
- [109] Neil W. Ashcroft and David Mermin. *Solid state physics*. Holt, Rinehart and Winston, 1 edition, 1976.
- [110] A Lanzara, P V Bogdanov, X J Zhou, S A Kellar, D L Feng, E D Lu, T Yoshida, H Eisaki, Atsushi Fujimori, K Kishio, J I Shimoyama, T Noda, S Uchida, Zahid Hussain, and Z X Shen. Evidence for ubiquitous strong electron-phonon coupling in high-temperature superconductors. *Nature*, 412(6846), Aug 2001. arXiv:cond-mat/0102227, doi:10.1038/35087518.
- [111] Z.-X. Shen, A. Lanzara, S. Ishihara, and N. Nagaosa. Role of the electron-phonon interaction in the strongly correlated cuprate superconductors. *Phil. Mag. B*, 82(13):1349–1368, 2002. doi:10.1080/13642810208220725.
- [112] A. Kohen, G. Leibovitch, and G. Deutscher. Andreev Reflections on $\text{Y}_{1-x}\text{Ca}_x\text{Ba}_2\text{Cu}_3\text{O}_{7-\delta}$: Evidence for an Unusual Proximity Effect. *Phys. Rev. Lett.*, 90:207005, May 2003. doi:10.1103/PhysRevLett.90.207005.
- [113] M. Kugler, Ø. Fischer, Ch. Renner, S. Ono, and Yoichi Ando. Scanning Tunneling Spectroscopy of $\text{Bi}_2\text{Sr}_2\text{CuO}_{6+\delta}$: New Evidence for the Common Origin of the Pseudogap and Superconductivity. *Phys. Rev. Lett.*, 86:4911–4914, May 2001. doi:10.1103/PhysRevLett.86.4911.
- [114] P. W. Anderson. The Resonating Valence Bond State in La_2CuO_4 and Superconductivity. *Science*, 235(4793):1196–1198, 1987. doi:10.1126/science.235.4793.1196.
- [115] C. M. Varma, S. Schmitt-Rink, and Elihu Abrahams. Charge transfer excitations and superconductivity in “ionic” metals. *Solid State Commun.*, 62(10):681–685, 1987. URL: <https://www.sciencedirect.com/science/article/pii/0038109887904078>, doi:[https://doi.org/10.1016/0038-1098\(87\)90407-8](https://doi.org/10.1016/0038-1098(87)90407-8).

- [116] P. W. Anderson. *A Career in Theoretical Physics*. World Scientific, Singapore, 1994. pp. 637–656, p. 570, p. 584.
- [117] J. M. Ziman. *Principles of the Theory of Solids*. Cambridge Univeristy Press, Cambridge, 1964.
- [118] T. M. Mishonov, S. I. Klenov, and E. S. Penev. Temperature dependence of specific heat and penetration depth of anisotropic-gap Bardeen-Cooper-Schrieffer superconductors for a factorizable pairing potential. *Phys. Rev. B*, 71:024520, Jan 2005. [arXiv:cond-mat/0212491](#), [doi:10.1103/PhysRevB.71.024520](#).
- [119] Todor M. Mishonov, Valery L. Pokrovsky, and Hongduo Wei. Thermodynamics of MgB_2 described by the weak-coupling two-band BCS model. *Phys. Rev. B*, 71:012514, Jan 2005. [arXiv:cond-mat/0312210](#), [doi:10.1103/PhysRevB.71.012514](#).
- [120] Todor Mishonov and Evgeni Penev. Thermodynamics of anisotropic-gap and multiband clean bcs superconductors. *Int. J. Mod. Phys. B*, 16(24):3573–3586, 2002. [arXiv:cond-mat/0206118](#), [doi:10.1142/S0217979202012074](#).
- [121] Todor M. Mishonov, Evgeni S. Penev, and Joseph O. Indekeu. Comment on “Anisotropic s -wave superconductivity in MgB_2 ”. *Phys. Rev. B*, 66:066501, Aug 2002. [arXiv:cond-mat/0204545](#), [doi:10.1103/PhysRevB.66.066501](#).
- [122] T. M. Mishonov, E. S. Penev, and J. O. Indekeu. Comment on “Anisotropic s -wave superconductivity: Comparison with experiments on MgB_2 by A. I. Posazhennikova *et. al.*”. *Europhys. Lett.*, 61(4):577–578, Feb 2003. [arXiv:cond-mat/0205104](#), [doi:10.1209/epl/i2003-00169-0](#).
- [123] J. J. Thomson. LXXXVIII. The forces between atoms and chemical affinity. *Philos. Mag.*, 27(161):757–789, 1914. [doi:10.1080/14786440508635150](#).
- [124] N. Bohr. On the Constitution of Atoms and Molecules. Part II. Systems containing only a Single Nucleus. *Phil. Mag.*, 26:476–502, 1913. [doi:10.1080/14786441308634993](#).
- [125] F. H. Read. A new class of atomic states: the ‘Wannier-ridge’ resonances. *Aust. J. Phys.*, 35:475–499, 1982. [doi:10.1071/PH820475](#).
- [126] J. C. Maxwell. *On the stability of the motion of Saturn’s rings*. Cambridge: Macmillan and Co., London, 1859. URL: <https://archive.org/details/onstabilityofmot00maxw/>.
- [127] J. Bardeen, L. N. Cooper, and J. R. Schrieffer. Theory of Superconductivity. *Phys. Rev.*, 108:1175–1204, Dec 1957. [doi:10.1103/PhysRev.108.1175](#).

- [128] N. N. Bogoliubov. A New Method in the Theory of Superconductivity. I. *J. Exp. Theory Phys.*, 7:41, 1958. URL: <http://jetp.ras.ru/cgi-bin/e/index/e/7/1/p41?a=list>.
- [129] Vladimir Anisimov and Yuri Izyumov. *Electronic Structure of Strongly Correlated Materials*. Springer-Verlag, Berlin, 2010. doi:<https://doi.org/10.1007/978-3-642-04826-5>.
- [130] Andrés Greco, Hiroyuki Yamase, and Matías Bejas. Origin of high-energy charge excitations observed by resonant inelastic X-ray scattering in cuprate superconductors. *Commun. Phys.*, 2:3, 2019. doi:[10.1038/s42005-018-0099-z](https://doi.org/10.1038/s42005-018-0099-z).